Wet torrefaction of verge grass

A pre-treatment to enable co-firing in a coal power plant

M.W. Verburg

Sustainable Energy Technology
MSc Thesis
report 2574

TU Delft Delft University of Technology

Wet torrefaction of verge grass

A pre-treatment to enable co-firing in a coal power plant

Master Thesis
Michiel Verburg
June 2013

Exam committee:
Prof.dr.ir B.J. Boersma
Dr.ir. A.J.J. Straathof
Dr.ir. W. de Jong
Ir. Y. Joshi

Sustainable Energy Technology
Faculty of Applied Physics
Delft University of Technology

Abstract

Current energy production is done in a way that cannot be sustained ultimately. As an alternative biomass is ideal since it can be used in the existing energy infrastructure without massive modifications and it is an energy carrier. In the future it can thus be used in the energy mix as storage to balance more intermittent renewables like wind or solar energy. There are however disadvantages that prevent large scale implementation of biomass currently.

In the Netherlands verge grass is available for co-firing in a coal power plant. The moisture content and its bioactivity however prevent direct co-firing on a large scale. A very new and promising pre-treatment technique to counter this is wet torrefaction. Because it does not evaporate the moisture it can be more efficient compared to dry torrefaction. Wet torrefaction also allows a precise temperature and thus process control, high heat transfer and a combined washing out of unwanted salts. This thesis focuses on wet torrefaction of verge grass to co-fire 20% of the thermal input of a coal power plant. To be able to do this a reaction model was set up using kinetic data from previous work on corn cob and cellulose. This model was tested against sugar maple wood meal and the results are very good. After only changing the material parameters the model was able to predict the trends very well and was within very close comparison to the original work.

Wet torrefaction experiments showed that verge grass decomposes very rapidly in contrary to the model. Xylan on the other hand decomposed slower than expected. The decomposition of bagasse was very hard to monitor because very little decomposition products were detected. A possible explanation could be that grass is very young biomass and thus has a low degree of polymerization. Xylan and bagasse are already treated prior to testing and this has only left over the toughest parts of the original material. Overall the three biomass species had a very high mass loss. Verge grass and bagasse retained only around 30% of the original mass and no solid mass was found with xylan. The solid fraction and the liquid fraction that could be accounted for is lower than half of the original mass.

Although additional tests are needed for accurate prediction of the decomposition of grass a design was made for a possible pre-treatment plant. This facility was regarded as a stand-alone facility and consists of several parallel CSTR’s and a heat exchanger. The total energy needed for the pre-treatment is around 8 times smaller than the energy returned. Although this seems very favourable due to the high mass loss more than half of the initial energy has been lost. When around 70% of the original mass is retained wet torrefaction is energetically favourable.

Contents

Acknowledgements

Without the help, guidance and wisdom from others this work would not have been the same.

Thank you Wiebren for your advice. You've pointed me in the right direction and to the right people when your practical knowledge sometimes ended.

Yash thanks for being my daily supervisor. Your experience has helped me and we had some interesting discussions on a lot of subjects and especially the energy landscape. Thanks also for honing the rough edges of my work.

My gratitude goes to Michel for almost always being around when I needed you and of course the inevitable answering of all my questions.

Bart Danon your knowledge and guidance on the test setup and HPLC analysis have added a great deal of the quality to the research part of this work.

At last my special thanks goes out to my parents and girlfriend for their patience. Not without reason is it called a virtue.

1. Introduction

An outlook on the future energy production is given. After that the necessity of biomass pre-treatment is given and the reason for this particular pre-treatment technology is explained. The boundary conditions are given in which the application of this pre-treatment is envisaged.

1.1. Outlook

Energy is a hot topic. In recent years it gained attention due to rising prices. With scarcity prices rise and this necessitates a search for alternatives. This has always been that way ('70s oil crisis, WWII Fischer-Tropsch process, isolation of South-Africa during apartheid, Brazil ethanol production). This time the search is however different and this is caused by two events:

- Easy to extract sources become depleted
- Developing countries step up to take their piece of the energy pie

This poses a problem for countries because a steady and affordable energy supply is vital for industry and every aspect of daily life. Rising prices are especially challenging for countries that are net energy importers. Energy is however a commodity where the political component is not to be forgotten. Being dependent on unstable regimes or oppressive rulers is being seen as more and more unwanted. Last but not least fossil fuels have the inherent trait that they cause high CO_2 emissions. In all possible directions the search is on for alternatives; shale oil and gas, under ice oil drilling, gashydrates and renewables.

1.2. Renewables

Renewables are the oldest forms of energy used by human beings. Wood has always been used for fire and windmills for food production and for pumping in the Dutch polders. In the meantime industrialization has taken place and due to their low efficiency renewables have to be "renewed" before they can be regarded as alternatives. Amongst these are solar, wind, water, geothermal and biomass. For the concerned reader: with water not large dams are meant but instead energy made from tides, waves or even salt water mixing with fresh water.
These renewables all have, except for one, an very important problem; they are not energy carriers. Especially with the intermittent nature of some of the renewables a new problem rises; storage of energy in very large amounts. Since power is not always needed when it is produced. From all renewables only biomass is not withheld by this challenge. One can argue that due to the predictive behavior of tidal and geothermal energy a simple adjustment of usage is needed. However our energy usage is not controlled in this top-down way. Therefore storage is necessary and a challenge for large scale application of renewables.

1.3. Biomass

Biomass and renewable both have debated definitions[1], however what all these definitions have in common is that they state the source and a time span in which this source is renewed. For this work a rather loose term is defined:

Biomass means:
a. organic matter derived from woods, grasses, agricultural feed or algae
or
b. waste organic matter
that can be renewed within 100 years.

Biomass is effectively the precursor of all fossil fuels. Another way of seeing this is that fossil fuels are nature's pre-treated biomass over thousands of years. With relative ease this process can be shortened turning biomass into a close resembling product which can thus act as a replacement in existing energy infrastructure and equipment.

When closely comparing biomass with fossil fuels some distinct differences are noticeable of which only the major common disadvantages are mentioned here:

- lower energy density
- high moisture content
- high processing costs
    - pre-processing/grinding (costs more energy than conventional)
    - transport
    - storage (bio-activity degrades biomass)
- inhomogeneous fuel characteristics
- different composition
    - burnout characteristics
    - different ash (ash thus not suitable for cement industry)
    - corrosion, slagging, fouling

One direction to which these disadvantages can be traced back to is that most biomass is a solid plant-like residue whereas oil and gas can flow nicely and coal is far more homogeneous. But even a wet waste stream such as cattle manure has these disadvantages except for perhaps the inhomogeneous characteristics.

1.4.Policy & challenges

In the Netherlands a sustainability policy is set because of rising energy prices and the call for cleaner energy production. The main target of this policy is that in 2020 of all energy produced 16% must be done in a sustainable way. For 2050 this target is set at 100%.[2]
For an electricity producers such as E.ON this is a huge task. Investments in energy production infrastructure span several decades and are therefore taken with care. With a new coal power plant[3] currently still under construction at the Maasvlakte (Maasvlakte Power Plant 3, MPP3) a search started on how to meet these targets.
Previous research for E.on concluded that co-firing verge grass in the MPP3 is one of the most feasible options. It is relative abundant[4] and because verge grass is not of food grade. Therefore the removal is being incentivized and with no competition for this source a steady price is expected.

Coal is compared with verge grass in

Table 1-1 with data taken from ECN.[5] Demolition wood is
added here because this also functions as a renewable alternative to coal. Where demolition wood compares to coal for roughly 3/5th in calorific value, verge grass is very different.

When taking a closer look at verge grass it shows the typical disadvantages of all biomass species and some specific problems of its own:

- Very high moisture content (ca. 60%)
- High chlorine content

Table 1-1: Properties of different fuels

	Coal	Demolition Wood	Verge grass	
LHV	24,24	16,59	5,42	MJ/kg
Moisture	11,50	8,60	60,00	%
Volatiles	27,88	70,65	-	%
fixed-C	48,50	18,83	-	%
Ash	12,12	1,92	3,36	%
	100,0	100,0	63,4	
Chlorine	265,50	914,00	1429	mg/kg

One of the possibilities for E.on is to directly co-fire verge grass, without pre-treatment.
When this is done the overall temperature in the boiler will be lower due to the high moisture content of grass. This seriously limits[6] the amount (<20%)of grass that can be co-fired in this way.
The high chlorine content will also cause more corrosion and HCL emissions.[6]
Storage of fresh grass necessitates extra precautions because of spontaneous combustion and degradation.
Another important thing is that the grinding of biomass costs more energy than coal.

1.5.Biomass pre-treatments for co-firing

As these disadvantages seriously limit the amount of grass that can be co-fired research is needed for a suitable pre-treatment. Several pre-treatment are available that enable direct co-firing of grass in a coal power plant. What these pre-treatments should achieve is to have a product that has similar properties as coal.

The following goals should be met for a pre-treatment to be successful:

- Lower moisture content (<15%)
- Higher LHV (>15 MJ/kg)
- Low energy usage during process
- Lower chlorine content (same as coal)
- Alter properties into coal properties (grinding & storage)

All pre-treatment technologies are at least capable of lowering the moisture content and raise the LHV to acceptable levels. There are differences for the other goals which are discussed more in detail. The heat needed for each pre-treatment could be delivered by steam diverted from the MPP3 or in a separate facility that can perhaps derive low value heat from a nearby source.

Drying

One possibility is to dry grass. Large scale drying is applied in for example tumble dryers.

- Dry grass has an LHV of 17,22 MJ/kg. [5]
- Drying of grass is very energy intense due to the high (60%) moisture content. [5]
- After drying it still has a rather high chlorine content. [5]

- A fibrous end product is expected which is not as brittle as coal. For this more grinding energy is required.[6]
- After additional densification less storage is needed, but it still is bulkier than coal and a dry storage is needed.

Torrefaction

Torrefaction is a rather new technology in the field of energy production. At a temperature of 250-320C biomass is heated in an inert environment. Due to the inert environment torrefaction is also called low temperature pyrolysis. Torrefaction causes the biomass to decompose a little and evaporates the moisture. The decomposition "breaks" the structure of grass which enables the removal of salts afterwards and it produces a brittle product. Torrefaction has been used in the coffee industry for the roasting of coffee beans for quite some time. However in the coffee industry oxygen (of air) is allowed during the process.

- Torrefaction of for example beechwood [5]raises the LHV of a dry product by approximately 10% depending on the reaction conditions. This comes at the cost of the loss of dry mass.[7]
- Due to the high temperatures needed for this process and the evaporation of all water even more energy is needed than normal drying. Some of this energy can be recuperated by the gasses that come of the grass. [7]
- Chlorine content is not affected, but can be washed out in an after-treatment. [5]
- After torrefaction a product very much resembling coal is produced. It is expected that the torrefied material can therefore be handled and stored just like coal. [7]

Wet torrefaction

A rather new technique that applies the same temperatures as torrefaction, however in liquid water instead of inert gas environment. This process is therefore called wet torrefaction. Water is thought to be a temperature buffer allowing for more precise control of the process. Water also has a higher heat transfer coefficient than gas allowing for a shorter residence time. Several mechanisms also point out that water plays an important role in the reaction chemistry.[9] Because of more control over the reaction conditions this process can also be used for the production of chemicals.[9]

- The LHV is expected to be changed in a comparable way as torrefaction.[8]
- The torrefied (biomass+water=) slurry can be fed through heat exchangers before and after the process to recuperate most of the energy that would have otherwise been lost due to evaporation of water. It is expected that this process costs less energy than drying or torrefaction.
- During the process chlorine automatically is removed by the process water. [8]
- Like torrefaction the product resembles coal and thus can be handled and stored like coal. [8]
- Due to fact liquid water is used the process however requires to be pressurized which in itself is challenging on this scale.

1.6.This work

This work is focused on a wet torrefaction treatment (WTT) of biomass as this is seen as a promising way of processing biomass and perhaps derive valuable chemicals. For the process a wide variety of names are in use: hydrothermal coalification/carbonization/upgrading/decomposition/degradation/conversion/treatment, torwash, hot pressurized water treatment, hydrolysis in near/subcritical conditions, hot water extraction,

hydrothermolysis, autohydrolysis, uncatalyzed solvolysis. It mostly depends on the required end-product and the background of the company/researcher.
What all these processes share is that **a form of biomass** be it whole or a component such as cellulose is being treated at **temperatures ranging from 150-374C** in **liquid water,** so there is **pressure** to keep it liquid, **without a catalyst added**.
The usage of wet torrefaction for energy production is quite new and the amount of terms used already indicate this. Some of the main directions of research focus on the production of carbon for usage in nano particles, sugars for chemical processes, enhancement of the enzymatic digestibility for the production of bio-ethanol or even catalyst free production of cellulose for paper. This has the implication that the information gathered was very shattered amongst sources, backgrounds and jargons.

Equipment

Due to the moisture content of grass a stand-alone facility is regarded, although this project is aimed at solely providing wet torrefied grass (WTG) for the MPP3. Transport costs play a large role in the costs of biomass co-firing. If grass is not available in the direct vicinity of the MPP3 they could be substantially higher, necessitating a separate facility.

Massflow

To get a rough idea of the grass flow that needs treatment a calculation is made in which 16% is co-fired unprocessed verge grass. The MPP3 has a capacity of 1070 MW with an efficiency of 46%[3]. This would require 372,2 MW_{th} to be provided by grass. With the LHV taken from ECN [5] of 68,7 kg/s of wet grass is needed.

Boundary conditions

A very rough process overview can be seen in Figure 1-1. Here water and grass go in a heat exchanger with on the other side the previous process mixture. This preheats the fresh mixture before it goes into the reactor. After the reactor the WTG and process water are separated.

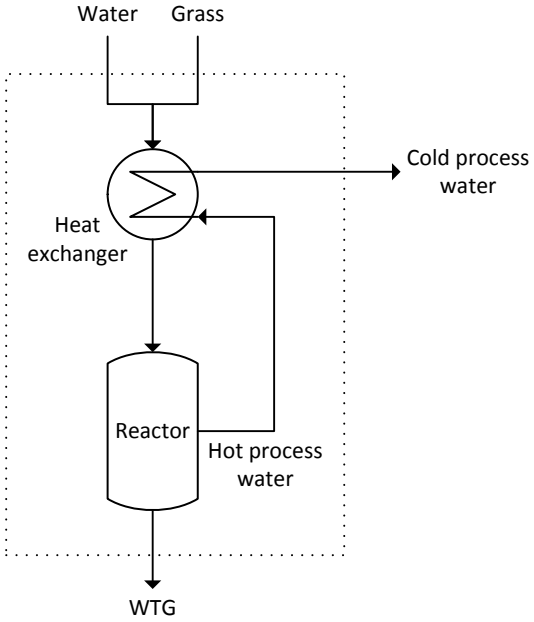

Figure 1-1: System of interest

This thesis focuses on making a design for the system inside the dotted line. First the reactor conditions need to be known and from that the mass and heat flows can be calculated. After that sizing of the equipment can be done.

1.7.Objective & outline

In this introduction some background information regarding the co-firing of biomass for a coal power plant is given. The coming chapters will focus more deeply on wet torrefaction of verge grass under the following objective:

> *Investigate wet torrefaction as a pre-treatment for pulverized co-firing of verge grass in the MPP3 coal power plant*

Chapter 2 focusses on a **model to predict the decomposition of grass** and this model is **validated with other sources of biomass**. In chapter 3 the **experimental method** is described and in chapter 4 **tests are performed to verify the model for specifically grass**. The **design of a facility in which grass can be processed** is the focus of chapter 5. The **conclusions** are reserved for chapter 6 and **recommendations** are for chapter 7.

1.8.References

1. P. Basu, Biomass gasification and pyrolysis; practical design and theory, Elsevier 2010, pp325
2. Rijksoverheid, Duurzame energie, 2012, http://www.rijksoverheid.nl/onderwerpen/duurzame-energie/meer-duurzame-energie-in-de-toekomst, accessed 10-4-2013
3. E.on, MPP3- een nieuwe centrale, 2013, http://www.eon.nl/corporate/Activiteiten/mpp3-een-nieuwe-centrale, accessed 10-4-2013
4. Energiebureau Overijssel, 2003, Verkennend onderzoek naar mogelijkheden voor de inzet van bermgras in Overijssel voor duurzame energie-opwekking, Enschede: BTG biomass technology group BV
5. *Energy research Centre of the Netherlands (*ECN), *Phyllis2 database for biomass and waste*, http://www.ecn.nl/phyllis2/, accessed: 8-5-2012
6. S. van Loo, J. Koppejan, The handbook of biomass combustion and co-firing, Earthscan 2008
7. P.C.A. Bergman, Combined torrefaction and pelletisation: the TOP process, ECN for SenterNovem, 2005
8. J.R. Pels, P.C.A. Bergman, TORwash: Proof of Principle - Phase 1, SenterNovem project number 0268-04-04-40-007, ECN 2006
9. N. Akiya, P.E. Savage, Roles of water for chemical reactions in high-temperature water, Chem. Rev. 102, 2002, pp 2725-2750

2. Modeling

An introduction into biomass chemistry is given along with the roles of water in the process. After that the model is presented for the different components. And finally the model is validated with data from research done on sugar maple wood meal.

2.1.Biomass

Biomass is comprised of cellulose, hemicelluloses, lignin and extractives. Cellulose, hemicelluloses and lignin are also called lignocellulosic components. The term comprised is used here because the composition is determined after a test like ASTM *D* 1106-96. Tests like these give fairly accurate results when performed on fresh biomass. For biomass that has been treated the results can become unclear. In some tests higher lignin percentages are found after treatment than before.[24]
For wet torrefaction this composition is important because the mass loss has been described by the decomposition of these components.
Other "components" of biomass are ash and protein. The ash content is more important for a comparison of heating value which we are interested in later. The protein content is of more interest to farmers and will therefore not be mentioned anymore in this work.
The composition used in this work is shown in the left column of Table 2-1. It is taken from an extensive database on biomass and waste from ECN.[1] On the right the composition is shown into its respective major components.

Table 2-1: Grass components sorted by major components

Verge grass		**Adjusted composition**	
glucose	32,9	cellulose	32,9
arabinose	2,9	hemicellulose	23,9
xylose	19,6		
rhamnose	0,3		
mannose	0,3		
galactose	0,8		
klason lignin	24,1	lignin	25,8
acid sol lignin	1,7		
extractives EtOH/toluene	3,2	extractives	16,5
extractives 95% EtOH	1,4		
extractives hot water	6		
pectin	5,9		
total	99,1	total	99,1

Of the three lignocellulosic components hemicellulose is the component that decomposes most easily in a hydrothermal treatment. It decomposes from as early as 150C[1], and can be totally decomposed after several minutes at 230C.[3] Cellulose on the other hand decomposes very late, from around 215C.[4] This thermal and chemical stability is due to its high degree of polymerization (DP) and its crystalline structure. Lignin decomposes more spread out then the former two, fractions of lignin start decomposing as early as hemicellulose[3] and almost all (>90%) lignin can be decomposed after 25 seconds at 365C.[5] This is caused by its heterogeneous structure. During experiments some of the lignin starts to repolymerize onto the original biomass. With longer reaction times a weight gain of the residue has been measured.[5]

An example of an industry in which the separation of lignocellulosic components takes place on a very big scale is the paper industry where large scale removal of hemicellulose and lignin is applied. This is not done solely in a hydrous environment but with the aid of sulphurous ions (Kraft and Sulphite process) or an organic solvent (Organosolv) to break down the lignin structure. As is later explained this has noticeable effects on the lignin produced and thus on the way the components can be analyzed.

2.2.Water

This passage on water serves as an illustration of the possible mechanisms behind wet torrefaction. And in a broader sense it illustrates the possibilities of water as a chemical reactant. This is mostly taken from the work by Akiya and Savage.[6]

Water recently gains attention as a reaction medium because there is a need for cleaner and safer processes. Another positive feature is that it is, depending on the grade, generally cheap and abundantly available. Water plays an important role in the wet torrefaction process. Besides partly being the eponym of the process, it plays an important role in the chemistry involved in that process. At elevated temperatures the properties of water change dramatically. Hydrogen bonds get weaker which relates to an obvious decrease in density.

It has a lower di-electric constant, which is related to its polarity. With a declining polarity water behaves more like an organic solvent does at ambient conditions. With this the solubility parameter of inorganic salts decreases as well.

What's also interesting is to see that the ionic product increases with this temperature rise.

In all, water at elevated temperatures can be thought of as an equivalent to acetone regarding its solvent properties at room temperature. The changes of some of the more important properties are mentioned in the Table 2-2.

Table 2-2: Comparison water-acetone

		Water 20C	Water 250C (sat. pres.)	Acetone 20C
Density	kg*m-3	998,2	799	791
Dielectric constant	ε_r	80,36	30	20,7 (25C)
Dynamic Viscosity	mPa*s	1,005	0,11	0,311
Cp	kJ*kg-1*K-1	4,183	4,87	2,160
log Kw	mol*kg-2	14,167	11	

The changes in properties have of course effect in the role of water in the chemical process. Water itself participates in reactions by hydrolysis and is sometimes found to be a hydrogen source. Due to the increase in ionic product water can also be seen as an acid/base catalyst. Thus reactions requiring acids require less acid or no acid at elevated temperatures when water is used as a reaction medium. When comparing wet torrefaction to dry, water also serves as a temperature buffer preventing local cold/hot spots. During pyrolysis temperatures within particles can be far higher[7] than the bed temperature and this can have negative effects on the products formed. In wet torrefaction this is prevented by the water surrounding each particle.

A lot of the mechanisms behind wet torrefaction are probably understood in a controlled environment with single components. But it is the combination of mechanisms and components together that makes it very hard to pinpoint exactly what governs a decomposition pathway. Verifying and explaining the complete decomposition pathway of glucose in water is already a very complicated tasks let alone a cocktail such as whole biomass.

2.3.Modelling of biomass decomposition

For this study on biomass decomposition a model was made on forehand to be able to determine an approximate optimum in residence time and temperature for a high LHV and a minimum of (initial) weight loss. Another reason is that it enables a better interpretation of the results obtained. Biomass decomposition is mostly modelled in two ways; using reaction kinetics and the severity factor[8] or severity parameter.[9]

Reaction kinetics

Reaction kinetics is used widely in chemistry and needs no introduction.
The use of reaction kinetics for modelling on forehand is based on the idea that quite a lot is known about the biomass being tested. The concentrations of the different lignocellulosic components and the extractives are used as input. With this a prediction can be made on how the biomass is going to decompose and what components are released.

Severity factor

The severity factor combines time and temperature into a single factor R_0 as can be seen in Equation 2-1. Weight loss and removal of different components are correlated to this R_0. From this correlation a model is made and this gives a quick insight to the decomposition behaviour. However no distinction is made, such as activation energy, to adjust a specific severity factor to a specific substance. Therefore no prediction can be made on possible valuable chemicals that can be extracted from the reaction mixture. And lumping time and temperature together "hides" the used reaction conditions so information for future use can be lost easily.

$$R_o = t * exp\left(\frac{T - 100}{14{,}75}\right) \qquad \text{Equation 2-1}$$

In all the use of the severity factor seems more appropriate as an engineering technique used for running a processing plant instead of explaining scientifically what is actually going on. Reaction kinetics give much more insight into the processes happening. Therefore modelling based on reaction kinetics was chosen for this work.

2.4.Components modelled

For the modelling only the lignocellulosic components are used. These components are the most common and abundant amongst biomass species and are therefore give results that are comparable. The extractives are assumed to be freed immediately from the grass once temperature in the reactor goes above 100C and therefore represent an immediate mass loss.
The ash is not modelled because the composition varies very much between species and ash is not as abundant as the other components. The ash composition is also affected by seasonal influences which can affect the results.

Cellulose

Cellulose is the most abundant of the components, up to 50% [4] in grasses. Cellulose is a homopolymer consisting of up to ten thousand D-glucose ($C_6H_{10}O_5$) monomer units and therefore sometimes regarded as the simplest of the three lignocellulosic components. However cellulose from different sources has different levels of polymerization and the configuration within actual biomass differ widely. This is illustrated by differences in behaviour in TGA measurements for different types of cellulose [11] shown in Figure 2-1 and Figure 2-2. The S-shaped curve (TG) represents the weight loss and the peak curve (DTG) represents the rate of weight loss. Cellulose from cotton does not

decompose completely and also shows a more spread out decomposition in comparison to the industrial derived cellulose. This makes the prediction of real biomass decomposition through modelling of cellulose as a model compound not as straightforward as one might think.

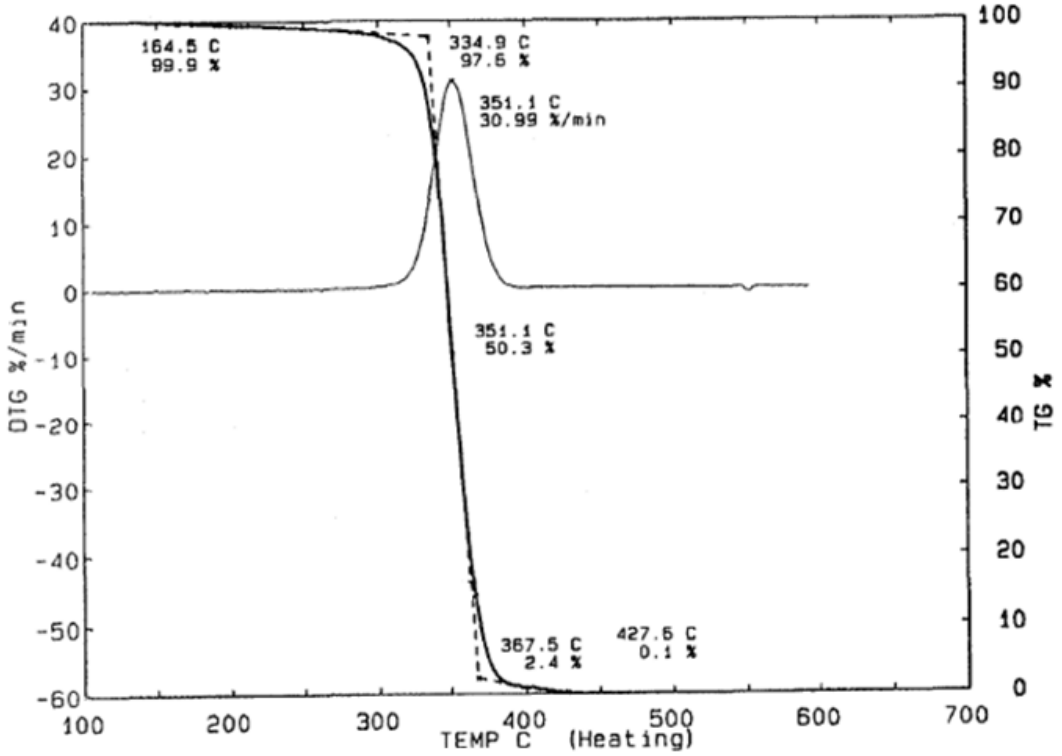

Figure 2-1: Cellulose (Baker analyzed) from Gaur [11]

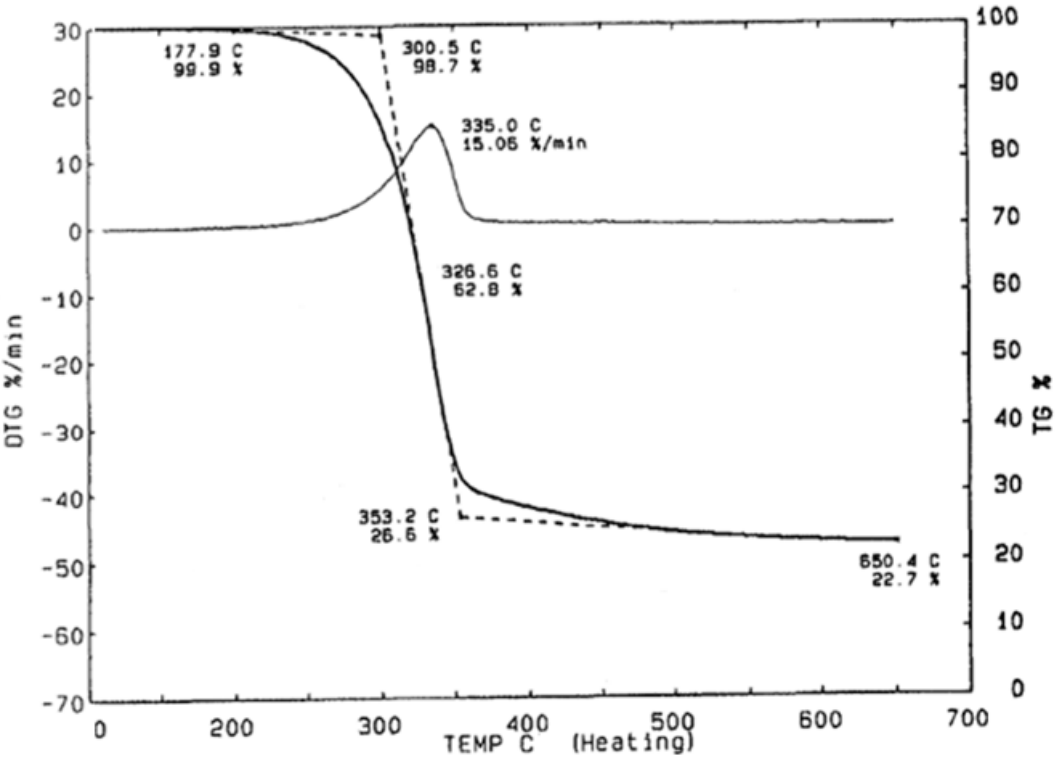

Figure 2-2: Cellulose (cotton) from Gaur [11]

Cellulose decomposition is mostly analysed by taking the model compound microcrystalline [12, 13, 14] cellulose, sometimes cotton [4] or filter paper [15] is being used. Other experiments focus on testing the decomposition products [14, 16] as well for a further understanding of the decomposition pathway.
Several reaction mechanisms have been suggested in literature.[13,14,16,42] In general these start from cellulose which degrades into oligosaccharides (cellobiose, cellotriose etc.), these degrade further into monosaccharides (glucose, fructose etc.) and these degrade furthermore leaving different pyrolysis (end) products (erythrose, 1,6 anhydroglucose etc) as can be seen in Figure 2-3. End products is more of an arbitrary term because usually the process is stopped due to the nature of the research instead of letting the reaction reach equilibrium.

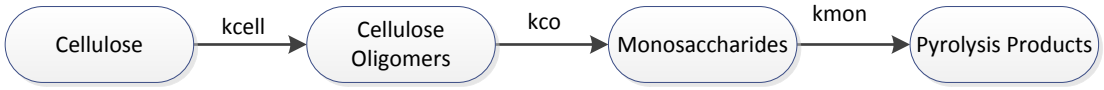

Figure 2-3: Commonly used reaction pathway

This work

The aforementioned scheme gives a good idea of what happens, although there are suggestions [13,18,19] that a competitive pathway exists into the pyrolysis products. Due to the these suggestion the model from Kamio [13] et.al. was chosen as a model for cellulose degradation.
In the work of Kamio pure cellulose was used in a 97 ml Hastelloy batch reactor. The heating rate used was approximately 10 K/min and maximum temperatures range from 170-280C with holding times up to 100 minutes. The solid concentration was 7%.

Table 2-3: Rate constants cellulose

	Activation energy Ea (kJ/mol)	frequency factor k0 (min-1)
kcell	141	7,3E+06
kco1	102	6,0E+07
kmon	130	1,0E+10
kco2	141	3,0E+11

The reaction pathway is depicted in Figure 2-4. This model doesn't only take the secondary pathway for the pyrolysis products into account but it also models macroscopic effects during the decomposition. Because cellulose has such a high level of polymerization the macroscopic effects are thought to be relevant even in modelling of biomass.

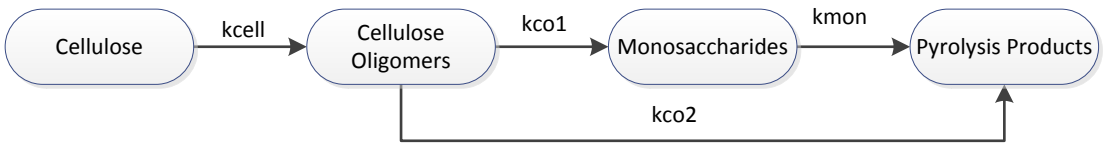

Figure 2-4: Reaction pathway of Kamio[13]

A cellulose particle is thought to be the dominant structure in biomass. It is assumed to have a spherical shape that decomposes at the surface by hydrolysis through water monomers. At the surface of the particle the concentration of water monomers is zero, thus this process is mass

transfer limited. The complete derivation of this is done in the work of Kamio [13]. The formulas used are explained here.

Decomposition of Cellulose

Cellulose is thought to undergo a hydrolysis reaction (1) by which the long cellulose polymer is split up into several smaller units such as cellobiose, cellotriose etc.:

$$\frac{dC_{cell}}{dt} = -k_{cell} * {C_{cell}}^{2/3} \qquad \text{Equation 2-2}$$

Where *cell* stands for cellulose.

In this formula *k1* is not the usual Arrhenius type equation therefore also C_{cell} has an exponent of 2/3. It is derived from the mass transfer limited particle model:

$$k_{cell} = \frac{3 * {C_{cel\_0}}^{1/3} * C_b}{75{,}7 * \rho * r_0 \left({}^{1}/_{k_c} * {}^{1}/_{k_s}\right)} \qquad \text{Equation 2-3}$$

Where *Ccel_o* is the concentration of cellulose at t=0, *b* is bulk, *ρ* is the molar density of a cellulose particle, r_0 is radius of cellulose particle, k_c is ass transfer coefficient of water monomer through the aqueous film surrounding the particle, k_s is the first order reaction constant.

The formed oligosaccharides have a reaction pathway (2) into the monomers glucose/fructose and directly into pyrolysis products:

$$\frac{dC_{oligo}}{dt} = k_{cell} * {C_{cell}}^{2/3} - k_{co1}C_{oligo} - k_{co2}C_{oligo} \qquad \text{Equation 2-4}$$

Where *oligo* is oligomer, *k2* and *k4* are normal Arrhenius type reaction equations.

The monomers are decomposed into pyrolysis products as well:

$$\frac{dC_{mono}}{dt} = k_{co1}C_{oligo} - k_{mon}C_{mono} \qquad \text{Equation 2-5}$$

Where *mono* is monosaccharides.

These degrade further (3) into the pyrolysis products erythrose, glyceraldehyde, glycoaldehyde, HMF etc:

$$\frac{dC_{pyro}}{dt} = k_{mon}C_{mono} + k_{co2}C_{oligo} \qquad \text{Equation 2-6}$$

Where *pyro* is pyrolysis products.

Hemicellulose

Hemicellulose is the second most abundant (16-38%) in grasses.[4] Hemicellulose is polymerized up to 200 units. In contrast to cellulose hemicellulose has a heterogeneous structure and consisting of mostly xylose but also mannose, galactose, rhamnose, arabinose and acetic acid and other minor components are present. Because of its heterogeneous structure and its small DP it is dissolved easily.

Because hemicellulose is made up of multiple components research on hemicellulose is mostly done on whole biomass[24,25]. This is justified by the fact that most research on hemicellulose is done at lower temperatures (<230C) at which cellulose and lignin are not affected. More detailed research is

focused on the monosaccharides[22,23] to further investigate the degradation pathway, analogous to cellulose.

Multiple researchers note a decomposition behaviour of hemicellulose which points to two types of hemicellulose: a fast decomposing fraction and a slower fraction. These are both decomposed into oligomers which in turn decompose into xylose. The research that focuses on the monosaccharides show that furfural is one of the main decomposition products. Besides furfural there is a whole range of reaction products being formed which are very low in concentration and are too many for this research to take into account.

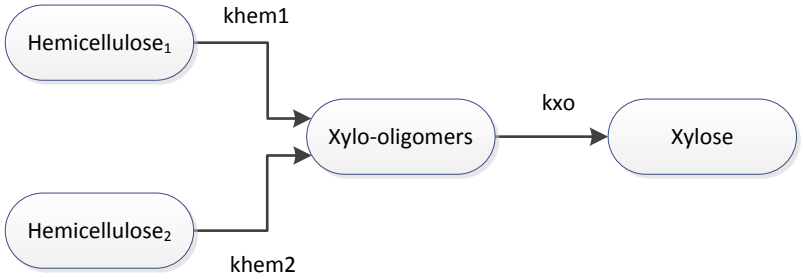

Figure 2-5: Commonly used reaction pathway hemicellulose

This work

One distinction from the models in literature [20,22,23,24,25] is the model from Naberlatz et.al seen in Figure 2-6. This model focuses on the complete decomposition pathway up to the pyrolysis products and it models arabinose and acetic acid as well. Because arabinose is the second most abundant sugar in hemicellulose[4] this monosaccharide can give important information on the decomposition pathway. Acetic acid is thought to play an important role in the autohydrolysis of biomass therefore this component is important as well.
In the work of Naberlatz corncob was used in a 25 ml stainless stell batch tubing-bomb reactor. The heating rate used was approximately 20 K/min and maximum temperatures range from 150-190C with holding times of 1,5-330 minutes. The solid concentration was 11%.

Table 2-4: Rate constants hemicellulose

	Activation energy Ea (kJ/mol)	frequency factor k0 (min-1)
khem1	127,3	4,9E+13
khem2	251,7	4,7E+26
kxo1	119	9,2E+11
kxo2	106,2	7,8E+10
kxo3	65,1	1,4E+06
kxyl	122,5	5,6E+12
kara	125,2	8,9E+12
kfur	132	1,3E+14

The model starts with two types of hemicellulose which decompose into oligomers. These oligomers decompose into the monosaccharides and acetic acid. The monosaccharides then decompose into furfural which is further decomposed into pyrolysis products. What these pyrolysis products are is

not elaborated in the work of Naberlatz. No further look was taken as furfural decomposition is regarded as very hard to predict under small changes in reaction conditions.

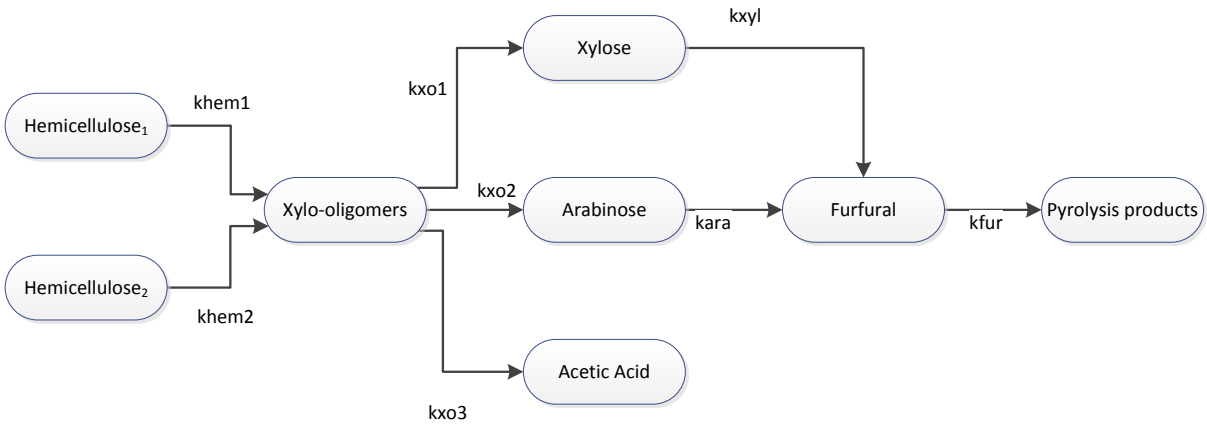

Figure 2-6: Reaction pathway of Naberlatz [43]

What is confusing in the work of Naberlatz is that hemicellulose is called xylan, although other components are modelled alongside of xylan. Therefore in this work hemicellulose is used because xylan could confuse readers into the idea that hemicellulose is made up purely out of xylose.

Previous studies on hydrothermal decomposition of acetic acid point out that no decomposition is expected on the time scale used for this research.
The research of McCollom and Seewald[26] is focused on the degradation of several organic acids in the presence of mineral assemblages (working as a catalyst). This is done using a gold bag in a stainless steel container. This stainless steel container is pressurized to prevent a gas phase in the gold bag. The experiments are done for example with pyrite-pyrrhotite-magnetite as the mineral assemblage. They report a loss of 9,4% after 527 hours and 43,8% after in 2545 hours at a temperature of 325C.
Another research is done by Palmer and Drummond[27] in vessels of different materials to investigate the catalytic activity of the vessel material. With temperatures ranging from 300-440C. They also have a time scale up to several hundred hours. In this research a gas phase is present.
Basagiannis and Verykios[28] furthermore report that for non-catalysed steam reforming in quartz tubes acetic acid degradation starts from approximately 400C in the absence of water and for 500C in the presence of water. Water is thus acting as an inhibitor of acetic acid decomposition.

At higher temperatures (>360C) D-xylose is found to decompose into glyceraldehyde and glycolaldehyde.[29] For lower temperatures (<220C) this is found not to be the case and the dominant reaction pathway leads to the formation of furfural.[30]

Decomposition of Hemicellulose

From observations amongst various types of biomass hemicellulose is modelled as two types, $hemicellulose_1$ which degrades (1) quickly and $hemicellulose_2$ which degrades (2) slower.
Hemicellulose is thought to consist of xylose, arabinose and acetic acid. There are more components, but these are the most abundant and thus measurable.
The mass of the different hemicelluloses is determined by the term *alpha*:

$$C_{hemi1} = C_{hemi} * alpha \qquad \text{Equation 2-7}$$

$$C_{hemi2} = C_{hemi} * (1 - alpha) \qquad \text{Equation 2-8}$$

Where *hemi* is the combined fraction of xylan, arabinan and acetyl groups, *hemi1* is hemicellulose type 1 and *hemi2* is hemicellulose type 2.
The different masses of these components are stated in mass percentage of the initial hemicellulose:

$$C_{xyl1} = X_{xyl1} * C_{hemi1} \quad \text{Equation 2-9}$$

$$C_{ara1} = X_{ara1} * C_{hemi1} \quad \text{Equation 2-10}$$

$$C_{ace1} = X_{ace1} * C_{hemi1} \quad \text{Equation 2-11}$$

$$C_{xyl2} = X_{xyl2} * C_{hemi2} \quad \text{Equation 2-12}$$

$$C_{ara2} = X_{ara2} * C_{hemi2} \quad \text{Equation 2-13}$$

$$C_{ace2} = X_{ace2} * C_{hemi2} \quad \text{Equation 2-14}$$

Where *xyl* is xylose, *ara* is arabinose, *ace* is acetic acid, *hemi* is hemicellulose and the number states the type of hemicellulose.

The fraction alpha and the composition of the two types of hemicellulose are determined by Naberlatz by using a Newton type minimization algorithm. In this work this values is used as well.
This gives the following mass balance for hemicellulose$_1$:

$$\frac{dC_{xyl1}}{dt} = -k_{hem1} * C_{xyl1} \quad \text{Equation 2-15}$$

$$\frac{dC_{ara1}}{dt} = -k_{hem1} * C_{ara1} \quad \text{Equation 2-16}$$

$$\frac{dC_{ace1}}{dt} = -k_{hem1} * C_{ace1} \quad \text{Equation 2-17}$$

And for hemicellulose$_2$:

$$\frac{dC_{xyl2}}{dt} = -k_{hem2} * C_{xyl1} \quad \text{Equation 2-18}$$

$$\frac{dC_{ara2}}{dt} = -k_{hem2} * C_{ara2} \quad \text{Equation 2-19}$$

$$\frac{dC_{ace2}}{dt} = -k_{hem2} * C_{ace2} \quad \text{Equation 2-20}$$

Where *k* is the reaction rate following the Arrhenius relationship:

$$k_i = k_{i0} * exp\left(\frac{-E_{ai}}{R * T(t)}\right) \quad \text{Equation 2-21}$$

Both types of hemicellulose degrade into the same oligomers. The oligomers stay separated in their components for ease of modelling:

$$\frac{dC_{o\_xyl}}{dt} = k_{hem1} * C_{xyl1} + k_{hem2} * C_{xyl2} - k_{xo1} * C_{o\_xyl} \quad \text{Equation 2-22}$$

$$\frac{dC_{o\_ara}}{dt} = k_{hem1} * C_{ara1} + k_{hem2} * C_{ara2} - k_{xo2} * C_{o\_ara} \quad \text{Equation 2-23}$$

$$\frac{dC_{o\_ace}}{dt} = k_{hem1} * C_{ace1} + k_{hem2} * C_{ace2} - k_{xo3} * C_{o\_ace}$$ Equation 2-24

Where *o* is oligomer.

These oligomers are further decomposed into the respective mono-components acetic acid, xylose and arabinose:

$$\frac{dC_{xyl}}{dt} = k_{xo1} * C_{o\_xyl} - k_{xyl} * C_{xyl}$$ Equation 2-25

$$\frac{dC_{ara}}{dt} = k_{xo2} * C_{o\_ara} - k_{ara} * C_{ara}$$ Equation 2-26

$$\frac{dC_{ace}}{dt} = k_{xo3} * C_{o\_ace}$$ Equation 2-27

Xylose and arabinose, being C5 sugars, both decompose into furfural:

$$\frac{dC_{fur}}{dt} = k_{xyl} * C_{xyl} + k_{ara} * C_{ara} - k_{fur} * C_{fur}$$ Equation 2-28

Where *fur* is furfural.

Which in turn is being decomposed (8) into certain degradation products:

$$\frac{dC_{degr}}{dt} = k_{fur} * C_{fur}$$ Equation 2-29

Where *degr* stands for degradation products.

Lignin

Lignin is the third most abundant component in grasses.[4] It is a heteropolymer consisting mostly of *p*-coumaryl alcohol, coniferyl alcohol, and sinapyl alcohol.[31] These are branched up to 10,000 units in a heterogeneous way, again the DP and configuration differ widely amongst biomass species. Lignin is bonded to hemicellulose causing some of the units to dissolve as easily as hemicellulose.

Several forms of lignin are available for usage as a model compound to test the decomposition. A few of them are mentioned here.
Large scale lignin (and hemicellulose) removal is done in the paper pulping industry for the production of cellulose. The most widely (>75%)[31] used Kraft process uses the sodium ion of sodium sulphate to break the intramolecular bonds in the lignin. After that there is a residue of sulphated phenolic components. The lignin produced this way has sulphates which alters the characteristics from normal lignin in biomass. Therefore no experiments were found using this type of lignin.

Lignin produced in an Organosolv process has the disadvantage that it has been repolymerized causing a stronger bond than the previous bond to the original biomass. This repolymerized lignin is

harder to dissolve in a hydrothermal treatment leading to a big error in using it as a model compound.

Another reason not to model lignin decomposition is that the temperatures and method of testing has a big influence. At moderate temperatures in a batch reactor lignin from biomass has been found to repolymerize on the original biomass. An example of this can be seen in the Figure 2-7 below taken from Mittal. Here very erratic behaviour can be seen in the percentage of lignin left at different holding times and temperature.
For these reasons no lignin decomposition is being modelled.

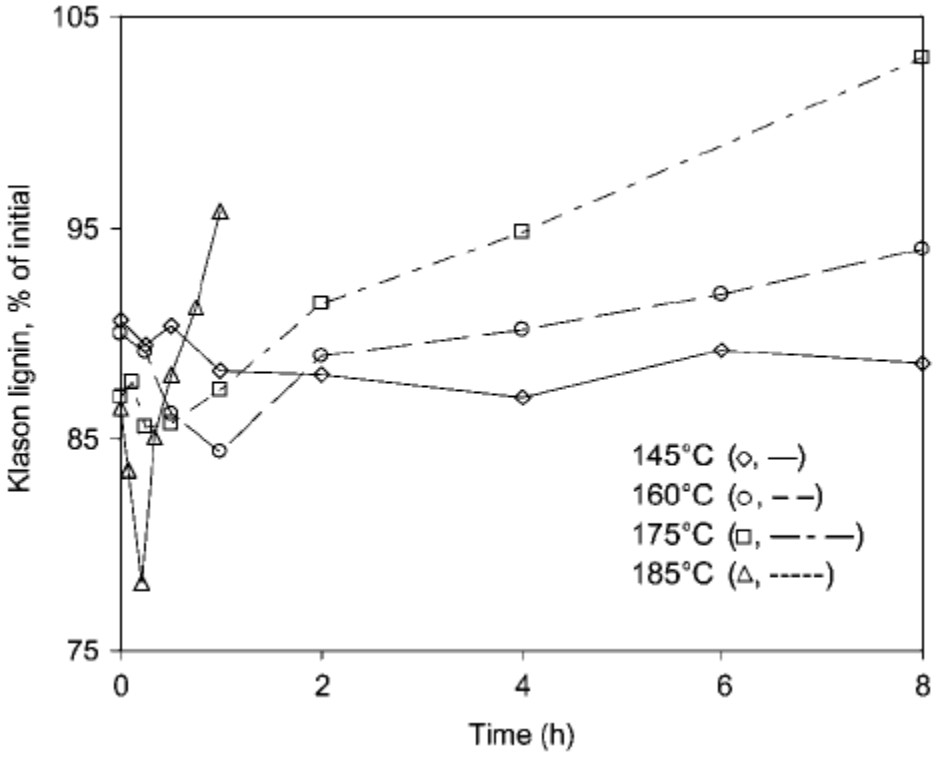

Figure 2-7: Percentage of Klason lignin after treatment

A logical step after testing the decomposition of model components is adding these up to predict the combined behaviour or even real biomass. Little is known on adding up of biomass model components. Most research is focused on single components regarded as waste streams of other processes (lignin from the pulping industry) or on pure components derived from traditional processes (cellulose from the pulping industry). The recent focus on biomass as a source of valuable chemicals and as an energy source has fuelled more research into the mechanisms behind biomass decomposition. Beginning at model components is the easiest way and from this the addition of model components is starting to gain attention.
Research done by Yoshida and Matsumura [32] uses cellulose, xylan and lignin as separate components in supercritical water gasification. The gaseous products (H_2, CO_2, CH_4) formed by these single components were used to predict the gaseous output when 2 of these products were combined. Between cellulose and xylan a linear correlation was found. Lignin combined with either cellulose or xylan displayed non-linear behaviour in the product gas. Therefore lignin can be regarded as disturbing a predictive model based on model components.

In a (dry) torrefaction research done by Nocquet et.al. [33] cellulose, xylan and lignin were again used as model components first and a combination in a next step. Here xylan and lignin display linear behaviour and is cellulose the disturbing component.
Due to the contradictory results from these two studies and a lack of more information the model components are simply added up in this work.

2.6.Model input

The model taken from Kamio uses cellulose as the input. The model from Naberlatz uses xylose, arabinose and acetic acid as the input for hemicellulose. Therefore the initial composition of major components as stated in Table 2-1 cannot be used. Rhamnose, mannose and galactose that are usually attributed to hemicellulose are therefore here regarded as extractives. The expectation is that hemicellulose is going to dissolve completely after wet torrefaction therefore treating them as extractives can be justified. As mentioned before the extractives are thought to boil off immediately. Lignin is thought not to decompose significantly and therefore stays in the residual solid mass. Therefore Table 2-1is adjusted for this and the used components are stated in Table 2-5.

Table 2-5: Grass components adjusted for modelling

Verge grass		Adjusted composition	
glucose	32,9	cellulose	32,9
arabinose	2,9	hemicellulose	22,5
xylose	19,6		
klason lignin	24,1	lignin	25,8
acid sol lignin	1,7		
rhamnose	0,3	extractives	17,9
mannose	0,3		
galactose	0,8		
extractives EtOH/toluene	3,2		
extractives 95% EtOH	1,4		
extractives hot water	6		
pectin	5,9		
total	99,1	total	99,1

The fuel properties of verge grass are given in Table 2-6. This data is taken from another research from the same database. [1] Due to differences in the determination methods the ash content of the verge grass is not exactly accounted for in the biochemical composition. However the ash content is not modelled therefore analyses of dried grass and wet torrefied grass can point to what happened with these ashes.

Table 2-6: Fuel properties of grass

Proximate Analysis	ar	dry	daf
Moisture content	60		
Ash	3,36	8,4	
Ultimate Analysis			
Carbon	17,84	44,61	48,7
Hydrogen	2,34	5,86	6,4
Nitrogen	0,7	1,74	1,9
Sulphur	0,05	0,13	0,14
Oxygen	15,56	38,9	42,47
Total	100	100	100
Calorific Values			
LHV	5,42	17,22	18,8
HHV	7,4	18,5	20,2

To be able to determine the areas of interest for the production of coal from grass the mass loss and the HHV were calculated. The Matlab code by which this was done can be found in the attachments. Results of these calculations are shown in Figure 2-8. For the determination of the HHV data was taken from.[34]

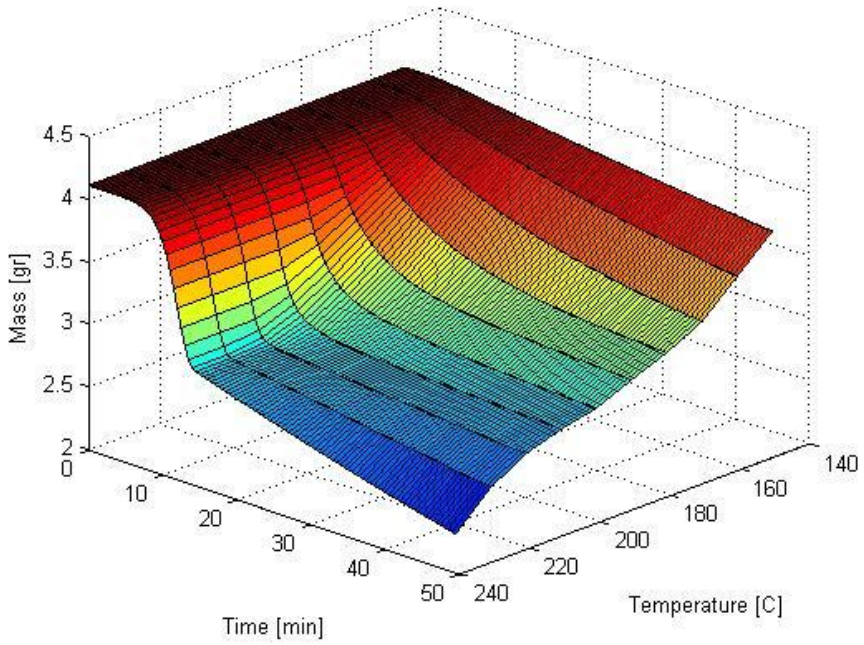

Figure 2-8: Mass loss

An area of interest is at 180-220C due to the plateau formed, as can be seen in Figure 2-8. This is caused by complete hemicellulose decomposition. This plateau forms an operating window if complete hemicellulose is required.

At higher temperatures cellulose degradation can be seen to take place and therefore higher temperatures >220C are interesting as well. Tests at these temperatures show verify the decomposition of cellulose.
By testing at these two areas the decomposition mechanisms can be verified and used for determining the appropriate reaction conditions for maximizing the energy yield of WTG.

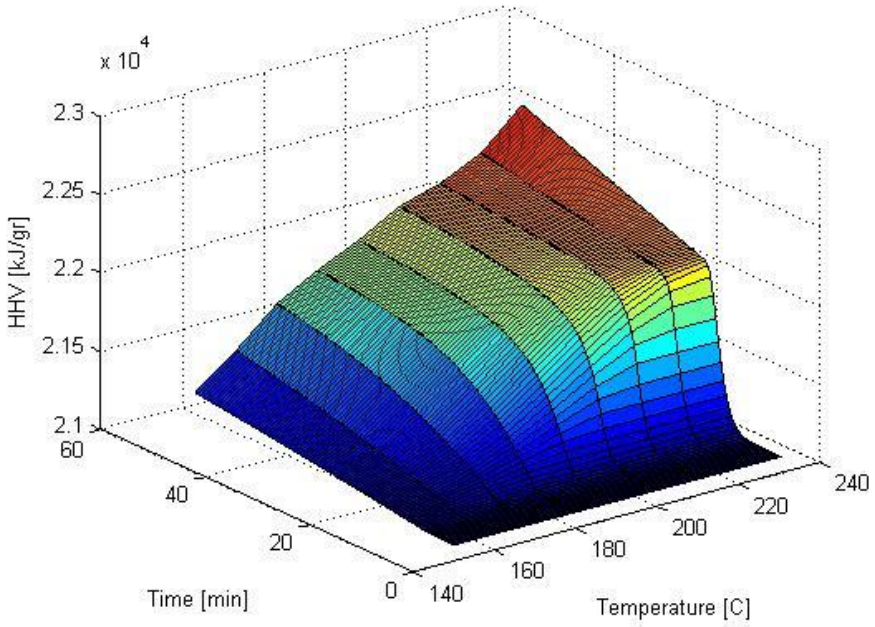

Figure 2-9: HHV of torrefied verge grass

2.7.Model Validation

The model is validated against data taken from Mittal et.al. [24] In the research from Mittal sugar maple wood meal (SMWM) is used, this is a very fine grind of sugar maple wood. The composition for this is taken from Mittal and can be seen in Table 2-7. The composition stated in the paper is on the left. The composition used as the input for the model is seen at the right. Some adjustments had to be made to use this to make a proper comparison. HMF is a decomposition product from glucose and furfural from xylose. Therefore these are added to their respective major component. Rhamnose, mannose and galactose are commonly assumed to come from hemicellulose however both Mittal and Naberlatz do not model them. For Naberlatz these sugars are not mentioned and Mittal doesn't show any results obtained other than from the composition at one specific condition. Due to their low concentrations they are regarded as extractives.

Table 2-7: SMWM components adjusted for modelling

Sugar maple wood meal		**Adjusted composition**	
glucose	45,5	cellulose	46
hmf	0,5		
xylose	15,1	hemicellulose	20,1
arabinose	0,6		
acetate	3,8		
furfural	0,6		
klason lignin	22,3	lignin	26,1
acid sol lignin	3,8		
rhamnose	0,8	extractives	8,5
mannose	2,4		
galactose	2,1		
extractives	3,2		
total	100,7	total	100,7

From the adjusted composition the fractions of arabinose, xylose and acetate are used in the model. In contrast to Naberlatz Mittal uses an alpha that varies according to temperature to distinguish between fractions of fast and slow hydrolysing hemicellulose. The alpha value from Mittal was also used as in input.
The measurements of Mittal are conducted with stainless steel reaction bombs in an oil bath. From this only data was used from the isothermal reaction condition therefore the measurement is regarded isentropic; the moment the reaction temperature is reached is regarded as the starting point.

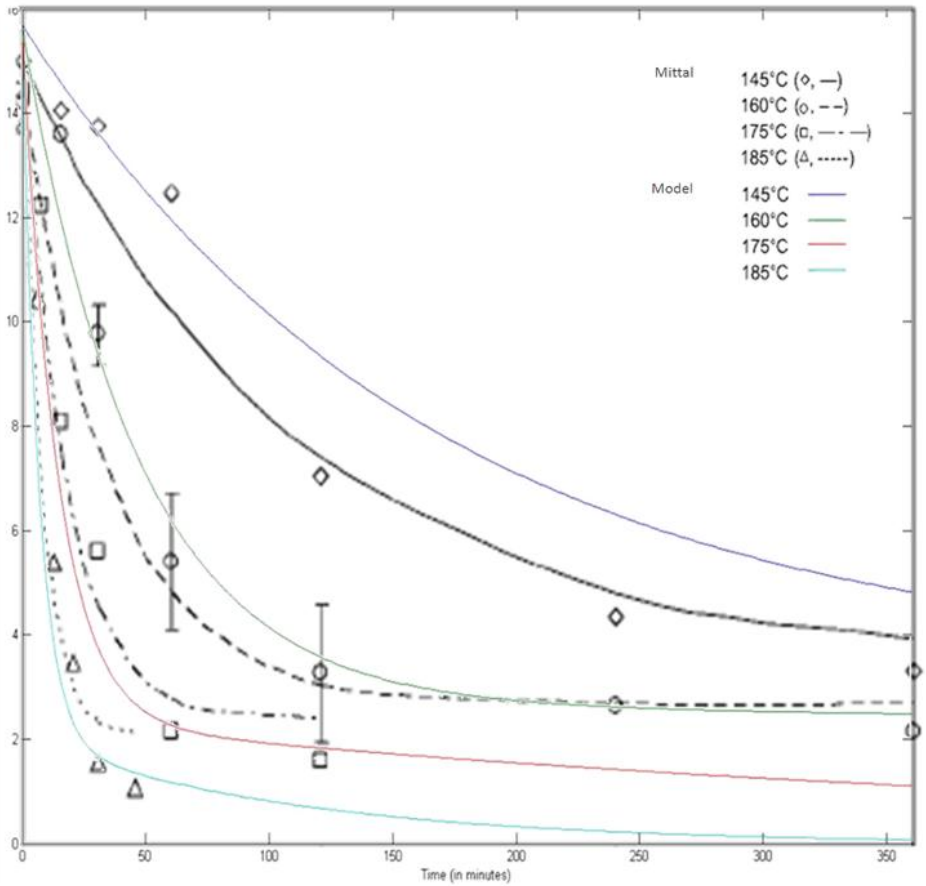

Figure 2-10: Percentage of xylan remaining in solid

As can be seen from the Figure 2-10 the xylan remaining in the fixed mass show a good prediction of the results obtained by Mittal. The overall trend prediction is good and the individual results show a good comparison.
For 145C the model offers a good prediction for the short time scale and underpredicts the degradation at longer holding times. The starting concentration seems to deviate a little as well. This might be due to the fact that the exact reaction temperature was not reached yet and that the assumption of isothermal behaviour is wrong.
For 160C the model predicts within the error margin of the measurements of Mittal.
For the higher temperatures the model predicts good overall. For longer holding times there are no measurements provided by Mittal therefore this can be an area of uncertainty. For the higher temperatures envisaged in this study this is a pity because under ideal circumstances longer holding times can substitute for higher temperatures from time to time.

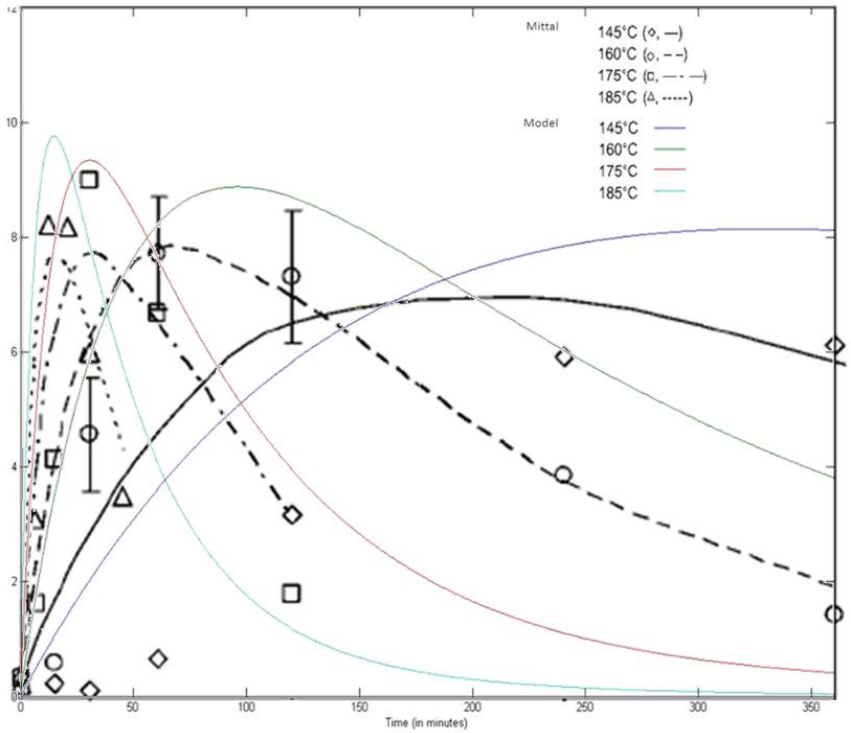

Figure 2-11: Percentage of xylooligomers in solution

The prediction of xylooligomers (XO) in Figure 2-11 seems to overestimate the total XO in solution but give an overall picture of what is happening.

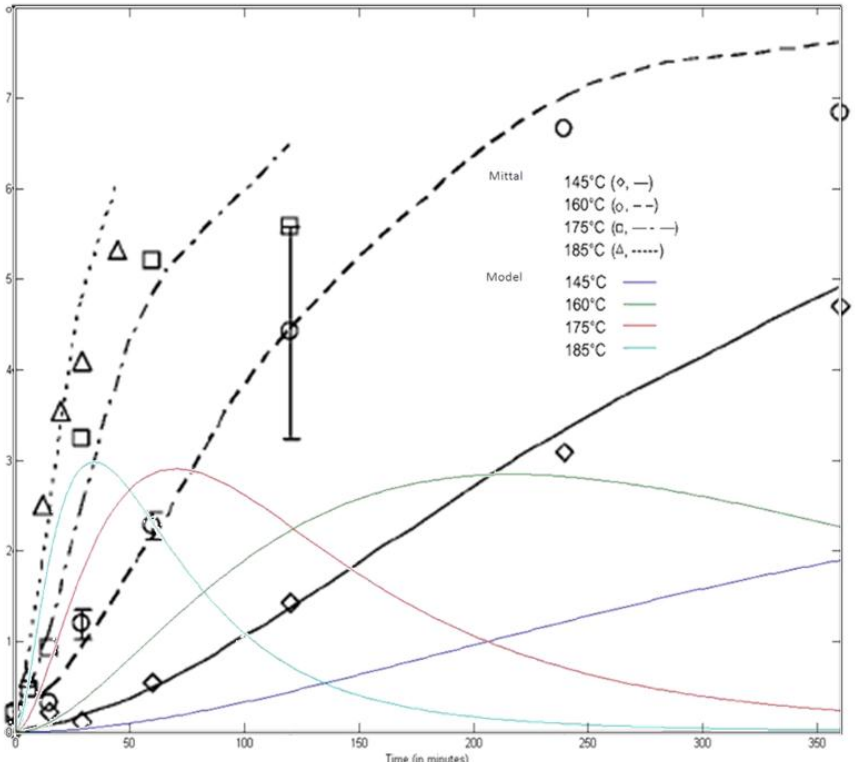

Figure 2-12: Percentage of xylose in solution

The model prediction for xylose in solution in Figure 2-12 deviates a lot from the measured results. This can partly be explained by the fact that the XO is over predicted resulting in a “slower” xylose coming into solution. On the other hand an overestimation of xylose decomposition causes a low maximum of xylose in solution. These deviations can be caused by the differences in the material and specifically differences in the acids liberated from the biomass. Perhaps a high chlorine content of corn cob in relation to the SMWM used by Mittal explains this difference. Chlorine can sometimes act as a catalyst in wet torrefaction.

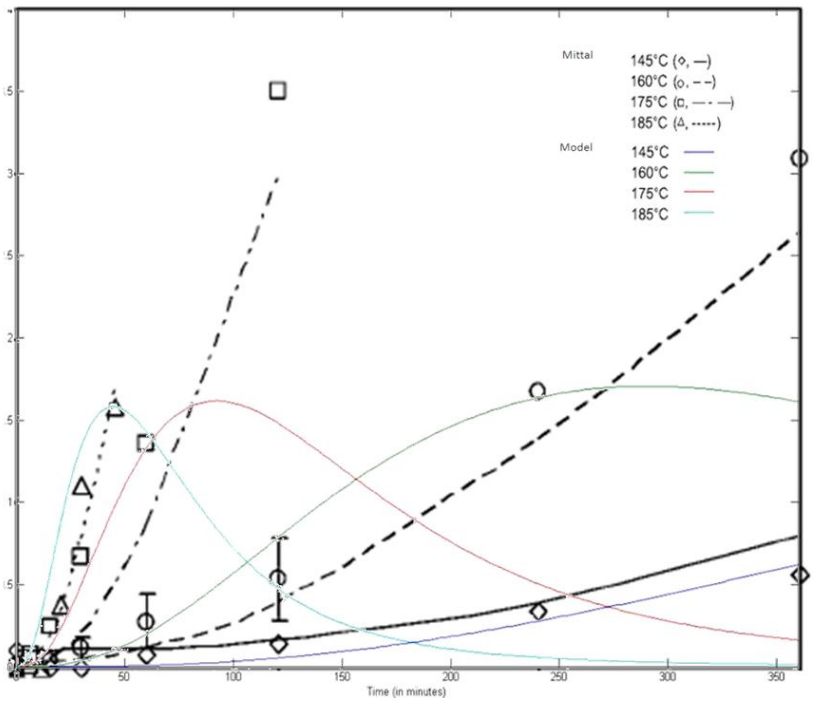

Figure 2-13: : Percentage of furfural in solution

The beginning of furfural formation is predicted reasonably well in Figure 2-13 however the decomposition is overestimated by the model. It starts to early for 160C and 175C, for 185C and 145C not enough data is supplied. Perhaps a different approach to the modelling of the single components can be done to make this prediction more accurate.

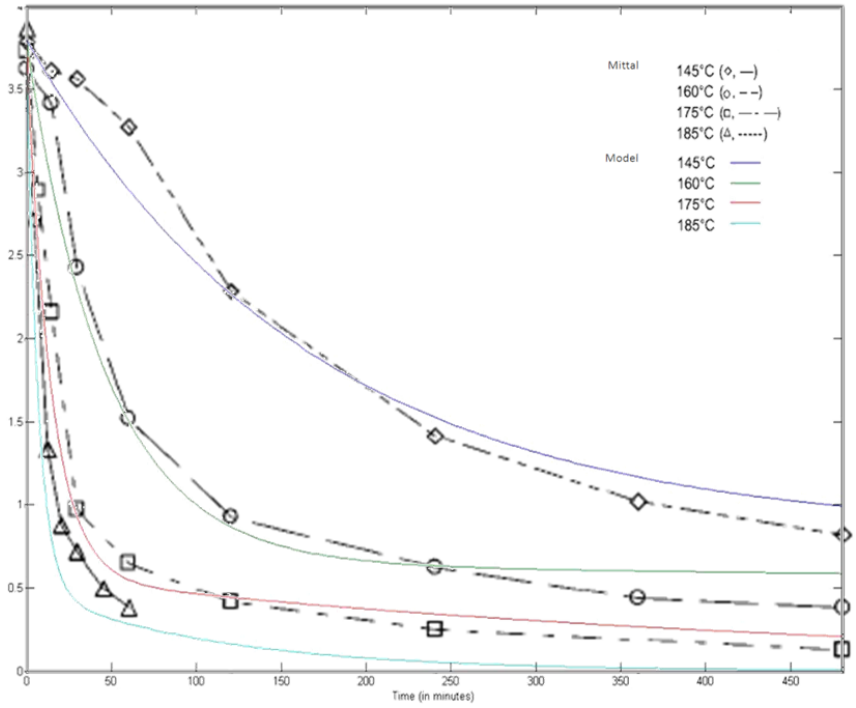

Figure 2-14: Percentage of acetyl in solid

The acetyl groups remaining in the wood in Figure 2-14 is predicted well overall. What can be seen from the measured results however is that isothermal behaviour is questionable. Again an S-shaped curse is seen from the figure.

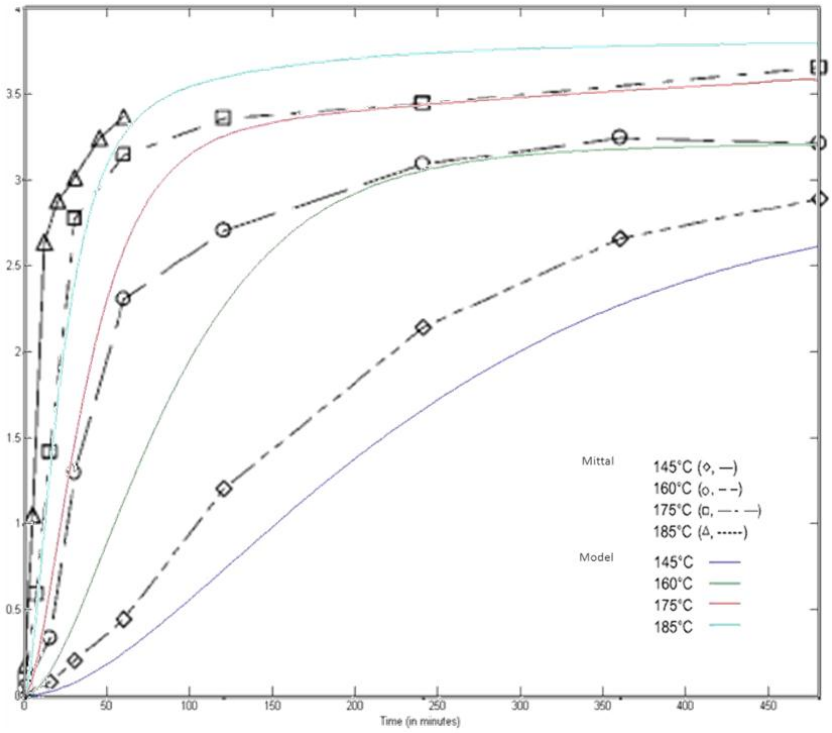

Figure 2-15: Percentage of acetyl in solution

Generally the same trends are visible for the acetyl groups in solution in Figure 2-15, however the model shows some lag in the release and "catches" up at longer holding times.

2.8.Conclusions

From the validation a couple of conclusions can be drawn:

- A very good approximation of mass loss is predicted.
- General acetyl behavior is predicted well.
- Behavior of single components are under predicted at longer holding times.

2.9.References

Intro biomass

1. *Energy research Centre of the Netherlands (*ECN), *Phyllis2 database for biomass and waste*, http://www.ecn.nl/phyllis2/, accessed: 8-5-2012
2. M.S. Tunc, A.R.P. van Heiningen, Hemicellulose extraction of mixed southern hardwood with water at 150C: Effect of time, Ind. Eng. Chem. Res. 47, 2008, pp 7031-7037
3. W.S Mok, M.J. Antal, Uncatalyzed solvolysis of whole biomass hemicellulose by hot compressed liquid water, Ind. Eng. Chem. Res. 31, 1992, pp 1157-1161
4. W. Schwald, O. Bobleter, Hydrothermolysis of cellulose under static and dynamic conditions at high temperatures, J. Carbohydrate Chem. 8, 1989, pp 565-578
5. O. Bobleter, R. Concin, Degradation of poplar lignin by hydrothermal treatment, Cell. Chem. Technol. 13, 1979, pp 583-593

Water (at these high temperatures)

6. N. Akiya, P.E. Savage, Roles of water for chemical reactions in high-temperature water, Chem. Rev. 102, 2002, pp 2725-2750
7. P. Basu, Burning rate of carbon in fluidized beds, Fuel 56, 1977, pp 390-392

Modeling of biomass decomposition

8. B. Yang, C.E. Wyman, Effect of xylan and lignin removal by batch and flowthrough pretreatment on the enzymatic digestibility of corn stover cellulose, Biotech. And Bioeng. 86, 2004, pp 88-95
9. G. Garrote, H. Dominguez, J.C. Parajo, Hydrothermal processing of lignocellulosic materials, Holz als Roh- und Werkstoff 57, 1999, pp 191-202

Cellulose

10. *Energy research Centre of the Netherlands (*ECN), *Phyllis2 database for biomass and waste*, http://www.ecn.nl/phyllis2/, accessed: 8-5-2012
11. S. Gaur, T.B. Reed, An atlas of thermal data for biomass and other fuels, NREL, 1995
12. M. Sasaki, B. Kabyemela, R. Maluluan, S. Hirose, N. Takeda, T. Adschiri, K. Arai, Cellulose hydrolysis in subcritical and supercritical water, J. of Supercrit. Fluids 13, 1998, pp 261-268
13. E. Kamio, S. Takahashi, H. Noda, C. Fukuhara, T. Okamura, Liquefaction of cellulose in hot compressed water under variable temperatures, Ind. Eng. Chem. Res. 45, 2006, pp 4944-4953
14. T. Minowa, Z. Fang, T. Ogi, G. Varhegyi, Decomposition of Cellulose and Glucose in hot-compressed water under catalyst-free conditions, J. Chem. Eng. Japan 31, 1998, pp 131-134
15. K. Mochidzuki, A. Sakoda, M Suzuki, Measurement of the hydrothermal reaction rate of cellulose using novel liquid-phase thermogravimetry, Thermochimica Acta 348, 2000, pp 69-76
16. B.M. Kabyemela, T. Adschiri, R.M. Maluluan, K. Arai, Kinetics of glucose epimerization and decomposition in subcritical and supercritical water, Ind. Eng. Chem. Res. 36, 1997, pp 1552-1558
17. M. Sevilla, A.B. Fuertes, The production of carbon materials by hydrothermal carbonization of cellulose, Carbon 47, 2009, pp 2281-2289
18. W.S. Mok, M.J. Antal Jr., Productive and parasitic pathway in dilute acid-catalyzed hydrolysis of cellulose, Ind. Eng. Chem. Res. 31, 1992, pp 94-100

19. T. Minowa, F. Zhen, T. Ogi, Liquefaction of cellulose in hot compressed water using sodium carbonate: Products distribution at different reaction temperatures, J. Chem. Eng. Japan 30, 1997, pp 186-190

Hemicellulose

20. D. Naberlatz, X. Farriol, D. Montané, Kinetic modelling of the autohydrolysis of lignocellulosic biomass for the production of hemicellulose-derived oligosaccharides, Ind. Eng. Chem. Res. 43, 2004, pp 4124-4131
21. K. Mochidzuki, A. Sakoda, M. Suzuki, Liquid-phase thermogravimetric measurement of reaction kinetics of the conversion of biomass wastes in pressurized hot water: a kinetic study, Adv. Ind. Science 7, 2003, pp 421-428
22. T.M. Aida, N. Shiraishi, M. Kubo, M. Watanabe, R.L. Smith jr., Reaction kinetics of D-xylose in sub- and supercritical water, J. of Supercrit. Fluids 55, 2010, pp 208-216
23. Z. Srokol, A.G. Bouche, A. van Estrik, R.C.J. Strik, T. Maschmeyer, J.A. Peters, Hydrothermal upgrading of biomass to biofuel; studie on some monosaccharide compounds, Carbohydrate Res. 339, 2004, pp 1717-1726
24. A. Mittal, S.G. Chatterjee, G.M. Scott, T.E. Amidon, Modeling xylan solubilization during autohydrolysis of sugar maple wood meal: Reaction kinetics, Holzforschung 63, 2009, pp 307-314
25. C.Pronyk, G. Mazza, Kinetic modelling of hemicellulose hydrolysis from triticale straw in a pressurized low polarity water flow-through reactor, Ind. Eng. Chem. Res. 49, 2010, pp 6367-6375

Acetic acid

26. T. M. McCollom, J. S. Seewald, Experimental study of the hydrothermal reactivity of organic acids and acid anions: II. Acetic acid, acetate, and valeric acid, Geochimica et Cosmochimica Acta 67, 2003, pp 3645–3664
27. D.A. Palmer, S.E. Drummond, Thermal decarboxylation of acetate. Part I. The kinetics and mechanism of reaction in aqeous solution, Geochimica et Cosmochimica Acta 50, 1986, pp 813-823
28. A.C. Basagiannis, X.E. Verykios, Reforming reactions of acetic acid on nickel catalysts over a wide temperature range, Applied Catalysis A: General 308, 2006, pp 182–193

D-xylose

29. M. Sasaki, T. Hayakawa, K. Arai, T. Adschiri, Measurement of the rate of retro-aldol condensation of D-xylose in subcritical and supercritical water, in: Hydrothermal reactions and techniques; S.H. Feng, J.S. Chen, Z. Shi, Worlds Scientific Publishing Co, 2003, pp 169-176
30. J.Qi L. Xiuyang, Kinetics of non-catalyzed decomposition of D-xylose in high temperature liquid water, Chin. J. Chem. Eng. 15, 2007, pp 666-669

Lignin

31. V.M. Roberts, Homogeneous and heterogeneous catalyzed hydrolysis of lignin, Phd thesis, TU Munchen, 2008

Adding up model compounds

32. T. Yoshida, Y. Matsumura, Gasification of cellulose, xylan and lignin mixtures in supercritical water, Ind. Eng. Chem. Res. 40, 2001 pp 5469-5474

33. T. Nocquet, C. Dupont, J.M. Commandre, M. Grateau, S. Thiery, M.H. Nguyen, S. Salvador, Mass loss and gas release during torrefaction of biomass and its constituents, European Biomass Conference and Exhibition, Milan, June 2012

Model input

34. A. Demirbas, Biodiesel: a realistic fuel alternative for diesel engines, Springer, 2008, pp23

3. Experiments

The materials and reactor setup that were used are introduced together with the test procedure. Followed by a short introduction of the different analytical methods that were applied.

3.1.Aim

The aim of the experiments is to verify the reaction mode. Two areas of interest were determined in paragraph 2.6; 180-220C and 260-300C.
Ideally the tests are done while maintaining a complete mass balance and thus measuring where all the solid, liquid and gaseous products go. In practice this is impossible with this setup. The gaseous products for example cannot be monitored. The components that can be monitored is the liquid fraction during the test and the solid fraction after the test. Of the liquid fraction the sugars and acetic acid in the solution are measured and the solid mass left in the solution will be measured as well. The sugars enable verification of the reaction mechanisms and the solid mass the serves as an overall measure of accuracy.
What has to be noted is that although two temperature ranges were of interest only 1 is tested. The reactor is rated for use up to 250C limiting the test to only the first temperature range.

3.2.Materials

The experiments were done using verge grass (180-200-220C), bagasse (180C) and xylan (180C). Bagasse and xylan were tested to make this work more comparable to other research on biomass.

The verge grass was freshly cut next to the P&E building at the TU Delft campus. Drying was done using a pre-heated Hereaus T-5050 oven at 50C for 24 hours. Before and after drying the grass was weighed carefully to determine the moisture content. Two batches of grass were dried of which the weighted average moisture content was 70%. Directly after weighing the sample was ground using a generic coffee grinder. The sample was ground until it was optically fine enough and thereafter is was sieved using a laboratory grade sieve with a mesh size of 250micrometer. The sieving was done to guarantee an even sample size to exclude heat transfer effects in the degradation of the grass. It was also done to prevent blockage in the reactor and for further processing of samples taken during reaction time. All grass samples (dried, ground and sieved etc) was stored in airtight plastic bags immediately after processing to prevent moisture uptake from the air.

Figure 3-1: Sieving

The xylan is derived from beechwood and was supplied by Sigma-Aldrich. It has a purity of at least 90% consisting of xylose and arabinose. The xylan was sieved before usage. The bagasse was provided from an undisclosed source in the form of pellets. The pellets were ground in the coffee grinder and then sieved like the grass. For each reaction demi-water was used as process water.

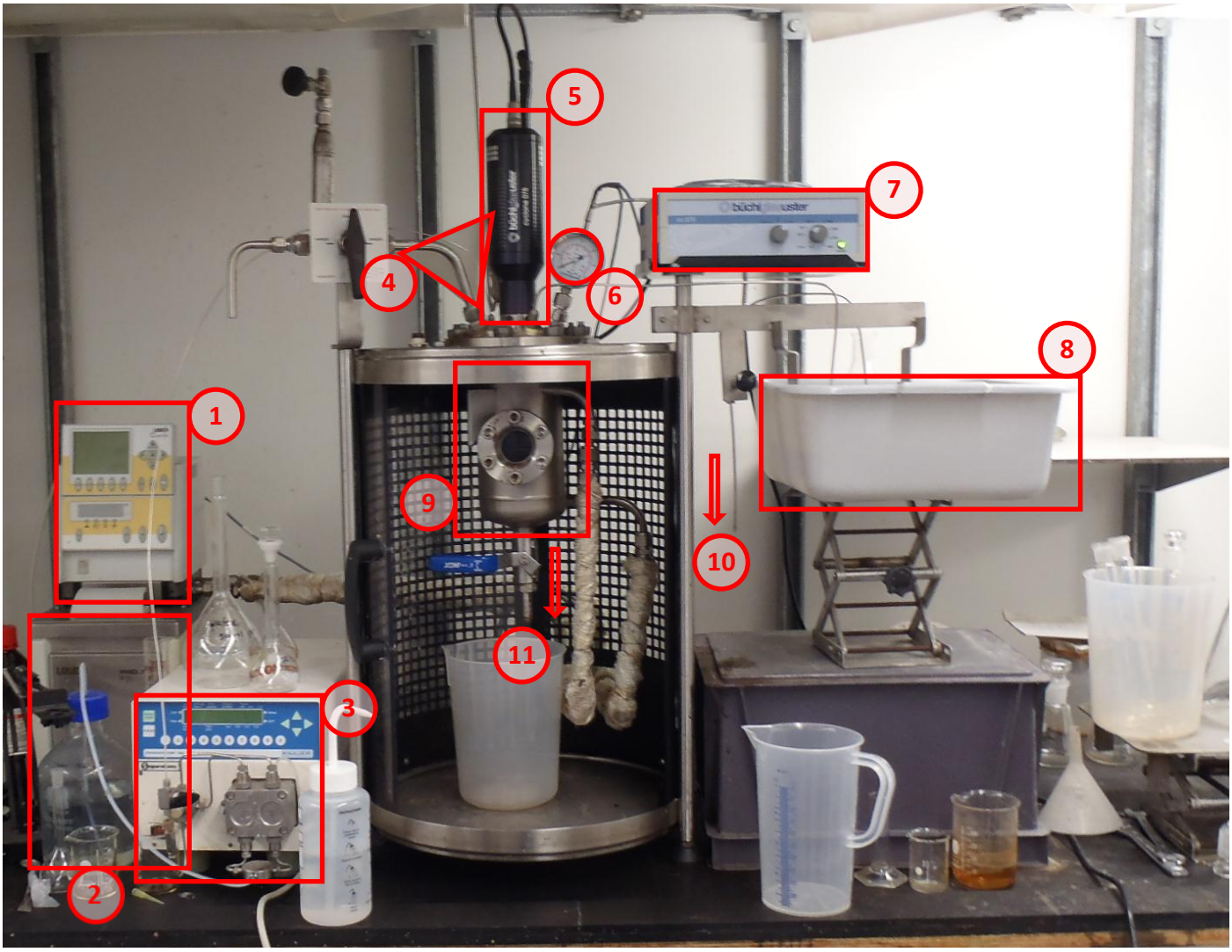

Figure 3-2: Test setup

1.	**Temperature controller oil bath**	**Lauda C Command**
1.	**Oil bath**	**Lauda Proline P5**
2.	**Pump**	**Knauer P1800**
3.	**Funnel for biomass insertion**	
4.	**Stirrer**	**Buchi Cyclone 075**
5.	**Manometer**	**generic Buchi provided**
6.	**Stirrer controller**	**Buchi CC 075**
7.	**Ice bath**	
8.	**Reactor**	**Buchi 1l metal Ecoclave with sightglass**
9.	**Primary outlet**	
10.	**Secondary outlet**	

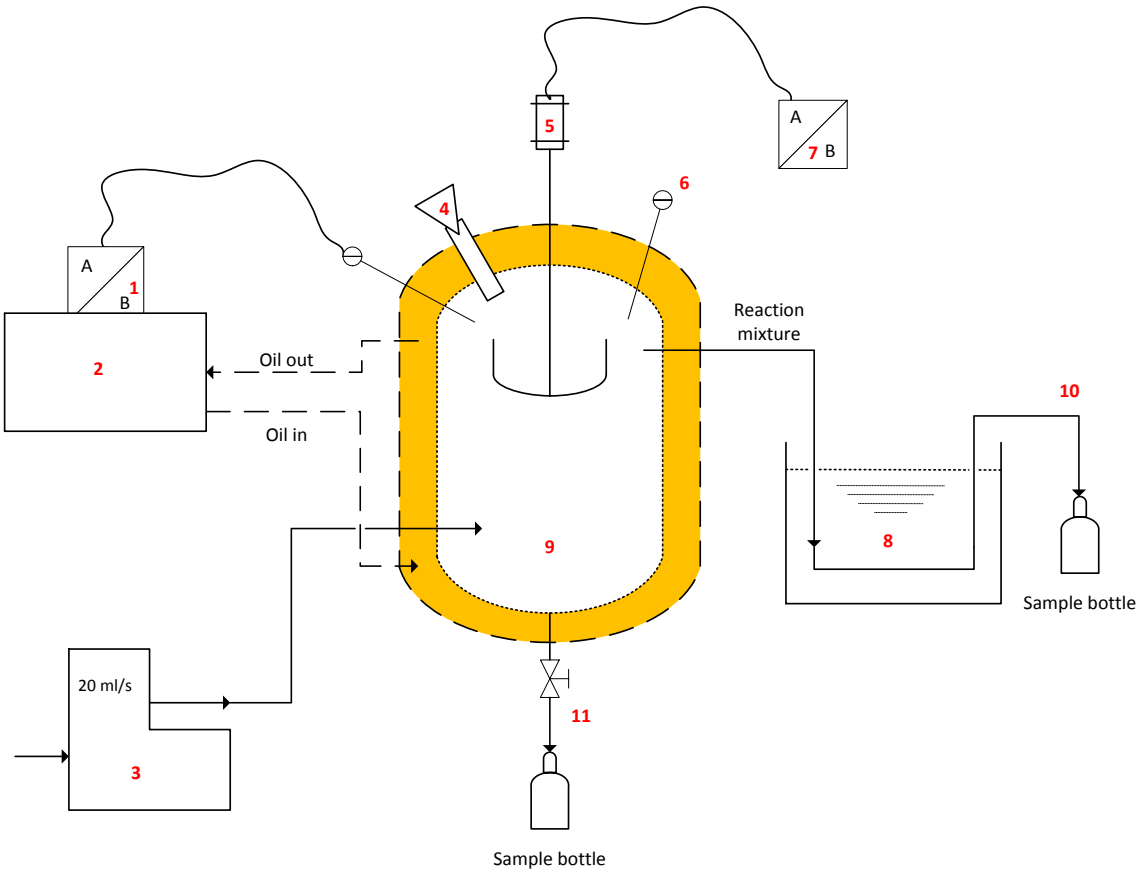

Figure 3-3: Graphic of test setup

3.3.Test procedure

The experiments were carried out using a 1l Buchi reactor as can be seen in Figure 3-2. A schematic representation can be seen in Figure 3-3. The reactor has a double wall through which the heating oil is pumped thereby heating the reactor.

- For each test 5 gram of biomass was used and 850 ml water. Although the reactor volume is 1 litre no more water was used because of expansion of the water.
- The reactor was heated to 90C together with 90% of the demi-water used for the reaction.
- When this temperature was reached the biomass was inserted into the reactor through a hole on the top side by using a funnel.
- To clean the funnel and get the remaining biomass in the rest of the water was poured in.
- The reactor was then closed using a Teflon sealed bolt.
- Then the temperature controller was set to the planned reaction temperature thus beginning the actual test.
- The stirrer was set at 500 RPM to get a homogeneous mixture.
- Every 6 minutes a sample was taken during the test. This was also done during heating up because the biomass is already decomposing. The temperature profile of the tests can be seen in Figure 3-4.
- After approximately an hour at reaction temperature the test was stopped and the reactor was cooled down. This was done by letting cooling water run through the oil bath. Thus cooling the oil that flows through the reactor outer wall.

Two sampling methods had to be used during the test. At higher temperatures the primary outlet could be used and at low (<180C) temperatures the secondary outlet had to be used. The primary outlet is preferred because here the reaction mixture runs through an ice bath before the actual sample is taken. This prevents evaporation of the reaction mixture and is safer. A minor disadvantage is that before the actual sample can be taken 13 ml of reaction mixture has to discarded because that resides in the tube and not in the reactor. With this method more reaction mixture is used per sample. At lower temperatures the primary outlet gets blocked by the then still relatively large biomass particles and the secondary outlet had to be used.

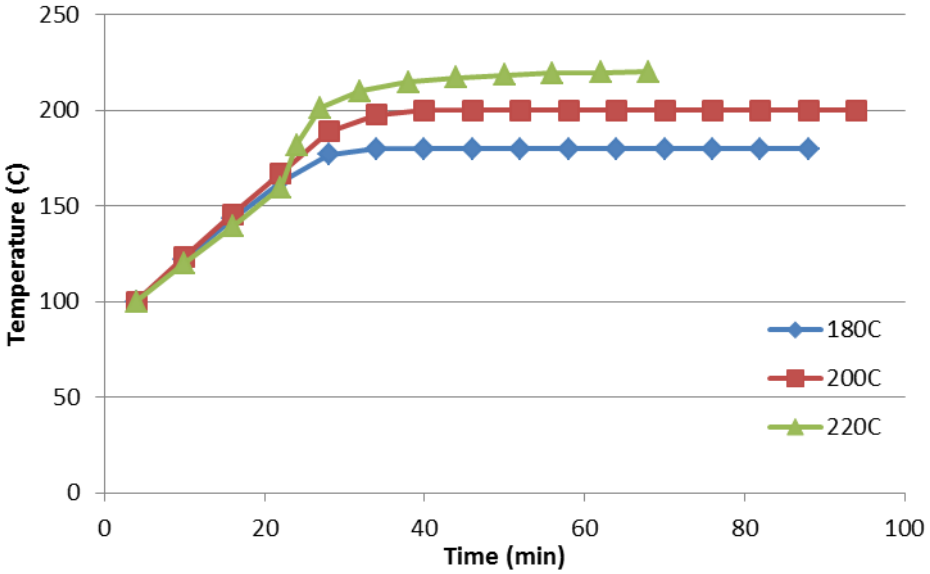

Figure 3-4: Temperature profile tests

The secondary outlet was used by opening the valve at the bottom of the reactor letting small bursts of reaction mixture and gasses out. This was collected in a pre-cooled Erlenmeyer flask under the reactor. Using a pre-cooled Erlenmeyer was done to condense as mush gasses as possible and for safety.

The measurement at 220C was troubled by a blockage of the primary outlet and therefore the secondary outlet had to be used. However after 4 measurements at this temperature the test was stopped. Due to the high temperature and pressure the sampling from the secondary outlet was determined to be unsafe. Therefore this test was not done completely.

From the Erlenmeyer sample then poured into a small plastic bottle (Figure 3-5) to enable the samples to be taken up by a generic 5mL syringe. The syringe was used to put the sample through a 0.45 µm Whatman syringe filter and then poured in a HPLC tube (Figure 3-5). Filtering is necessary to prevent blockage of the HPLC-pump.
A black settlement can be seen at the bottom of the plastic bottle, this is the solid residue that needs to be filtered. The HPLC tubes are aligned from the left (first sample) to the right (last sample).

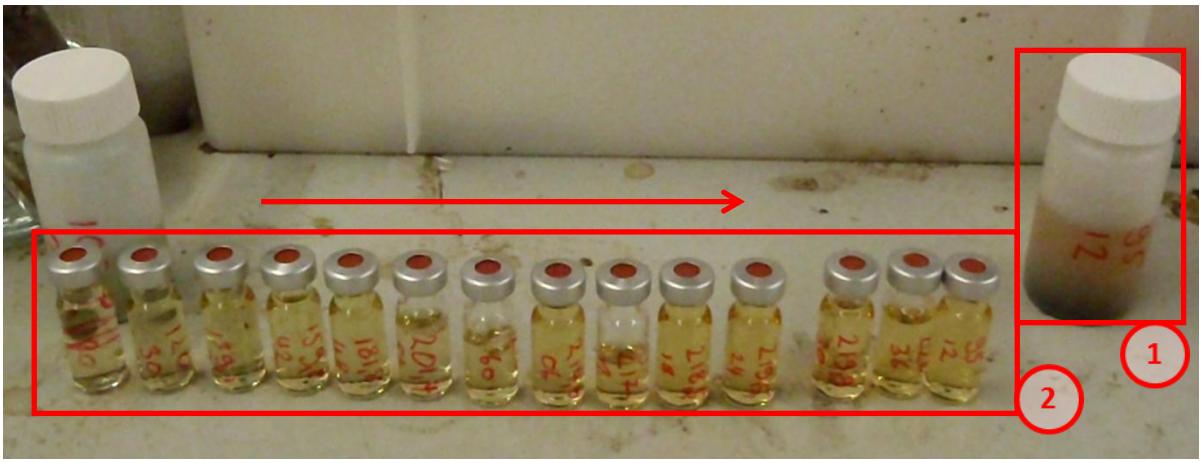

Figure 3-5: Plastic bottle and samples in HPLC tubes

1. **Plastic bottle**
2. **HPLC tube**

3.4.Analysis

The samples taken from the reactor contain water, dissolved decomposition products (sugars etc.) and solids. The liquid samples are thought to be homogeneous and thus representative of the total reaction mixture. The solid samples however still resemble small grass particles, combined with a small sample size the solids are regarded as non-representative and discarded.
The reaction mixture that is left over from the sampling and after the reactor cooled down is also used for analysis. From this the solid mass was filtered and weighed. The fluid was also weighed.

Figure 3-6: Filtering of reaction mixture

Due to constraints such as time, money and therefore measurement tools there are limits to what was analyzed. In the case of the liquid fraction only completely hydrolyzed monosaccharides and some of the decomposition products can be measured. Oligosaccharides cannot be measured.
The solid fraction left over will be compared to the prediction from the model. The results from the TGA will also be used for this.

Liquid analysis

The liquid samples were analyzed by using a HPLC. A Rezex RHM column was used at 50C and a mixture of 0,005N H_2SO_4 at a flow rate of 0,6 ml/min as the eluent and a run time of 60 min. The actual determination was done by UV-Vis (Varian Model 310) and RI (Varian Model 350) spectroscopy in parallel. The sampling was done using a Marathon XT auto-sampler.
Some measurements were also analyzed by using an alternative column, the Aminex HPX-87H at 60C with 0,005N H_2SO_4 as an eluent at 0,6mL/min. The same spectroscopic set-up was used.
The calibration of both columns can be found in the attachments. With all results the used column is mentioned.
Furthermore a graphic representation of the retention times is shown in Figure 3-7. As can be seen some of the components overlap.

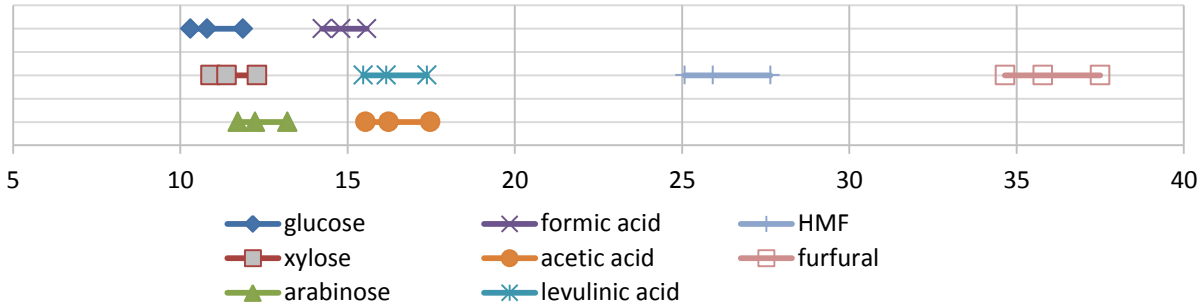

Figure 3-7: Detectable components at their retention time

A typical result from one sample is shown in Figure 3-8. Here you see different peaks for different components found in the solution at their respective retention time.
Comparing peaks cannot be done because a higher peak from a different component does not correspond directly to a higher concentration. Different components behave differently in the spectroscopic measurement, therefore a calibration is needed. The surface of each peak is calculated into their respective concentration from calibrated values.
Glucose and xylose show relatively good, although they are very close together. Acetic is a bit close to the other acids, what might cause amplification. Furfural is very clear on its own.

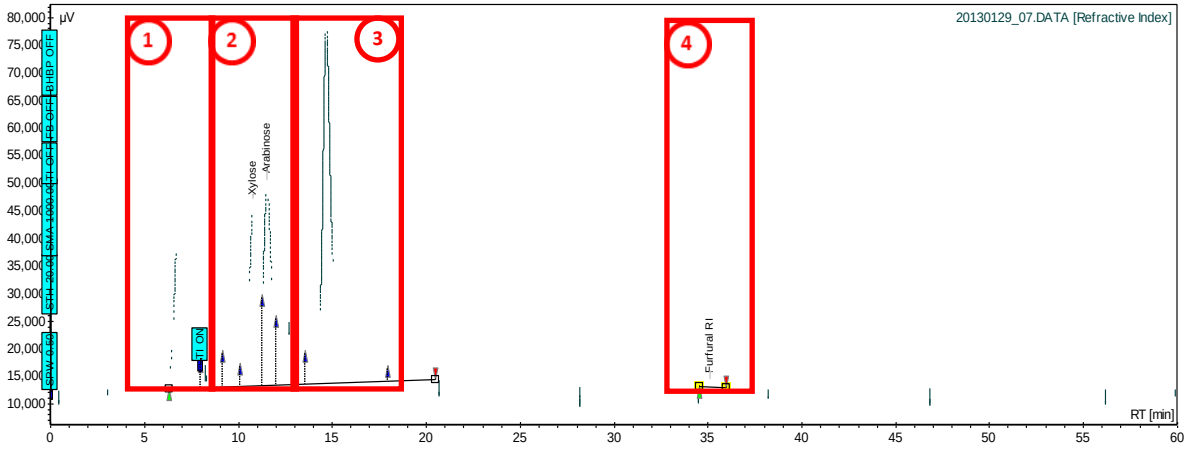

Figure 3-8: HPLC diagram 60 min. with components

1. **Oligomers**
2. **Monosaccharides**
3. **Acids**
4. **Furfural**

Sometimes the area of a curve is hard to determine because the HPLC graphs can sometimes look like Figure 3-9. Here the baseline is going up and a lot of peaks are melted together. This makes analyzing HPLC diagrams not always easy.

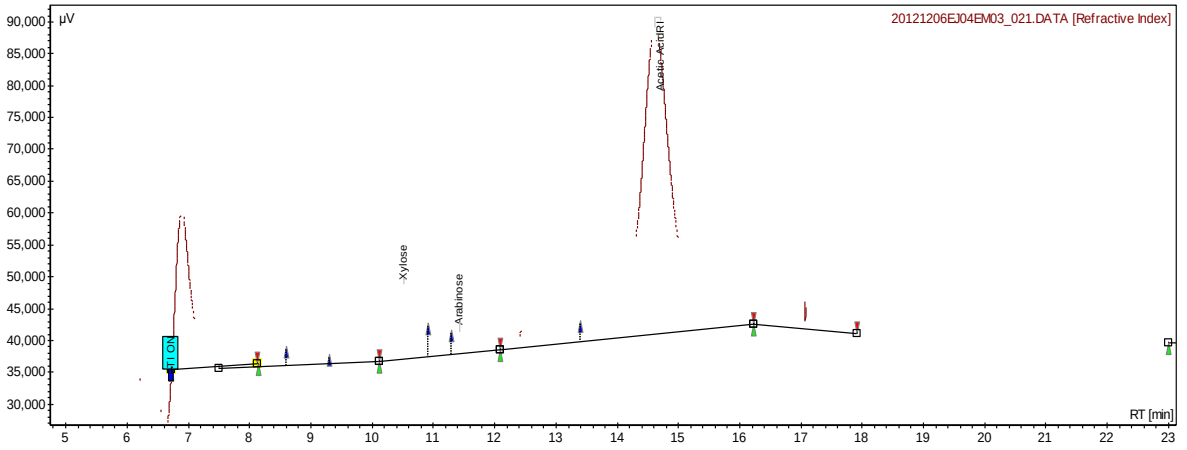

Figure 3-9: HPLC diagram 23 min. baseline going up

Solid analysis

The solid samples were tested by using a Texas Instruments SDT Q600 TGA. The temperature of the gas fed over the sample can be seen in Figure 3-10. Nitrogen is fed at 100 ml/min which is heated up to 105C with a temperature ramp of 10C/min. The nitrogen of 105C is fed for 5 minutes to evaporate all water present in the sample.
After evaporation the nitrogen was heated up further until 700C to release all volatiles. This is again done with a ramp of 10C/min. After 700C air was fed into the TGA to burnout the fixed carbon, this was done with a ramp of 10C/min until 1000C.

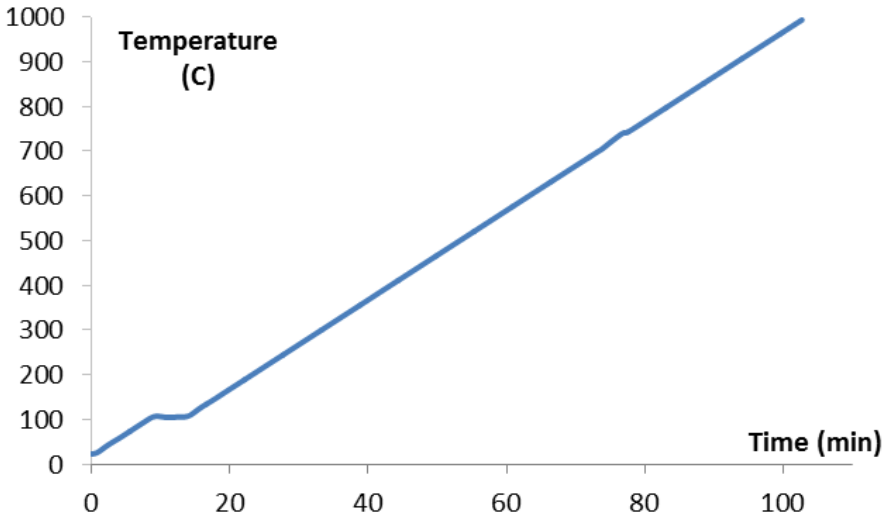

Figure 3-10: Temperature profile TGA

In Figure 3-11a typical TGA result is shown. The weight loss at a certain temperature points to a certain composition. In the beginning the moisture content can be determined. After that the lignocellulose is being decomposed. At the end the fixed carbon content can be determined and the residue is the ash content in the sample.

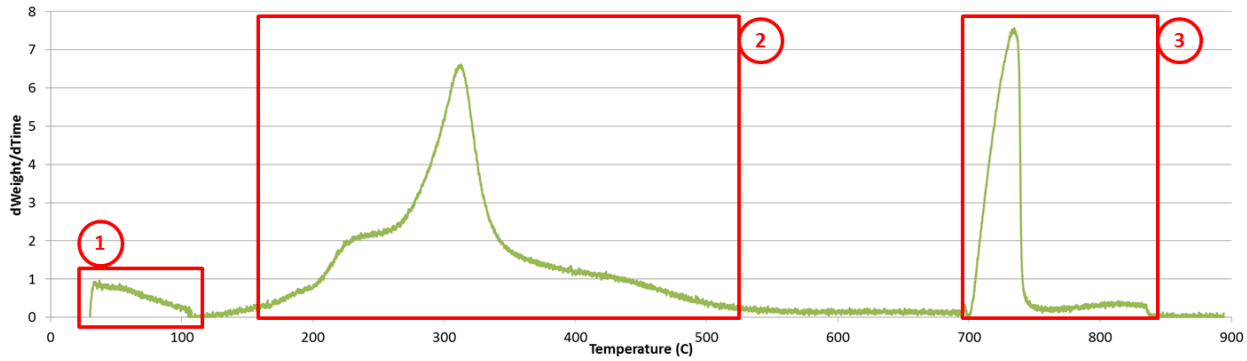

Figure 3-11: Complete TGA diagram biomass

1. **Moisture**
2. **Volatile matter/Biomass components**
3. **Fixed carbon**

What is generally thought to happen with biomass in a TGA is that the first components to decompose are hemicellulose and lignin. Lignin is thought to decompose very slowly up until higher temperatures. Hemicellulose decomposes more abruptly. This is depicted in Figure 3-12.

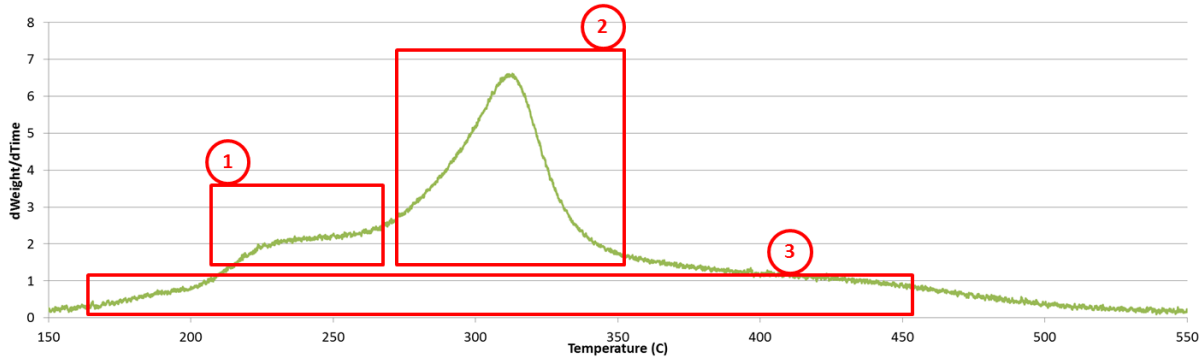

Figure 3-12: Biomass components TGA diagram

1. **Hemicellulose**
2. **Cellulose**
3. **Lignin**

Apart from the diagrams which point to structural differences some more data can be used from the TGA. Since all extractives are thought to have been removed during treatment all mass that has been removed in the TGA during the heating up to 110C is thought to be water. All mass that is removed after 700C is thought to be fixed carbon and the residue to be ash.

4. Results

The results from the liquid analysis are presented first. Since this is the most important method for analysing the decomposition pathway the conclusions of this are also drawn. Thereafter the solid analysis after drying is given and the results from the TGA. Physical changes are monitored and discussed by SEM images.

4.1.HPLC RHM-column

The results from the HPLC with the RHM column are given first. These results are sorted into the product being analysed. After that the results from the HPX column are compared to the RHM column. All results are given in concentrations.
The calibrated values have a linear relation between concentration and spectroscopic surface area. This linear relation is in the form of Equation 4-1.

$$y = a * x + b \qquad \text{Equation 4-1}$$

However the b-values obtained from the calibration are sometimes negative and sometimes positive. In the work used here the concentration are rather low. Therefore the b-value is not used because it has a very big influence on the calculated concentration

Xylose

The dissolved xylose from grass is depicted in Figure 4-1. Initially a very high xylose concentration can be observed with all tests and after about 30 minutes the xylose decomposition rate is overtaking the formation rate.
Initially the concentration of xylose in all tests is expected to be the same due to the same reaction conditions, as can be seen in the temperature profile in Figure 3-4: Temperature profile tests. After 22 minutes the temperatures start to deviate due to flattening out of the test at 180C and here is where deviations should show up. What is also odd is that the line of 200C crosses the 220C line. It is expected that xylose decomposes faster at higher temperatures.
One of the causes of this could be that 5 gram of grass is not enough to get a representative mixture of grass. Another possibility could be a measurement error caused by inhomogeneous mixing inside the reactor. It might be that in the mixture of 220C there was a hump of grass which later loosened up. That would also explain why the values are later on about the same as those of 200C. Another possibility is that the liquid samples are not representative of the reaction mixture.

What can also be observed is that the model does not give an accurate prediction. The test results show a very high initial xylose concentration where the model shows no decomposition of hemicellulose. Furthermore it seems that the model under predicts the xylose concentration. A very fast formation rate of xylose and a slower decomposition rate can be the cause of this.

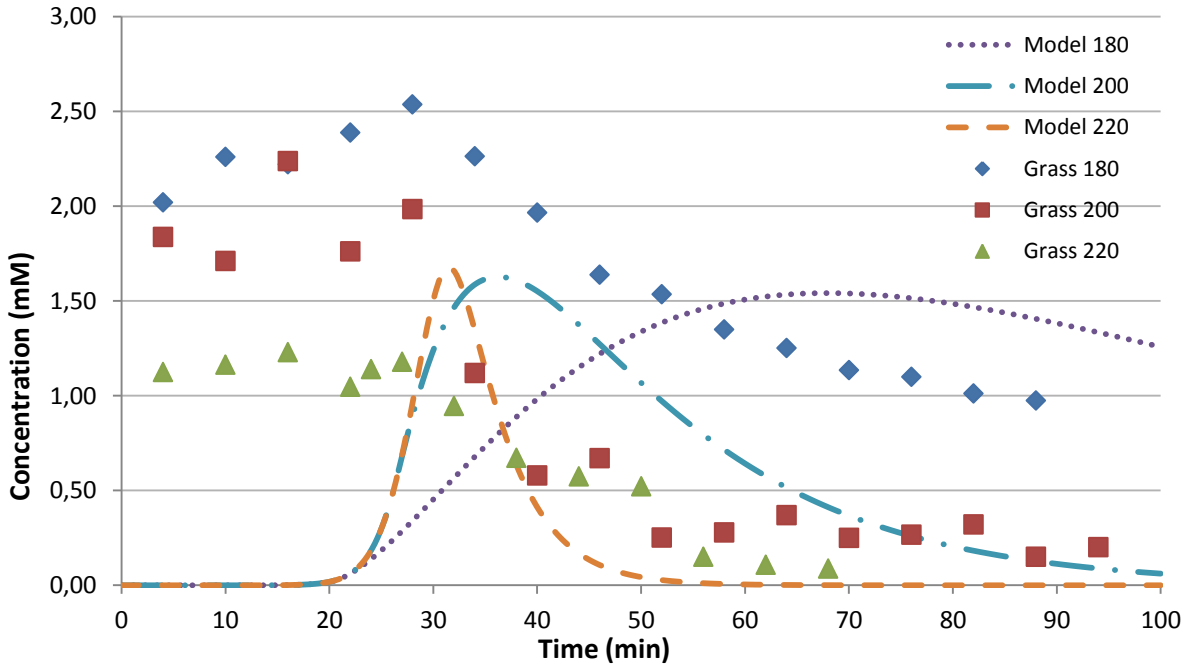

Figure 4-1: Verge grass xylose in solution

The dissolved xylose from different biomass species is depicted in Figure 4-2. The behaviour displayed by xylose is opposite of that from grass. Where grass shows a very high initial concentration and a decline preceding that of the model, xylan starts of slowly and does not reach a concentration peak nor is the highest value near the value predicted by the model.
The very different composition from grass can point to a tougher structure to break up. This can be caused by a higher degree of polymerization of xylan.

For bagasse the concentration of dissolved xylose was very low. Nothing can be said about the model results in comparison to the test results from bagasse. The reason for bagasse to have a very low concentration of xylose can be due to the fact that bagasse has already been processed and that the sugars that are removed easily are already removed.

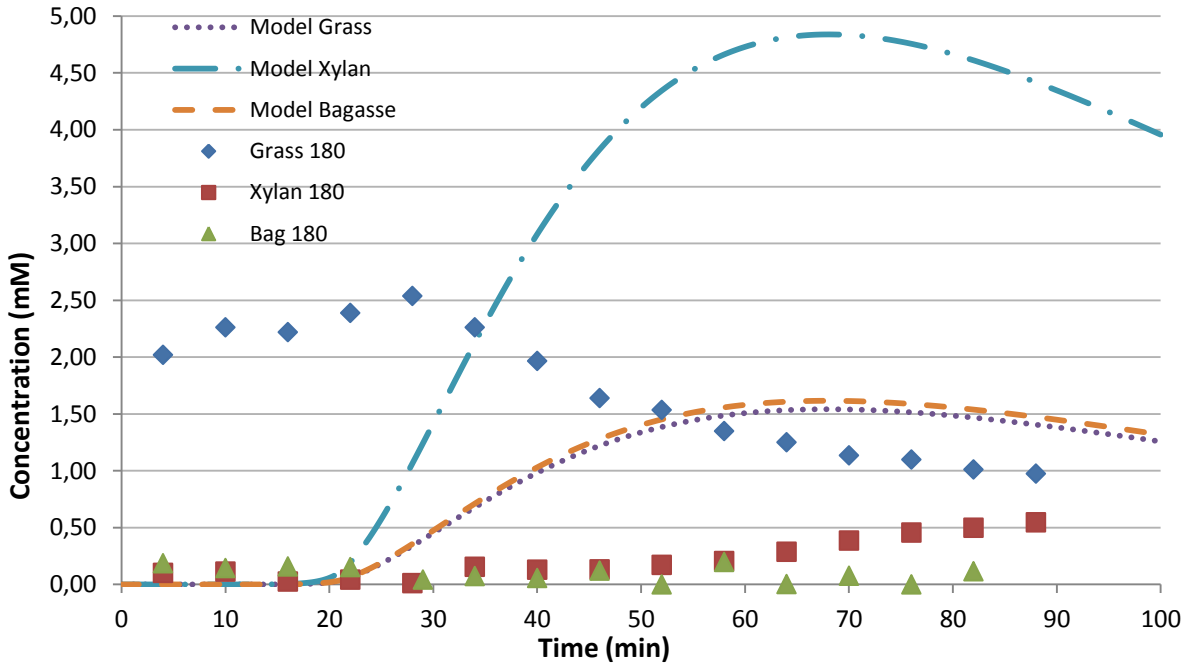

Figure 4-2: Biomass xylose in solution

Furfural

The dissolved furfural from grass detected by RI spectroscopy is depicted in Figure 4-3. What should be noted is that again the first samples are taken under similar reaction conditions and it is thus not expected that the concentrations already differ before 22 minutes.
At 180C some is furfural formation can be observed, although very low and slowly rising. At 200C there is a very low concentration furfural and initially furfural formation was not observed in the measurements. This is caused by a very erratic HPLC graph like the example given in Figure 3-9. The high concentration of 220C is unexpected. It is very clear that furfural formation is taking place at 220C.
As can be seen in Figure 4-1 the xylose concentration of grass at 220C is lower for the same initial conditions. It could be that this xylose is quickly converted into furfural. That would explain the high furfural concentration. The fact that this behaviour is differing from the other tests could point to a contaminant in the reactor.

No justifiable trend can be seen between the test results. This questions the validity of these results. Therefore the model and the test results cannot be compared. If only the results from 180C are valid the slow formation of furfural is can be explained by the slow decomposition of xylose.

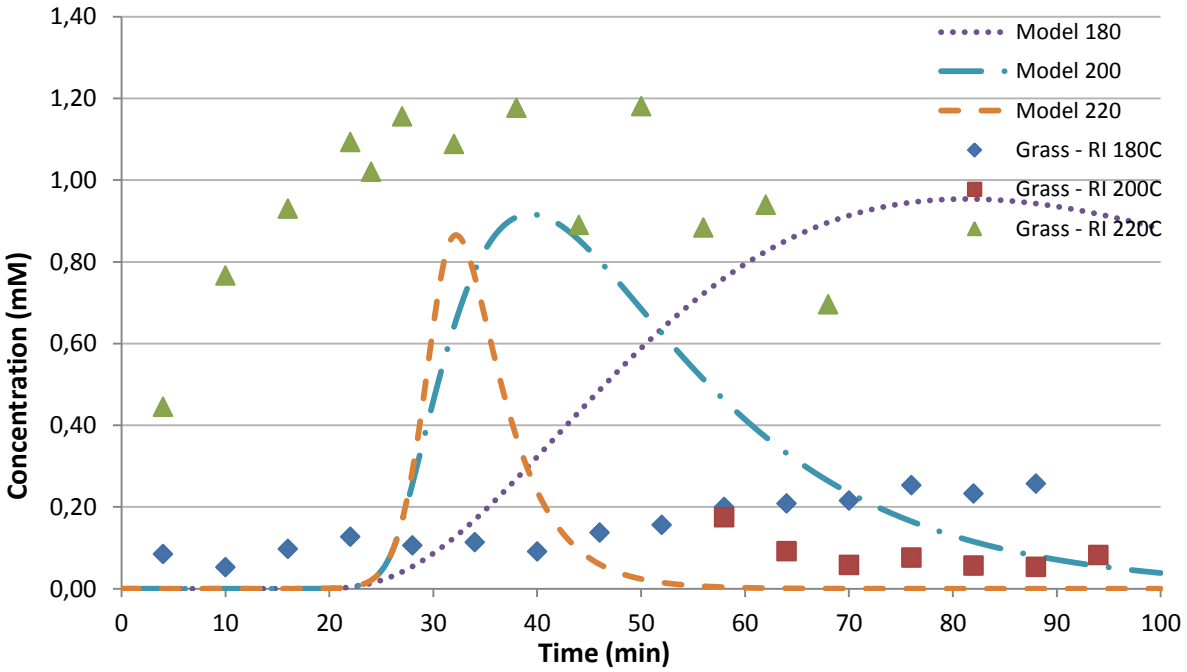

Figure 4-3: Verge grass furfural in solution detected with RI

The dissolved furfural from grass detected by UV spectroscopy is depicted in Figure 4-4. The concentrations for 180C and 220C show the same trend as observed by RI spectroscopy. Those of 200C differ a lot. This could be caused by the erratic behaviour of the HPLC at 220C
What causes the substantial higher values obtained by UV spectroscopy is unclear. Because this is seen at both 180C and 220C this must be caused by a systematic error.

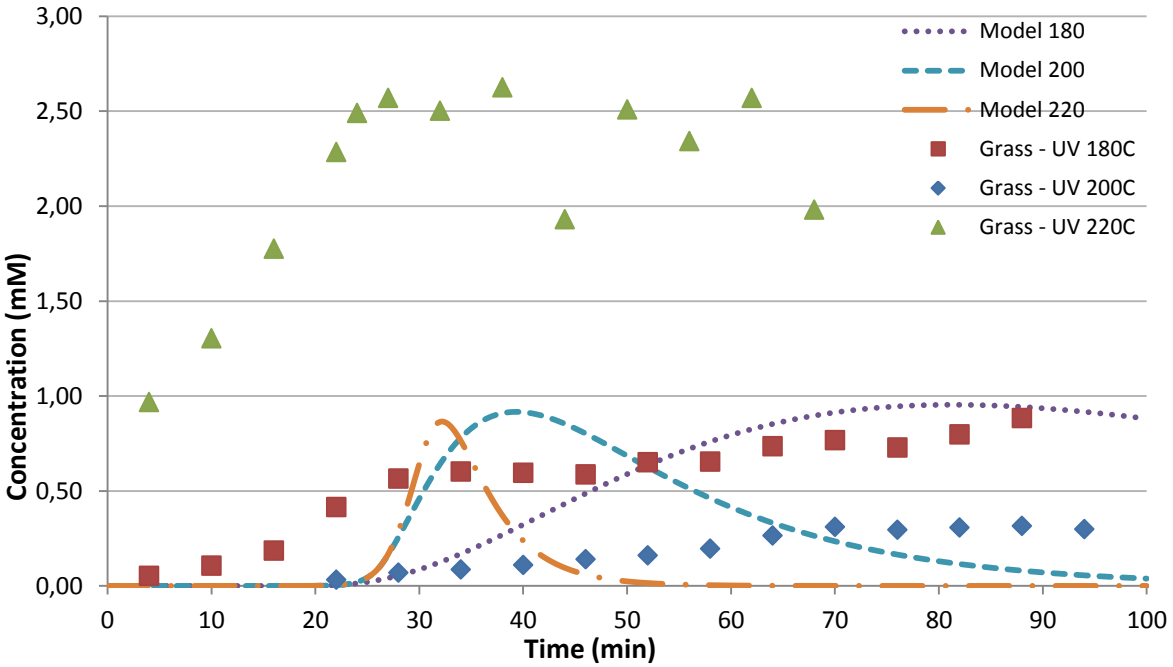

Figure 4-4: Verge grass furfural in solution detected with UV

The dissolved furfural from different biomass species is depicted in Figure 4-5: Biomass furfural in solution What is interesting is that furfural decomposition from xylan can be distinguished very clearly in low concentrations and xylose only after 28 minutes as can be seen in Figure 4-2 above. This is especially interesting because xylose is thought to be the precursor to furfural. This means that the furfural being formed from xylan does not come from xylose.
It could be that arabinose is responsible for the furfural. Another possibility is a poor resolution at the area of interest in the HPLC diagrams. As mentioned in the explanation of the HPLC techniques the sugars are very concentrated and furfural is very clear to distinguish at a retention time of 35,46 minutes.
The concentration from the test results show a rise that begins earlier than predicted. This can be caused by the high initial xylose concentration. The formation of furfural is although rather slow and this is in line with the slow decomposition of xylose from xylan.

No furfural was observed in the samples from bagasse. This is in line with the low concentrations of xylose observed in bagasse in Figure 4-2.

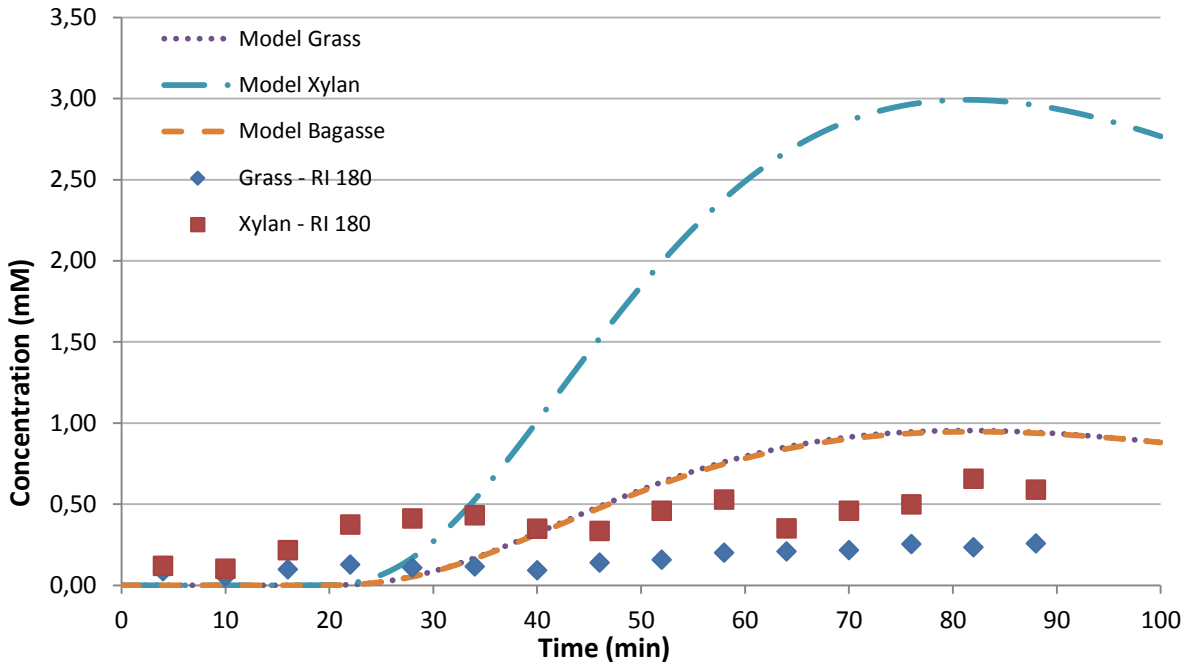

Figure 4-5: Biomass furfural in solution

Glucose

The dissolved glucose from grass is depicted in Figure 4-6. For glucose similar behaviour is observed as that of xylose. This is surprising because from the modelling one would expect cellulose to decompose a lot slower. Even that slow that no significant glucose should be measured. It seems that glucose bonding in grass is different from that in corn cobs from the work of Naberlatz [1] or in sugar maple wood meal as in previous research [2].
Again however the same differences can be observed between the tests at different temperatures. The initial concentration of 180C is the highest and stays the highest, where in the beginning the same concentrations are expected. Only after 22 minutes is a deviation expected.

Possible causes are the sugar distribution inside of the reactor is not evenly.
Sample dilution. Or a structural lower value due to HPLC base line.
Too small sample size used and therefore low sugar content which leads to big measurement errors.

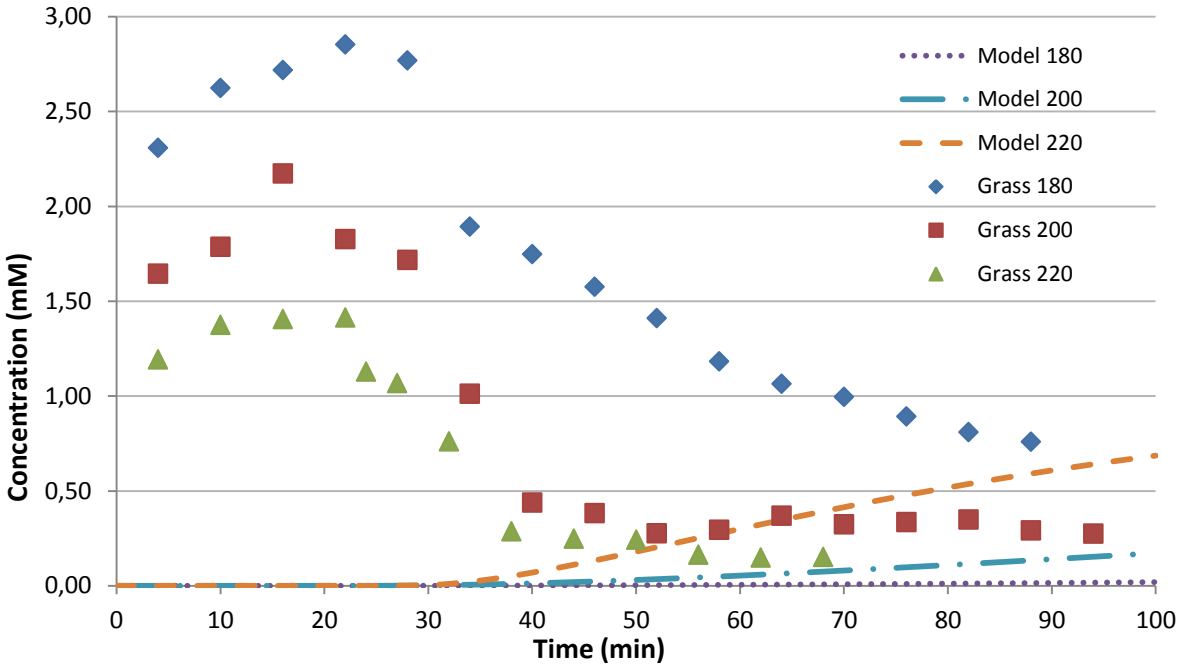

Figure 4-6: Verge grass glucose in solution

The dissolved glucose from different biomass species is depicted in Figure 4-7. Xylan is not depicted here because the concentrations were too low. This is of course logical due to the fact that the supplier guarantees a 90% xylose content.
Bagasse again shows very low concentrations of glucose which is in line with the model results.

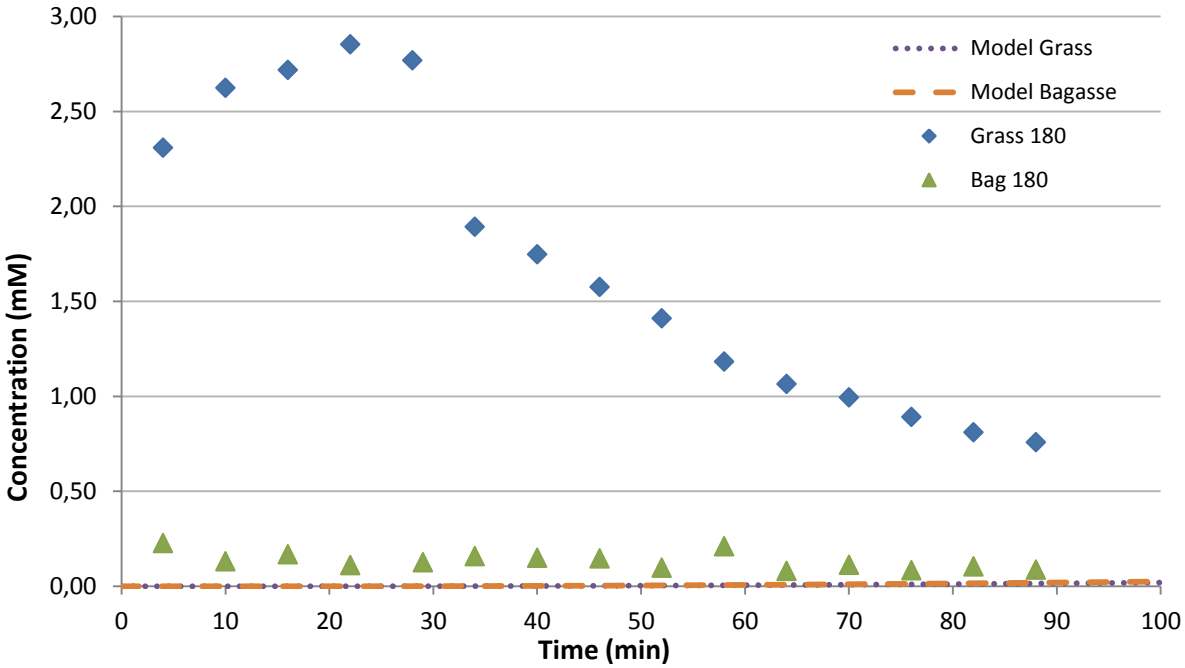

Figure 4-7: Biomass glucose in solution

Acetic acid

The dissolved acetic acid from grass is depicted in Figure 4-8. The concentration of acetic acid are the highest of all products formed. The concentration stays more or less the same for all tests. This high concentration is remarkable because this is not observed in other studies. The concentration of acetic acid at 220C shows however very erratic behaviour, but in all it is considered constant.
It could be that grass has an exceptional high concentration of acetal-groups. It can also be that other acids are adding to the acetic acid peak in the HPLC diagrams. Another possibility is that acetic acid is being formed as a decomposition product.
Due to the fact that no initial acetic acid content was known this was not used as an input for the model. The model does on the other hand predict no decomposition of acetic acid, which is observed in Figure 4-8.

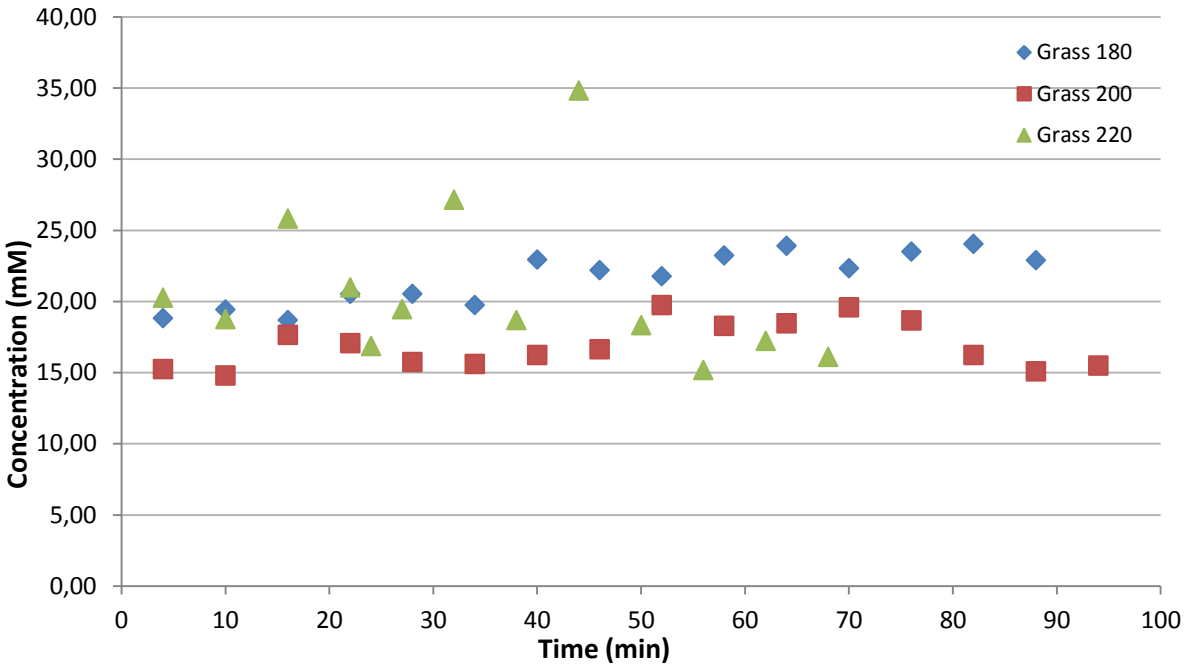

Figure 4-8: Verge grass acetic acid in solution

The dissolved acetic acid from different biomass species is depicted in Figure 4-9. The first value for xylan seems to be an error in the measurement. Apart from this xylan shows the same high amount of acetic acid as bagasse. From the initial xylan this is not expected.
Again the reasons mentioned by grass could be accountable for the high concentration of acetic acid in xylan. It could be that other acids that are hydrolyzed affect the spectroscopy much more than acetic acid.

Acetic acid concentrations from bagasse are again low, but measurable compared to the other results from bagasse.

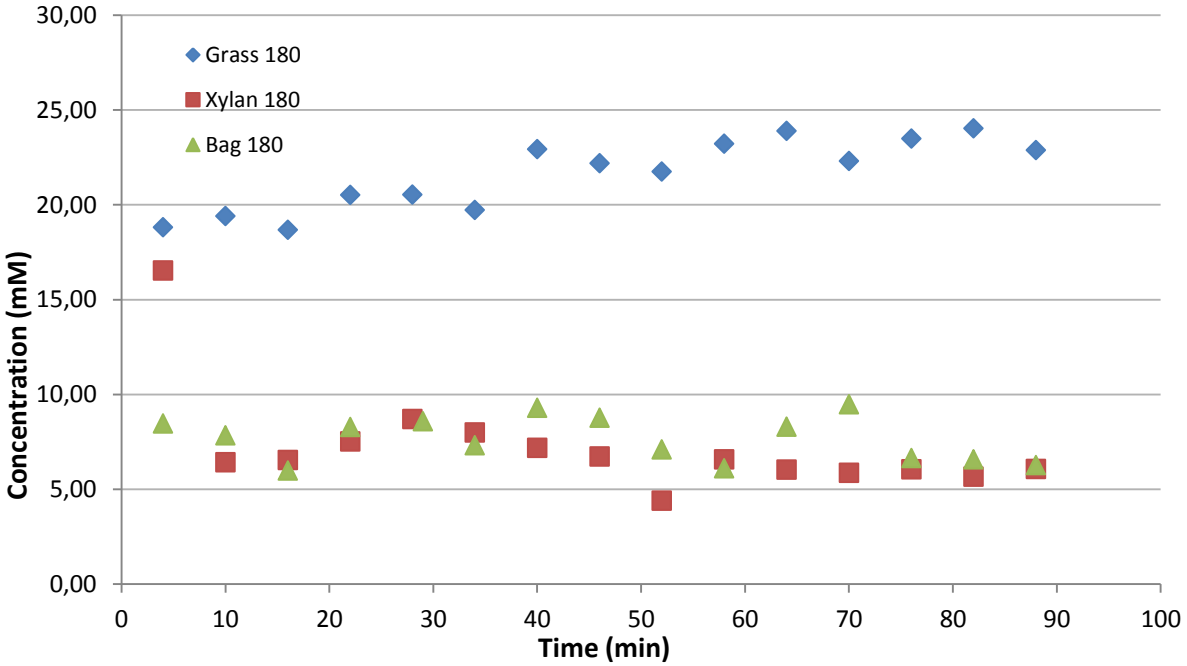

Figure 4-9: Biomass acetic acid in solution

Other components

Although the columns were calibrated for more components than the ones mentioned here none of those were usable. The values were either way too low to be significant or they were too hard to distinguish in the HPLC diagram "fusing" into the more dominant components such as xylose, glucose and acetic acid.

Conclusions RHM-column

Grass has very high initial concentrations of xylose and glucose pointing to a very quick decomposition which was not predicted. Furfural formation is observed, but due to the variation of the results nothing more can be said. Acetic acid formation is very quickly and is not decomposing as predicted.

The predicted and obtained results differ that much that the model cannot be used for predicting the behaviour of grass during wet torrefaction. Combined with the differing results from the experiments more measurements are needed to get more insight into the reactions governing the decomposition of grass.

Xylan has on the other hand very low concentrations of xylose and furfural compared to the model and grass. It seems that xylan has a much harder to decompose structure. Tests at higher temperatures and longer holding times can give more insight into the decomposition behaviour.

4.2.HPLC HPX-column

Here the results are shown from the HPX column. In general these results showed relative comparable results xylan. For grass the results deviate more.

Xylose

Differences between the initial RHM column and the HPX for xylose from grass can be seen in Figure 4-10. The trend observed in the RHM curve can also be observed in the HPX curve. The initial concentrations are high and drop off after 30 minutes. Although the initial concentrations are differing a bit after 40 minutes the values converge.

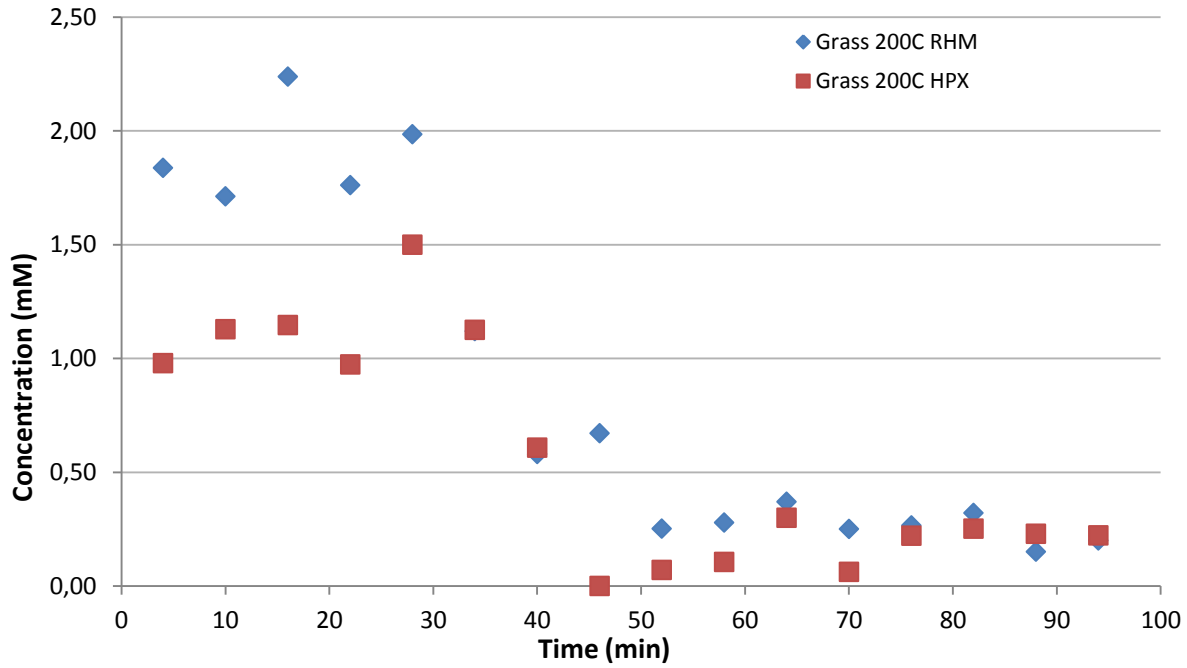

Figure 4-10: RHM-HPC comparison xylose from verge grass 200C

Differences between the initial RHM column and the HPX for xylose from xylan can be seen in Figure 4-11. Here similar behavior is observed between the curves of the different columns although the RHM results are a little lower.

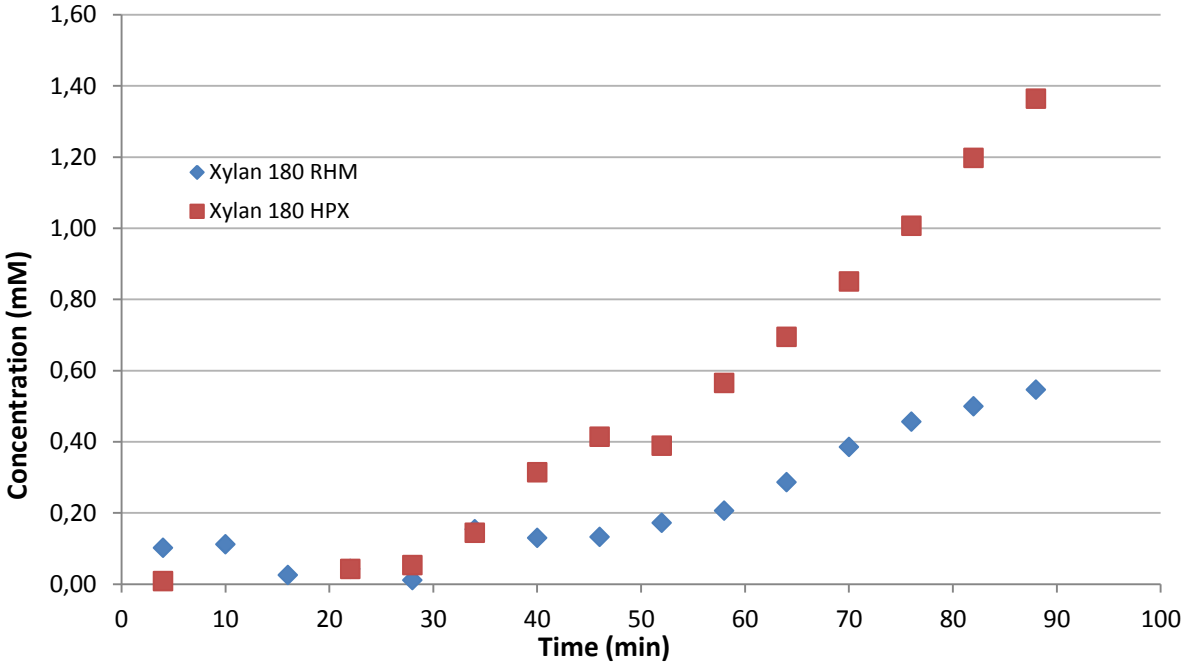

Figure 4-11: RHM-HPC comparison xylose from xylan

Furfural

Differences between the initial RHM column and the HPX for furfural from grass can be seen in Figure 4-12. The results obtained by UV spectroscopy are very comparable between the two columns the RI values are not. The cause of this could be that the RI measurements are corrupted in a way.

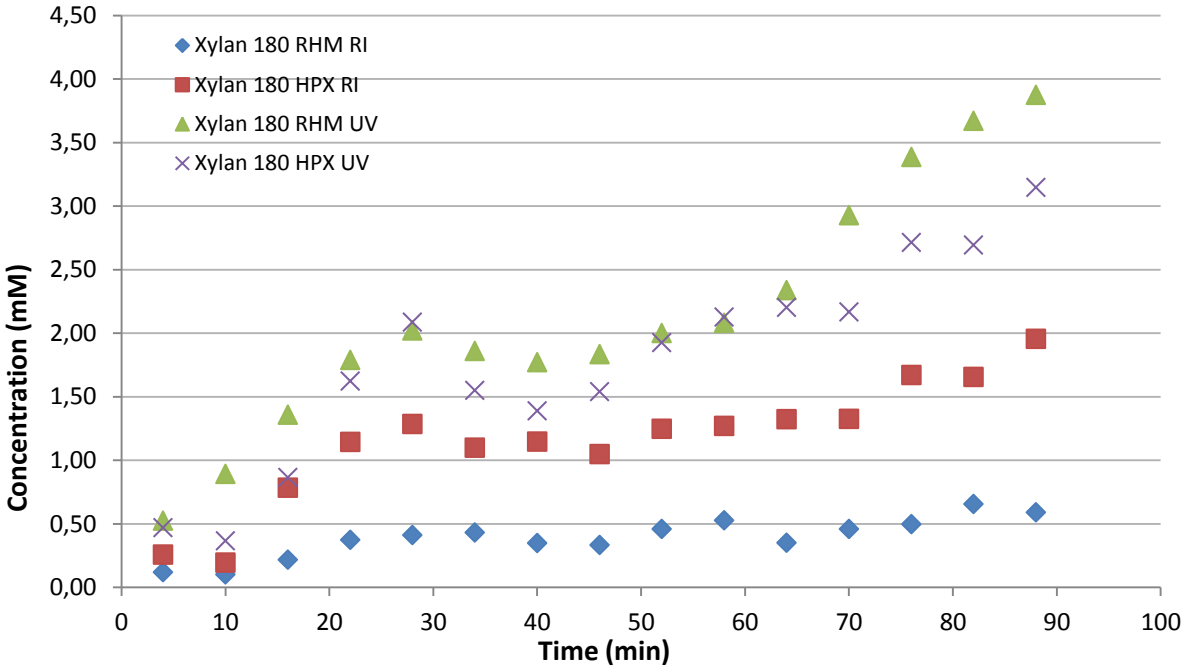

Figure 4-12: RHM-HPC comparison furfural from grass

For xylan the HPX column shows the same behaviour although it is a little “exaggerated”. A reason for this could be the low concentrations of furfural.

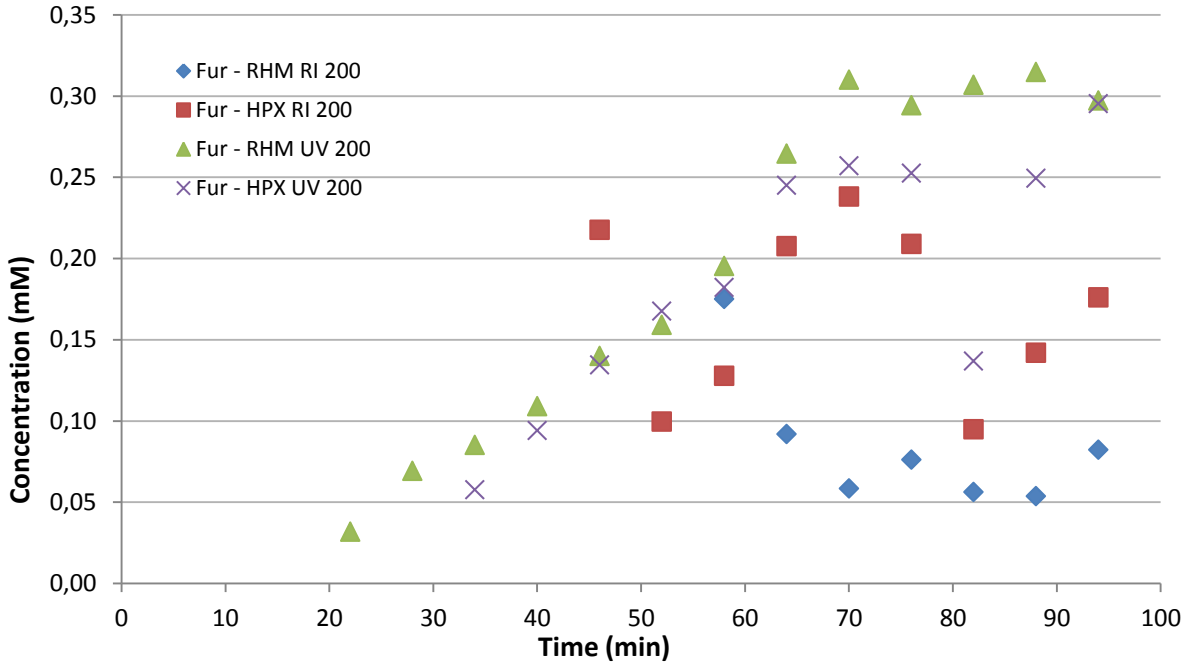

Figure 4-13: RHM-HPC comparison furfural from xylan

Glucose

Differences between the initial RHM column and the HPX for glucose from grass can be seen in Figure 4-14. The same results are observed here as with xylose. Initial values that differ a lot and after 40 minutes they converge.

This error seems to be systematic and can be due to interpretation of the HPLC diagrams.

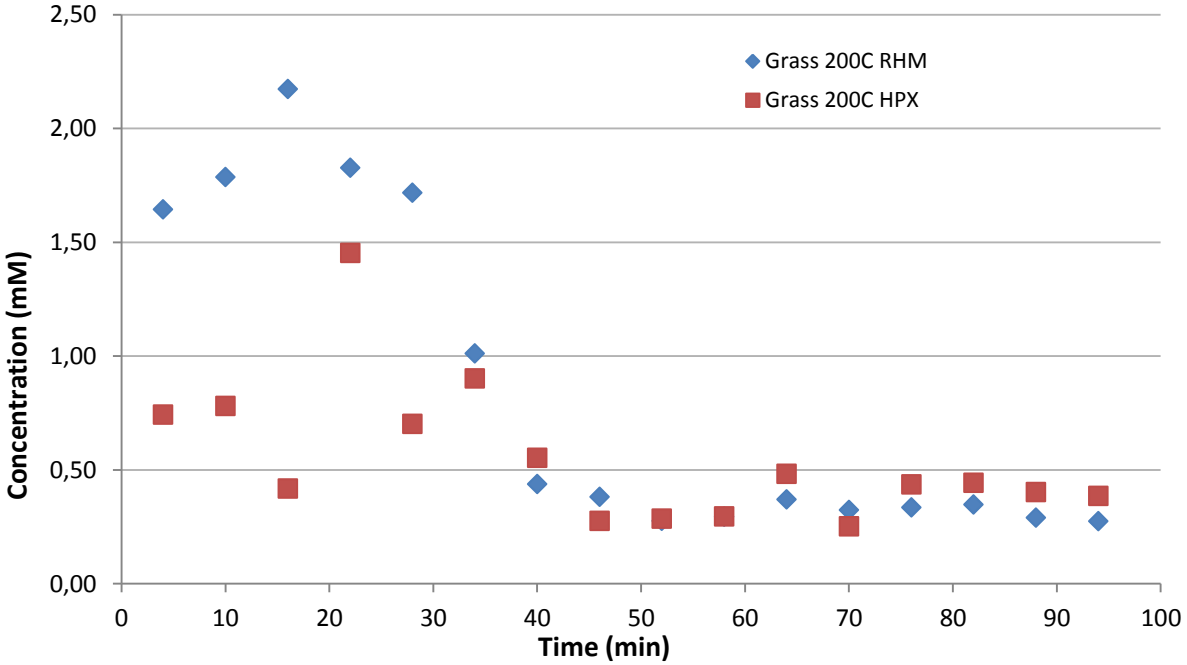

Figure 4-14: RHM-HPC comparison glucose from verge grass 200C

The glucose content is that low in the xylan samples that no glucose was detected by using the HPX column.

Acetic Acid

For the HPX column acetic acid was not calibrated therefore not results are shown here for xylan and grass at 200C. A peak was visible which might be acetic acid, but this is not certain. This peak cannot be calculated back to concentrations and is therefore not shown.

Conclusions comparison RHM-HPX

For xylan a good agreement between the different columns was observed. Although the values differed here and there similar concentration patterns were observed. It might be that a higher concentrations of products give better results.
For grass the story is a little different; it seems that the value obtained by RI spectroscopy have a big error in them. The reason for this can be can be caused by a contamination of the sample.

4.3.Conclusions HPLC

Xylose and glucose from grass is decomposed quickly compared to xylan. This points to a whole different structure. From a mechanistic point this seems logical since xylan comes from beechwood which has a much tougher structure than grass.
However what is not expected is the amount of glucose in the reaction mixture. This points to a very loose connection of glucose in grass. This could be caused by the fact that the grass around our faculty is constantly being mowed and that in fact very young grass was used. Grass species can have a length up to 60 cm and what was used for this test was hardly longer than 15 cm.
At 220C furfural formation is higher than at lower temperatures. This could be caused by a faulty measurement or point to a different formation pathway of furfural.
Very high acetic acid concentrations are measured. If this is caused by other acids or unusual high levels of acetic acid should be pointed out by further research.
Bagasse shows very low concentrations of all products. This could be caused by a much tougher structure of because. Perhaps tests at higher temperatures show better results.
In general higher concentrations of biomass should be used in this setup because for some tests the HPLC result was below the lowest calibrated value.
Differences between calibrated values can be relatively big. Xylose shows a difference of 0,08 gr between the calibrated values from the RHM and the HPX. This partly explains the biggest deviations already.

4.4.pH results

For some samples the pH was measured. Not all could be done because for a pH measurement more sample is needed which would drain the reactor. The results from these measurements are shown in Figure 4-15: pH of grass tests.

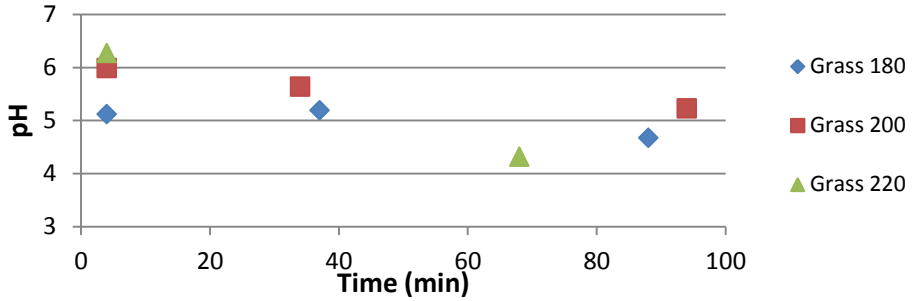

Figure 4-15: pH of grass tests

These measurements could explain the differences observed in the concentration of xylose. Acidity helps to hydrolyse xylose. For 220C the xylose concentration was low compared to 180C. This could be caused by the low acidity. On the other hand the low pH could point to the other direction: at 220C grass was not decomposed as much as at 180C although the reaction conditions are the same.

4.5.Solid mass

After cooling down the reactor residue was filtered to separate the solid from the liquid part. The solid was left on the filter to be air dried. Some solid samples are shown in Figure 4-16. The sample from 180C has a more fibrous structure than the other samples. Clearly the more severe reaction conditions had an impact.

The results from the drying are shown in Table 4-1. At longer holding times more of the solid mass has decomposed this can be seen by the difference from 180C and 200C. For 220C nothing can actually be said because this test was not as long as the others.

Figure 4-16: WTG after drying

In the same process bagasse decomposes a little less mass than grass. This mass loss however is not accounted for in the HPLC samples. It might be that higher order oligomers were present in the

mixture which were not detected by the HPLC. Another possibility is that gasification has taken place already.
The samples of grass were air dried with different drying times. It seems that treatment at 180C still leaves some hydrophilic components which are removed by a treatment at 220C. It can also be that even at 200C all the hydrophilic components are removed, but this is not clear because of the longer holding time of 15 days. However in general grass loses a lot of its hydrophilic components and can be dried naturally very well compared to fresh grass.

Table 4-1: Different drying characteristics

	% of original	reactor time in minutes	days of drying	% mass loss after 24h in 50C oven
Grass 180C	23,4	88	4	4,6
Grass 200C	21,8	94	15	1,9
Grass 220C	25,6	68	2	2,8
Bagasse 180C	24,6	88	-	-
Fresh grass (from Haket [1])	-	-	7	70 (after TGA)

4.6.TGA

After drying the grass solids were tested in a TGA. Tests were performed in duplicate since the sample size used in a TGA is several micrograms. The results of the TGA can be seen in Figure 4-17 and Figure 4-18. Only temperatures between 110C and 550C are shown. This is because up to 110C a lot of water is evaporated as explained earlier. And after 550C the solid carbon content is burnt up this is analysed later.

TGA different grass samples

The WTT grass is compared to dried and fresh grass. These results are normalized from 110C because all water is thought to have evaporated after that point. The normalization was done in order to give a good comparison of the dry mass of every sample. What can be seen immediately is that actually not all water was evaporated from the fresh grass. This is not spectacular since the water content was approximately 60% as mentioned earlier. However for dried grass and wet torrefied grass no immediate mass loss is detected after 110C immediately so it is safe to say all water is evaporated.
A clear distinction is seen between wet torrefied grass and unprocessed grass.

This is the first shoulder in the graphs of unprocessed grass. You can see this shoulder is completely lacking in wet torrefied grass pointing to a complete removal of hemicellulose. Another thing to see is that the main peak is much later in WTG, this could be caused by removal of easy to remove cellulose or changes in the cellulose structure. Overall the peak is higher and more concentrated in temperature due to the earlier mentioned removal of hemicellulose.
The fact that the peak of treated grass comes late can be caused by the lack of catalyst. Most catalytic components are thought to be washed out during treatment.

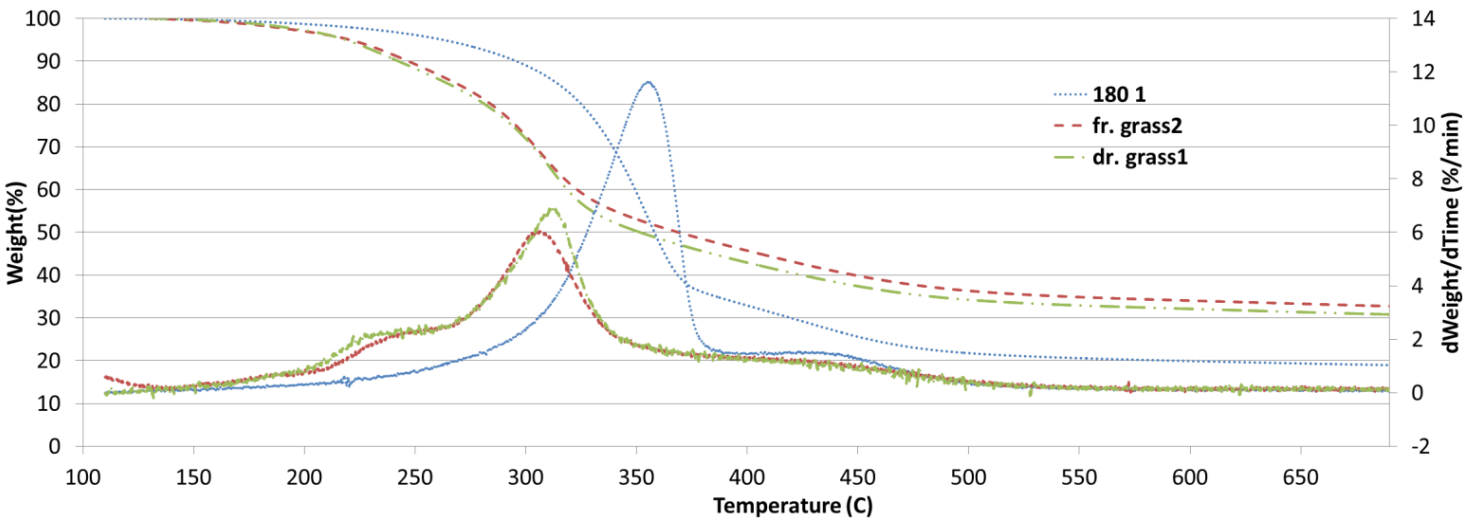

Figure 4-17: Grass compared to WTG in TGA diagram

The different samples of fresh grass show very different behaviour. This is probably caused by an uneven sample size. Due to the moisture percentage of 70 different biomass components can be more abundant. The dried grass samples fit together rather nice. A small difference can be seen between the two samples that were processed.

TGA different wet torrefaction temperatures

No real big differences can be seen between the wet torrefied samples from the TGA diagram. The 180C samples have a peak which comes a little earlier in time. This can be caused by differences in the structure by the treatment or the fact that the easy to remove components are removed. The 200C samples are both very similar compared to the sets of 180C and 220C. The 220C samples look very much like the 200C samples. Perhaps all hemicellulose is really gone and only pure cellulose and lignin are left. These can then behave the same in a TGA measurement.

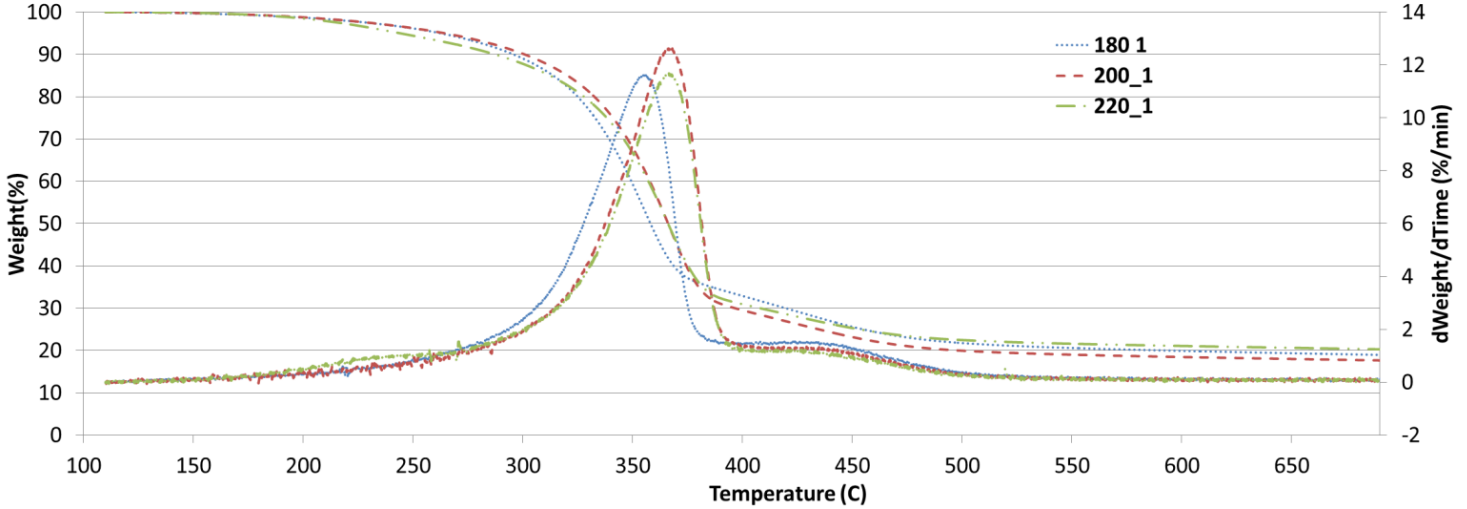

Figure 4-18: Different WTG compared in TGA diagram

A trend is seen that higher temperature result in a lower moisture content . The results from the TGA experiments contradict the results from oven drying as from Table 4-2. From oven drying the

treatment of 200C resulted in the lowest moisture percentage. Due to very small sample sizes an error can be introduced.

The biochemical and fixed carbon percentages differ a little. Generally the idea is that the volatile matter is decreasing after a higher temperature or longer holding times as can be seen from the torrefied beechwood from the Phyllis database [4]. However the TGA does not give a definite answer because at 220C the volatile matter decreases again. It could be that too little data is available to predict anything. Bigger differences between the tested temperatures could be of more value for making an accurate prediction.

Table 4-2: Fuel properties different sampels

	av. 180	av. 200	av. 220	av. fresh	av. dried	beechw. torr. 240	beechw. torr. 260	
moisture	4,03	2,98	2,41	69,55	4,43	0	0	ar
ash	1,62	3,1	4,16	7,4	9,67	0,35	0,4	db
volatile matter	82,86	84,13	83,07	73,34	76,36	80,88	76	daf
fixed carbon	17,14	15,87	16,93	26,66	23,64	19,12	24	daf

One would expect that longer holding times and higher temperatures result in less biomass and more ash. And that can be seen from Table 4-2. However since nothing is known of the contents of this ash one cannot simply connect the higher ash content to a lower percentage of biomass that is left. The percentage of mass left after treatment from Table 4-1 also puts this in doubt.
The ash percentages of unprocessed and wet torrefied grass however are not comparable. The wet torrefied grass probably has a much lower chlorine content because this is thought to have been washed out.

4.7.SEM

To get an idea of the physical changes of verge grass pictures were made with a SEM. What can be seen is that dried grass in Figure 4-19 already has undergone some changes. The outer wall is open and the internal structure is visible. What can also be seen is that the vascular structure in the grass has been altered. So it is safe to say that relatively moderate drying at 50C can already alter the structure of grass.
The effect of a WTT is also noticeable in the structure as can be seen in Figure 4-20. At 180C still some structure can be seen at the right side of the figure. Perhaps this is the outer wall that has been opened. The major structural parts of the grass leaf is still visible.
At 200C in Figure 4-22 the outer wall is still visible on the left side and at the background in the middle. Major inner structures are still visible as well.
At 220C in Figure 4-21 no outer wall can be seen. The major structures still seem to be intact. Small white dots are also visible in the 220C. At 200C they are also visible but in a much smaller amount. In other research this has been attributed to lignin reforming.

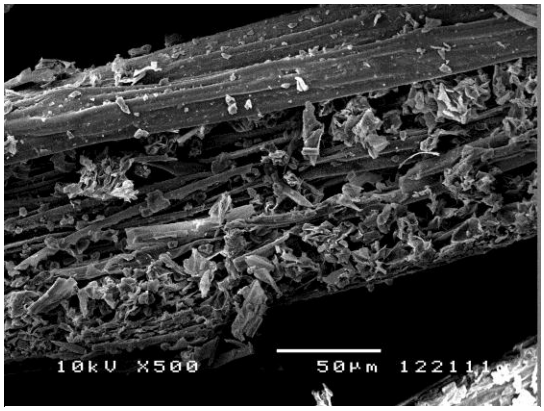

Figure 4-19: Dried grass

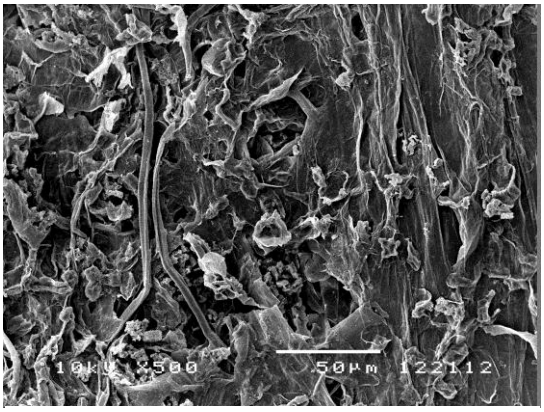

Figure 4-20: Grass 180C

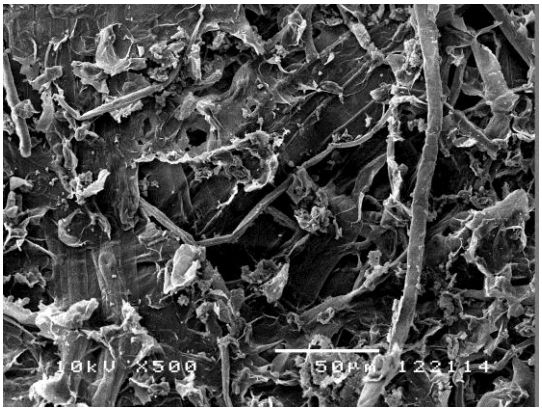

Figure 4-22: Grass 200C

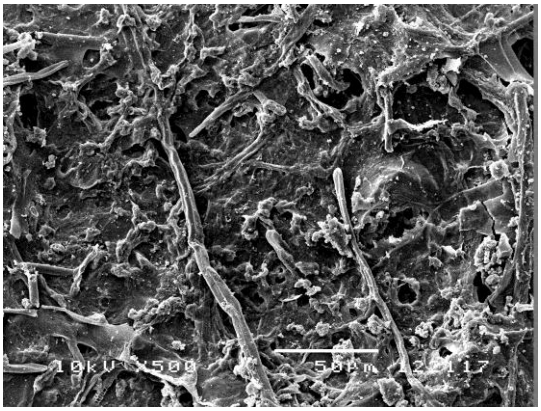

Figure 4-21: Grass 220C

In Figure 4-23: White dots grass 220C a detailed view of the white dots is shown from the WTT at 220C.

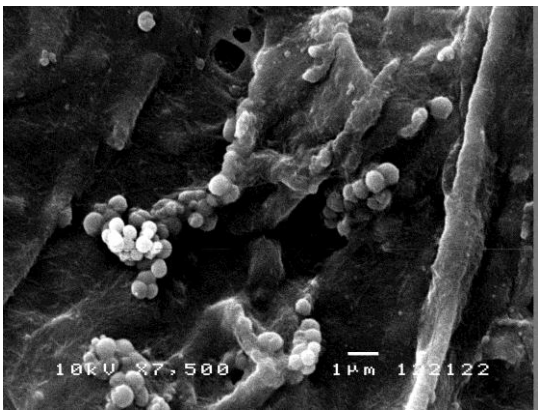

Figure 4-23: White dots grass 220C

4.8.References

1. D. Naberlatz, X. Farriol, D. Montané, Kinetic modelling of the autohydrolysis of lignocellulosic biomass for the production of hemicellulose-derived oligosaccharides, Ind. Eng. Chem. Res. 43, 2004, pp 4124-4131
2. A. Mittal, S.G. Chatterjee, G.M. Scott, T.E. Amidon, Modeling xylan solubilization during autohydrolysis of sugar maple wood meal: Reaction kinetics, Holzforschung 63, 2009, pp 307-314
3. C. Haket, On-site drying of verge grass for large scale co-combustion, Master thesis, TU Delft, 2012
4. *Energy research Centre of the Netherlands (*ECN), *Phyllis2 database for biomass and waste*, http://www.ecn.nl/phyllis2/, accessed: 8-5-2012

5. Equipment

With the parameters of interest known the requirements can be determined for the equipment needed to process verge grass. First a general layout is described and from that the mass flows are calculated. After that the necessary energy needed is calculated and this is all summed up and compared against alternatives.

5.1.General layout

Verge grass is harvested and thereby cut into smaller (<50mm) pieces. No contamination is expected to be in the harvested grass. After harvesting it is transported to the processing facility and there it is stored in a small bunker. By a conveyor it is transported to the mixing tank were it is mixed with recycled process water. After mixing it is pumped to the required pressure to be fed through the heat exchangers. Of these heat exchangers one is fed by the process water which is derived from the parallel reactor. The other is fed by a steam source or another heat source to provide the extra heat needed. Ideally this would be steam from either the Maasvlakte power station or in the case of a separate processing plant waste heat from an adjacent facility.
Once the reaction mixture is in the reactor it is being stirred to prevent any grass from sinking to the bottom. After the needed reaction time the bottom valve is opened up to let the reaction mixture flow through the heat exchanger. After having given of most of its heat the mixture is being filtered either by a passive or an active system. The WTG seems to be hydrophobic from small scale tests and natural drying is observed with good results. However for large scale processing further research is needed because it might be that big piles of WTG behave differently.

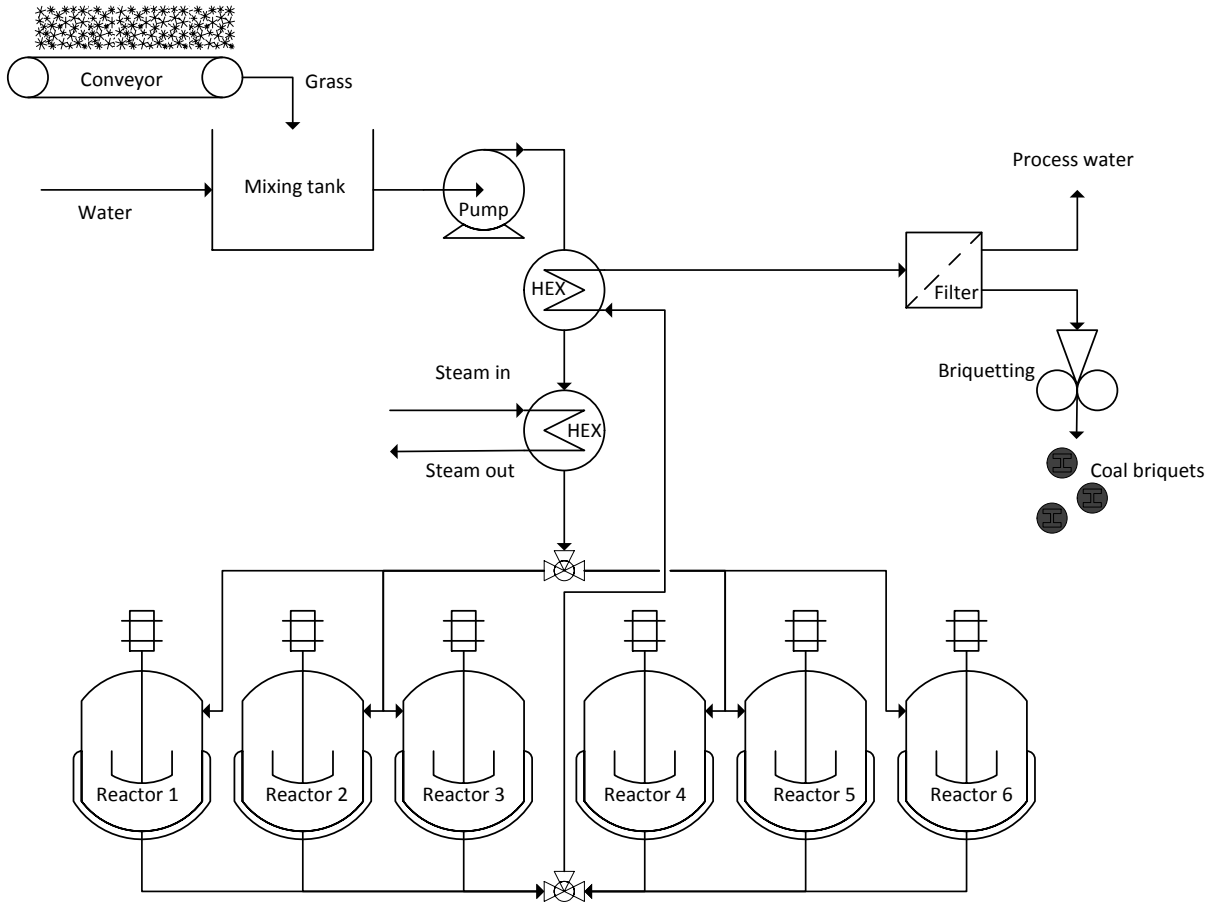

Figure 5-1: WTG equipment

The process water can be further processed to collect all valuable chemicals (xylose, glucose, furfural etc.). From the relative dry mixture briquettes are made that can be processed further or stored. It is expected that these briquettes have similar properties as coal and as such can be fed into the existing coal power plant infrastructure as coal. No problems are foreseen with grindability or degradation due to storage such as is expected with unprocessed grass.

The most important for the design of the equipment are the properties of the treatment. For the calculations done here a temperature of 250C and 15 min was chosen. Because the treatment is done in liquid water the temperature of the treatment is directly linked to the pressure of the treatment. A lower temperature would result in a longer reaction time and thus bigger equipment. On the other hand would higher temperatures result in smaller equipment which needs to sustain more severe conditions. The chosen temperature and time seem to be a good compromise between size and severity.
Further research should optimize between time and temperature.

Although grass was never tested at these temperatures an estimation of the properties of WTG after this treatment is made based on the results from the model and results from the tests. Preference was given to the test results as these are more relevant to the process. Wherever needed data was used from the model. All data used can be seen in Table 5-1.

LHV_wet	5,42	MJ/kg
mc	60	%
LHV_dry	17,22	MJ/kg
H_evap	2,45	MJ/kg
LHV_wtg	22	MJ/kg
mass loss	70	%
t_treat	15	min
t_treat	900	s
P_treat	3990	kPa
T_treat	250	C
added water	50	%
Cp_grass	4,18	kJ/kg/K
T_ambient	15	C

Table 5-1: Characteristics treatment

5.2.Amount of grass/Mass flows

As mentioned in the introductory chapter it is envisaged to co-fire 20% of the electrical energy of the MPP3. This power plant has a rated output of 1,07 GWe. For the co-firing of 20% of WTG the expectancy is that apart from the heating value all other characteristics are the same as the conventional coal used.
The electrical energy produced from WTG is:

$$P_{wtg} = P_g * \%_{co} = 200\ MW \qquad \text{Equation 5-1}$$

P_{wtg} is the power generated from WTG, P_g is the total power generated and $\%_{co}$ is the percentage that is co-fired.

With a thermal efficiency of 46% the thermal input of WTG is then:

$$P_{th} = P_{wtg} * \eta = 435\ MW \qquad \text{Equation 5-2}$$

P_{th} is the thermal input and η is the efficiency.

With the thermal input the mass flow of WTG needed for co-firing of 20% can be calculated:

$$\dot{m}_{WTG} = {}^{P_{th}}/_{LHV_{WTG}} = 19{,}76\ {}^{kg}/_{s} \qquad \text{Equation 5-3}$$

m_{WTG} is the mass flow of WTG and LHV_{WTG} is the lower heating value of WTG.

The moisture left after the tests is <5% therefore all moisture is thought to be out of the WTG. However a lot of mass is lost during the WTT. This is something that deserves further research. For now however this mass loss is taken into account for determining the mass flow of raw grass:

$$\dot{m}_{gr} = \frac{\dot{m}_{WTG}}{(1-\%_{mc})*(1-\%_{ml})} = 164{,}7\ {}^{kg}/_{s} \qquad \text{Equation 5-4}$$

m_{gr} is the mass flow of grass, $\%_{mc}$ is the moisture content and $\%_{ml}$ is mass loss

As can be seen in Figure 5-1 the grass is mixed before it is pumped through the heat exchanger. For this 50% of water is added to the mass of grass. This number is thought to liquefy the grass stream enough . More research is needed on the flow characteristics of grass and water-grass mixtures because this is important in the further processing of these streams.
The water-grass mixture stream is therefore:

$$\dot{m}_{mixt} = \dot{m}_{gr*(1+\%_w)} = 247{,}0\ {}^{kg}/_{s} \qquad \text{Equation 5-5}$$

m_{mixt} is the mass flow of the mixture of grass and water, $\%_w$ is the percentage of water added

For the uninformed reader this might seem a big amount of grass-water mixture, however in the MPP3 the mass flow of steam coming out of the boiler is around 820 kg/s. [5]

5.3.Heat exchanger

After the mixing the mixture goes through the first heat exchanger. This is a single-pass shell-and-tube heat exchanger with a tube layout of 30°. This heat exchanger is fed by the reaction mixture leaving one of the other parallel reactors. For the properties of the mixture the properties of water are used since only 15% (50% * 70%) of the reaction mixture is biomass.
The total heat transfer rate between two fluids in a heat exchanger can be determined by:

$$Q = U * A_{hex} * \Delta T_{lm} \qquad \text{Equation 5-6}$$

Q is the total heat transfer, U the overall heat transfer coefficient, A_{hex} the total heat exchanger surface and ΔT_{lm} the log mean temperature difference (LMTD).

Of this the total heat exchanger surface is not known, neither are all temperatures for the LMTD. The use of an approximate value for the overall heat transfer coefficient will be explained later.

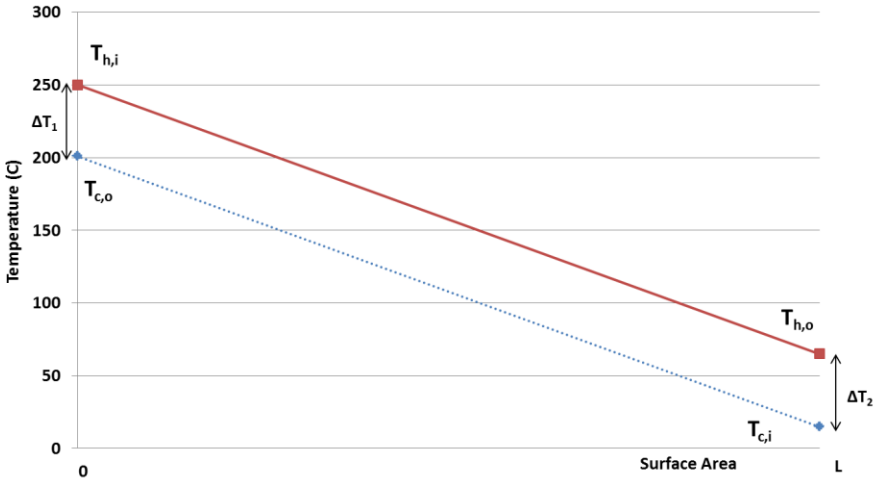

Figure 5-2: Temperature profile heat exchanger

The inlet temperature of the hot flow is 250C, this means there is no heat loss after leaving the reactor. The inlet temperature of the cold flow is equal to the ambient temperature of 15C. The outlet temperature of the hot flow is thought to be 65C this gives a ΔT_2 of 50C. The temperature difference is the driving force behind heat transfer and this is a value used in industry [1].
The total heat transfer can also be calculated by the heat transfer from the hot flow:

$$Q_h = \dot{m}_{mixt}(h_{hi} - h_{ho}) \quad \text{Equation 5-7}$$

Q_h is the heat transfer from the hot flow, h_{hi} the enthalpy from the hot inflow and h_{ho} the enthalpy from the hot outflow.

The heat transferred to the cold flow:

$$Q_c = \dot{m}_{mixt}(h_{co} - h_{ci}) \quad \text{Equation 5-8}$$

Q_c is the heat transfer from the hot flow, hc_i the enthalpy from the hot inflow and hc_o the enthalpy from the hot outflow.

No heat loss to the environment is assumed and thus is the heat flow from the hot flow equal to the heat flow to the cold flow:

$$Q_h = Q_c \quad \text{Equation 5-9}$$

From this the enthalpy of the unknown outlet temperature of the cold flow can be calculated:

$$h_{co} = (h_{hi} - h_{ho}) + h_{ci} = 877{,}5 \ {}^{kJ}/_{kg} \quad \text{Equation 5-10}$$

This corresponds to a temperature of 201,1C.
With all temperatures known the log mean temperature difference can be calculated:

$$\Delta T_{lm} = \frac{\Delta T_1 - \Delta T_2}{ln\left({}^{\Delta T_1}/_{\Delta T_2}\right)} \quad \text{Equation 5-11}$$

With:

$$\Delta T_1 = T_{hi} - T_{co}$$ Equation 5-12

$$\Delta T_2 = T_{ho} - T_{ci}$$ Equation 5-13

$T_{h,i}$ is the temperature of the hot inflow, $T_{c,o}$ is the temperature of the cold outflow, $T_{h,o}$ is the temperature of the hot outflow and $T_{c,i}$ is the temperature of the cold inflow.

And thus:

$$\Delta T_{lm} = 49{,}44\ C$$

With the Q known and the ΔT_{lm} an estimation of the size of the heat exchanger can be made.

The overall heat transfer coefficient is of course not known for the grass-water mixture. An approximate value for this is taken from the book of Kakac [1]. An overall heat transfer coefficient for water to water in a shell and tube heat exchanger ranges from 1300-2500 W/m2*K. With a modest 1800 W/m2*K the area needed for heat exchanging is calculated by manipulating Equation 5-6:

$$A_{hex} = \frac{Q}{U * \Delta T_{lm}} = 2261\ m^2$$ Equation 5-14

The tube sizing depends largely on the material being transported through the heat exchanger. Especially with mixture blockage can easily become a problem and therefore needs to be prevented. Therefore the tubing is chosen with an outside diameter of 70mm and an inside diameter of 63mm. This should not give any problem with an estimated grass size below 50mm. The tubes are bundled as 700. Thus the length is:

$$L_p = \frac{A_{hex}}{N_t * d_o * \pi} = 14{,}69\ m$$ Equation 5-15

L_p is the length of the pipes, n_p the number of pipes and d_o the outside diameter of the pipes.

With the outside diameter of the tubes and the number of tubes known the inner diameter of the shell can be calculated. First the cross-sectional area needed for a single tube is calculated:

$$A_{x,t} = (CL){P_T}^2 = 6{,}66 * 10^{-3}\ m^2$$ Equation 5-16

$A_{x,t}$ is the cross-sectional area per tube, CL is the tube layout constant, P_t the pitch size.

The tube layout constant for this configuration is 0,87 [1] and the pitch size usually is between 1,25-1,50 [1] times the outside diameter of the tubes. Here 1,25 is chosen because the particles in the processed grass are smaller than those in unprocessed grass and blockage should not be an issue.

The inner diameter of the shell can then be calculated to give an idea of the size:

$$D_{i,s} = \sqrt{\frac{4 * N_t * A_{x,t}}{\pi * CTP}} = 2{,}53\ m$$ Equation 5-17

CTP is the tube count calculation constant.

The tube count calculation constant is a constant that accounts for the incomplete coverage of the shell diameter. For a one-pass heat exchanger the tube count calculation constant is 0,93 [1].

The book of Kakac [1] furthermore notes that the ratio of L_pipes/D_shell is a value ranging from 5-15. For this configuration this ratio is:

$$L_{pipes} / D_{shell} = 6{,}63 \qquad \text{Equation 5-18}$$

5.4.Heat needed

As calculated before the cold outflow 201C and there is thus extra heat needed to further heat up this flow. The extra heat that is needed to further raise the temperature of the reaction mixture to 250C is:

$$Q_{c,2} = \dot{m}_{mixt}(h_{250} - h_{201}) = 51{,}75\ MW \qquad \text{Equation 5-19}$$

$Q_{c,2}$ is the heat flow needed in the second heat exchanger, h_{250} the enthalpy of water at 250C and h_{201} the enthalpy of water at 201C.

In the case of the MPP3 this could be steam derived from the steam cycle in the powerplant.

5.5.Size of reactor

This mixture is thought to have a density comparable but not as high as water. Since nothing is known about this the density is estimated to be 800 kg/m3. With the parallel reactors and the recuperation of heat through the heat exchangers a minimum of 3 reactors are needed for continuous operation. To prevent these reactors becoming too big a number of 6 reactors were chosen. This gives a volume per reactor of:

$$V_r = \frac{\dot{m}_{mixt} * t_t}{N_r * \rho_{mixt}} = 46{,}32\ m^3 \qquad \text{Equation 5-20}$$

V_r is the reactor volume, t_t the treatment time, N_r the number of reactors and ρ_{mixt} the density of the mixture.

With a reactor diameter of 4 m the height becomes:

$$h_r = \frac{V_r}{d_r * \pi} 4{,}2\ m \qquad \text{Equation 5-21}$$

h_r is the reactor height and d_r the reactor diameter.

5.6.Auxillary devices

If the mixture is pumped through the heat exchanger and after that heated up by steam to the right temperature the pressure needs to be at least above the vapour pressure of 3,99 MPa. The energy needed to pump the mixture to this pressure is:

$$P_p = \frac{\Delta P * \dot{m}_{mixt}}{\eta_p * \rho_{mixt}} = 1{,}45\ MW$$ Equation 5-22

P_p is the pump power, η_p is the pump efficiency and ΔP is the pressure difference.

No significant losses are expected through the heat exchanger or the other tubing. Most power will be needed for pumping the mixture to the right pressure.

For the decomposition of grass inside the reactor some stirring is needed as well. For this the viscosity of water is used at 250C. Nothing is known about the viscosity of the mixture so for investigating the feasibility of this installation tests on the viscosity is needed.
No calculations are noted here because the energy needed for stirring is negligible. The calculation for this can be found in the attachments.

5.7.Filtering & briquetting

In the Figure 5-1 above also an installation for filtering and briquetting of the WTG is shown. Several possibilities exist to remove the moisture from the WTG after it is treated. From the hydrophobic behavior after several days of drying in air it is expected that mechanical drying can be applied. However it is expected that the WTG is going to behave very differently when dried on a large scale. More research is therefore needed to make an appropriate estimation of the right technique and power needed for mechanical drying. The field of mechanical drying is very diverse however as can be seen by a guidebook[7] and textbook[6] on mechanical drying.
For briquetting the same applies more or less. The WTG clogs together nicely when dried in air as can be seen from the pictures on page . However the treatment foreseen is at higher temperatures than tested at which lignin should be still be present to clog the material together. The water content can also play an important role and it can be that a little higher moisture content produces the best briquettes for storage and further processing. More research is therefore needed for the determination of the briquetting process as well.

5.8.Energy balance

All the power needed to process the grass flow is summed up in Table 5-2. As can be seen quite an energy input is required for the processing of the grass. The heat provided in the form of steam could have otherwise have been used for power production and for the pump electrical energy is needed as well.

Table 5-2: Energy balance WTT

Q_net	-51,75	MW	E_w.t.	435	MW
P_pump	-1,45	MW			
P_stir	0,00	MW			
E_needed	-53,20	MW	E_prod	435	MW
			E_net	381,58	MW

This means that where normally the total thermal input is:

$$Q_{th,t} = \frac{P_g}{\eta} = 2173\ MW$$ Equation 5-23

$Q_{th,t}$ is the total thermal input.

The heat flow needed for the WTT is subtracted from the total thermal input:

$$Q_{th,wtt} = Q_{th,t} - Q_{c,2} = 2122\ MW$$ Equation 5-24

$Q_{th,wtt}$ is the total thermal input with the WTT.

If electricity is still produced with the same efficiency the amount of electricity is then:

$$E_{wtt} = Q_{th,wtt} * \eta = 976{,}2\ MW$$ Equation 5-25

E_{wtt} is the electric energy produced with the WTT.

From this still the pump power has to be subtracted to get the net electrical energy production:

$$E_{net,wtt} = E_{wtt} - P_p = 947{,}7\ MW$$ Equation 5-26

$E_{net,wtt}$ is the net electric energy produced with the WTT.

This represents a loss of electric energy of 2,5 % compared to the situation without treating and co-firing grass. Perhaps in real life this effect can be counteracted by processing a little more WTG to be fired in the boiler.

5.9.Comparison to dry grass

When dry grass is co-fired less fresh grass is required, due to the high mass loss (70%) during the WTT. For co-firing dry grass a mass flow is needed of:

$$\dot{m}_{dry} = {Q_{th}}/{LHV_{dry}} = 25{,}25\ {kg}/{s}$$ Equation 5-27

LHV_{WTG} is the lower heating value of dry grass.

The mass flow of water in the fresh grass that needs to be evaporated is:

$$\dot{m}_{water} = \frac{\dot{m}_{dry}}{(1-\%_{moist})} * \%_{moist} = 37{,}87\ {kg}/{s}$$ Equation 5-28

For the drying of the mass flow this amount of heat is required:

$$Q_{dry} = \dot{m}_{water} * h_{evap} = 92{,}66\ MW$$ Equation 5-29

h_{evap} is the enthalpy of evaporation of water.
Compared to the WTT this is a lot more. However this comparison cannot be made directly because drying can be done with lower temperature steam. A real comparison can be done in further research.

Per kg comparison

To compare the different treatments the required energy per kg of grass is calculated. This is done by subtracting the energy for the treatment from the LHV from the biomass fired. The LHV values and mass percentages are taken from Table 5-1.

Wet-dry
Although drying grass has a net zero effect energetically from Table 5-3. and would only add operational costs and a need for additional equipment it can be beneficial from an operational point of view. Co-firing wet grass cannot be done unlimited. The high moisture content would ultimately lower the boiler temperature. This has negative effects on the burning biomass in the boiler and on the reachable steam temperature. For (co-)firing biomass with such a high moisture content a completely different boiler design is needed. Separating the drying from the firing can thus be exergetically favourable due to the low temperature nature of drying of grass.

Dry-WTG(30%)
The WTT clearly has a very negative impact on useful energy production. This is however not related to the energy needed for treatment but by the nature of the treatment of grass. The high percentage of mass loss during treatment results in an unacceptable low energy yield. Further research on this mass loss is needed otherwise WTT is an unsuitable process for upgrading grass towards an energy source useful for firing in the MPP3.

WTG(30%)- WTG(70%)
For the feasibility it is interesting to note that if 70% of all mass is retained, all hemicellulose is removed, the energy balance is favorable for WTG. Further research can focus on the mass loss of grass or can be aimed at looking at a wet waste stream that does not show this high mass loss.

Table 5-3: Per kg comparison treatments

	Wet	Dried	WTG (30%)	WTG (70%)	
M_in	1	1	1	1	kg
M_out	1	0,4	0,12	0,28	kg
E_biom.	5,42	6,89	2,64	6,16	MJ
E_treatm.		-1,47	-0,22	-0,22	MJ
E_net	5,42	5,42	2,42	5,94	MJ

References:

1. S. Kakac, H. Liu, Heat exchangers: selection rating and thermal design, CRC Press, 1998, pp249-270
2. M. Zlokarnik, Stirring: theory and practice, Wiley-VCH, 2001, pp70-79
3. *Energy research Centre of the Netherlands (*ECN), *Phyllis2 database for biomass and waste*, http://www.ecn.nl/phyllis2/, accessed: 8-5-2012
4. E.on, MPP3- een nieuwe centrale, 2013, http://www.eon.nl/corporate/Activiteiten/mpp3-een-nieuwe-centrale, accessed 10-4-2013
5. Internal E.on MPP3 design document, 2006
6. R.J. Wakeman, E.S. Tarleton, Solid/liquid separation: scale-up of industrial equipment, Elsevier 2005, pp1-35
7. H. Pierson, B. Perlmutter, Selection of Liquid - Solid Separating Equipment, TCE Today 2009 (this is a series of article that appeared in June pp49-50, July/August pp53-55 and October pp48-50), also available through http://www.bhs-filtration.com/rental/Selection%20of%20Liquid-Solid%20Separating%20Equipment.pdf

6. Conclusions

Modelling

- In the modelling a good comparison was seen between 2 biomass species. The model taken from the study into corn cob showed very similar results when used for sugar maple wood meal (SMWM). Benchmarking with more results could lead to a better model. Looking into more advanced modelling methods might be needed then.

Experimental setup

- The reactor can be used up to 250C and this limits the test range. In practice this is further limited by the heating rate that can be achieved. Because the reactor cannot be heated higher than 250C the heating oil can neither be heated further. This results in a very small to no temperature difference, the driving force behind the heating rate.
- The sampling method is not suitable for tests with solid particle that pass through a sieve bigger than 250 micrometer. Already with the solid particles used blockage of the primary sampling tube happened. At higher temperatures this results in dangerous situations.
- Gasses that are produced during the tests cannot be measured. This results in a loss of gaseous products during sampling at the secondary sampling tube. This includes evaporation of products that are liquid at room temperature such as furfural. At the primary sampling tube this is prevented. However after the test the gaseous products such as CO2, H2 can again not be measured.
- Some of the solid mass stays behind in the reactor after the tests. Even though the reactor can be flushed some will remain fixed at the reactor walls. Another disadvantage is that some of that mass can be released during a later test releasing a solid carbon-like product.

Measurement equipment

- Only single components (glucose, xylose acetic acid) can be measured. No oligomers are available for calibration and these are thus no quantative measurement is possible. This again limits the possibilities to get a complete mass balance.

Results

- All results are totally not in line with the results obtained from modelling. The results are furthermore on the low side compared to calibrated values.

HPLC of grass

- Grass shows very high concentrations of dissolved glucose, xylose and acetic acid. This is very remarkable since this should point to a very rapid decomposition of grass. This is in line with the high mass loss seen after the tests. This contradicts the results from the model. The cause of this could be that grass has a very different structure from the biomass used for modelling. It could be that the degree of polymerization of grass is very low.
- Research done for another master thesis at P&E (done by Vini Mangkasuputra) has also shown a result that points to a very low DP. In a mechanical dewatering test a high level of glucose and xylose has been found in the released liquids.
- The high concentration of acetic acid deserves some extra attention because this is also not expected. This high concentration could be caused by a very high level of acetyl groups in hemicelluloses from grass. Another possibility could be that the acetic acid comes from xylose decomposition.
- Furfural shows very high concentrations only at 220C, this is very strange especially since at the other tests the conditions in the beginning are the same.

HPLC of xylan and bagasse

- Xylan decomposes very slow in comparison to the predictions. Xylose and furfural are being measured and their behaviour is in agreement.
- Bagasse shows a very low concentration of dissolved sugars and thus no comparison could be made between the model and test results.

HPX-RHM comparison

- The HPX column shows very similar results from the results obtained by the RHM column for xylan. For grass the results were less distinct. This could be caused by a contamination introduced into the liquid sample.

Solid samples

- As said before a relatively high mass loss was observed. This is not in line with the model results. This points to different decomposition behaviour in comparison to corn cob used in the work of Naberlatz.
- The solid samples obtained after the test were air dried and after this were very dry (<5 wt% moisture). Large scale should give information regarding scaling up and possible drying techniques usable at larger scale.
- The solid samples that were dried were still very fibery. It looked like the structure of cardboard used in structural pieces. This does not have the brittleness such as coal. At higher temperatures this brittleness is expected.
- The solid sample obtained from bagasse also had a relatively high mass loss. A reason for this could be that bagasse is already a processed form of biomass and thus relatively broken up and thus susceptibly to decomposition in WTT.

TGA

- The tests performed with the TGA showed a very distinct change in composition. The hemicelluloses “shoulder” was not visible anymore and the cellulose related peak is shown at a much higher temperature. The more volatile components are thus regarded to be decomposed.
- What deserves more attention is that the volatile matter is less in WTG than in fresh grass. This is the opposite of what is expected.

SEM

- The SEM pictures showed a small change in structure between the different samples of grass. No spectacular differences were observed. What can be seen is that at higher temperatures more white dots are visible. What these white dots are is unknown.

Equipment

- From the calculations done on the equipment it is observed that treating grass at the same facility as were it is to be co-fired has a negative impact on electrical energy production. This impact is negative and around 2,5%. This is caused by the heat needed for the processing. The implementation of the WTT should thus be carefully done to minimize impact on the total power production.
- The high mass loss observed in the tests limit the implementation of the WTT. The amount of WTG that results is so low that co-firing grass directly is energetically more favourite. This is thus advised for E.ON. A wet waste stream that retains most of its mass would make such a treatment economically feasible.

Overall

- The overall conclusion is that wet torrefaction of verge grass is not suitable for E.ON as a pre-treatment for co-firing. Simply too much mass is lost during the process. Wet waste streams that retain more mass can be viable. Another possibility could be that the treatment is "tweaked" for getting the right chemicals during grass decomposition. These chemicals could then be sold negating the negative effects of the high mass loss.
- Grass and bagasse show a very high mass loss which is not accounted for in dissolved sugars. The decomposition mechanisms is thus completely different from that used for modelling.

7. Recommendations

For this method

- Do a test on forehand to get acquainted with the method and its limitations
- Use higher solids concentrations, 5 gram in 850 ml water gives low HPLC peaks
- Find a HPLC column which specifically separates monosaccharides more clearly
- Perform biochemical analysis on dried grass and reactor residue, a very clear HPLC reading is essential
- Use acid hydrolysis to dissolve all oligomers as well
- Look into the high mass loss
- Find a way to account for gases released

Different method

A totally different method can be applied which has been done by other researchers. This method uses a heated oil bath in which small reactor tubes are placed. The tubes are then removed one by one at the required reaction time and quenched in an ice bath. This enables more precise analysis of the solid fraction and with the right precautions the gaseous fraction as well. Perhaps the mass balance can be closed in this way. This method also prevents the measurement being influenced by possible release of carbon residue from the reactor wall from previous tests. A downside of this method as that no internal stirring takes place.

Different process

Another possibility is that a search goes further into a very different process. One of the possibilities is to look at higher temperatures, what was not possible with the used test setup. What also limits research into higher temperatures with the current stup is the time needed for sampling. At higher temperatures the decomposition takes places quicker and currently around 1,5 minute is needed for sampling. This is too much to get insight into the reaction behaviour at higher temperatures.

Another possibility is to look at a process that uses two steps to convert grass into WTG. This process would use one step at a lower temperature (around 150C) to release the sugars from grass. These can then be processed into valuable chemicals or ethanol. At a higher temperature the solid residue can be made into a coal like solid.

Attachments I: Matlab main file

```
global T_max T_init vT NC Ccel_0
Tc=160;
Tstart=90;
T_max=Tc+273;
T_init=Tstart+273;
vT=10;   %Heating rate (tfinal/ntimes * K/min)
NC=12;
% Biomass composition
Pct_Hemi=0.236;
Pct_Cel=0.329;
Pct_Lig=0.225;
Pct_Tot=Pct_Hemi+Pct_Cel+Pct_Lig;
Pct_Ash=0;
Pct_Extr=1-Pct_Tot-Pct_Ash; %The extractives boil off immediately and are
thought to have no influence on the initial HHV
% Biomass weights
Biom=5;  %Total biomass in reactor (g)
Chemi_0=Biom*Pct_Hemi;
Ccel_0=Biom*Pct_Cel;
CLig_0=Biom*Pct_Lig;
CAsh_0=Biom*Pct_Ash;
% Initial condition
C0=zeros(1,NC);
C0(1)=Chemi_0*0.8;
C0(2)=Chemi_0*0.2;
C0(9)=Ccel_0;
% Specification of integration
tfinal = 50;
ntimes = 100;
tout   = linspace(0, tfinal, ntimes);
% Options
opts = odeset ('AbsTol', sqrt (eps), 'RelTol', sqrt (eps));
% The integration
[tsolver, cout] = ode15s (@componentrates, tout, C0, opts);
% HHV values
HHV_hemi=1.86E4;    %kJ/g
HHV_cel=1.86E4;     %kJ/g
HHV_lig=2.658E4;    %kJ/g
% Original E(nergy)C(ontent) daf
OEC_hemi=HHV_hemi*Pct_Hemi;
OEC_cel=HHV_cel*Pct_Cel;
OEC_lig=HHV_lig*Pct_Lig;
OEC_tot=(OEC_cel+OEC_hemi+OEC_lig)/Pct_Tot;
% EC & Masses
Cout(:,1)=(cout(:,1)+cout(:,2));
Eout(:,1)=Cout(:,1)*HHV_hemi;   %EC attributed by the Hemicellulose
Cout(:,2)=cout(:,9);
Eout(:,2)=Cout(:,2)*HHV_cel;    %EC attributed by the Cellulose
Cout(:,3)=CLig_0;
Eout(:,3)=Cout(:,3)*HHV_lig;    %EC attributed by the Lignin
Cout(:,4)=CAsh_0;
Cout(:,5)=(cout(:,1)+cout(:,2)+cout(:,9)+CLig_0+CAsh_0);    %Total mass
Cout(:,6)=(cout(:,1)+cout(:,2)+cout(:,9)+CLig_0);           %daf mass
Eout(:,4)=(Eout(:,1)+Eout(:,2)+Eout(:,3))./Cout(:,6);
HHV(:,2)=Eout(:,4);
```

```
% Plotting
plot(tout,Eout);
xlabel('Time (min)')
ylabel('HHV (kJ/gr)')
title(['Decomposition of Biomass at T=' num2str(Tc) ' (C)'])
legend('Hemicellulose (kJ)', 'Cellulose (kJ)', 'Lignin (kJ)', 'Total daf
(kJ/gr)');
axis([0 tfinal 0 OEC_tot*2])
```

Attachments II: Matlab reaction equations

```
function rcomp = componentrates(t,C);
% The hemicellulose data was taken of Naberlatz et. al.
% Species and reactions might be a bit confusing, therefore:
% % C(1)= xylan type 1
% % C(2)= xylan type 2
% % C(3)= xylose oligomers
% % C(4)= xylose
% % C(5)= furfural
% % C(6)= decomposition products
% % C(7)= arabinose
% % C(8)= acetic acid
% The cellulose data was taken of Kamio et.al.
% % C(9)= cellulose
% % C(10)= oligomers
% % C(11)= monomers
% % C(12)= pyrolysis products
global T_max T_init vT NC Ccel_0
R=8.3144621;
Cb=7000;
rho=555;
r0=8E-5;
kc=0.001;
T_r=vT*t+T_init;
% T_r=T_max;
if T_r>T_max
    T_r=T_max;
end
% Reaction constants
% % Hemicellulose
k(1)=exp(31.52)*exp(-127300/R/T_r);
k(2)=exp(61.41)*exp(-251700/R/T_r);
k(3)=exp(27.55)*exp(-119000/R/T_r);
k(4)=exp(29.36)*exp(-122500/R/T_r);
k(5)=exp(32.48)*exp(-132000/R/T_r);
k(6)=exp(25.08)*exp(-106200/R/T_r);
k(7)=exp(29.82)*exp(-125200/R/T_r);
k(8)=exp(14.18)*exp(-65100/R/T_r);
% % Cellulose
ks=7.3E6*exp(-141000/R/T_r);
k(9)=180*Ccel_0^(1/3)*Cb/((75.7*rho*r0)*(1/kc+1/ks));
k(10)=3.6E9*exp(-102000/R/T_r);
k(11)=6E11*exp(-130000/R/T_r);
k(12)=1.8E13*exp(-141000/R/T_r);
% The stoichiometric matrix
stoi = [-1 0 1 0 0 0 0 0 0 0 0 0;...
        0 -1 1 0 0 0 0 0 0 0 0 0;...
        0 0 -1 1 0 0 0 0 0 0 0 0;...
        0 0 0 -1 1 0 0 0 0 0 0 0;...
        0 0 0 0 -1 1 0 0 0 0 0 0;...
        0 0 -1 0 0 0 1 0 0 0 0 0;...
        0 0 0 0 1 0 -1 0 0 0 0 0;...
        0 0 -1 0 0 0 0 1 0 0 0 0;...
        0 0 0 0 0 0 0 0 -1 1 0 0;...
        0 0 0 0 0 0 0 0 0 -1 1 0;...
        0 0 0 0 0 0 0 0 0 0 -1 1;...
```

```
        0 0 0 0 0 0 0 0 0 -1 0 1];
% initialize a column vector
rcomp = zeros(NC,1) ;
% the rates of the individual reactions
% % Hemicellulose
r(1) = k(1) * C(1);
r(2) = k(2) * C(2);
r(3) = k(3) * C(3);
r(4) = k(4) * C(4);
r(5) = k(5) * C(5);
r(6) = k(6) * C(3);
r(7) = k(7) * C(7);
r(8) = k(8) * C(3);
% % Cellulose
r(9) = k(9) * C(9)^(2/3);
r(10) = k(10) * C(10);
r(11) = k(11) * C(11);
r(12) = k(12) * C(10);
% Using the stoichiometry matrix, the component rates are:
for i=1:NC
    rcomp(i) = sum(stoi(:,i).*r(:));
end
```

Attachments III: Calibration line Rezex RHM

Calibration curve for Rezex RHM-monosaccharide

Arabinose-RI

Start [Min]	Time [Min]	End [Min]
11.71	12.23	13.2

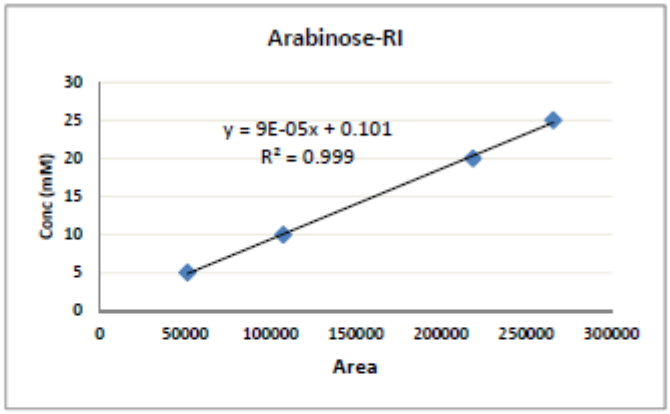

Furfural-RI

Start [Min]	Time [Min]	End [Min]
34.65	35.78	37.5

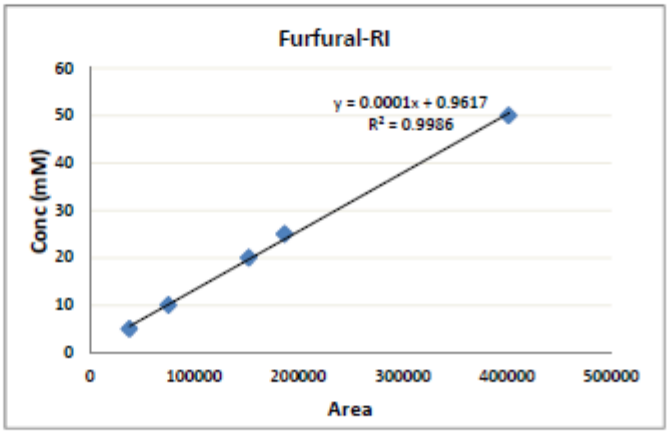

Furfural-UV

Start [Min]	Time[Min]	End [Min]
34.59	35.46	37.11

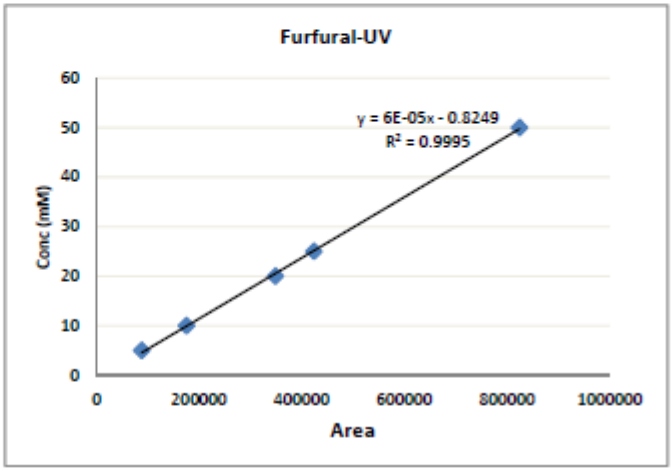

Acetic acid-RI

Start [Min]	Time [Min]	End [Min]
15.53	16.22	17.47

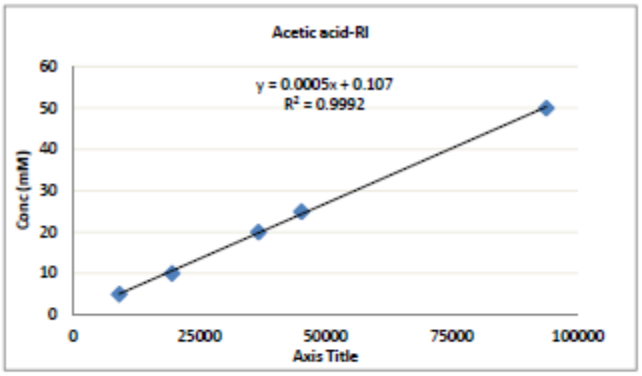

Oxalic acid-UV

Start [Min]	Time [Min]	End Time[Min]
6.96	8.15	8.64

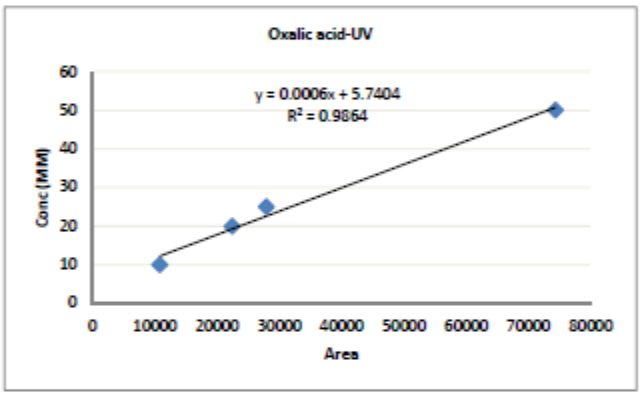

HMF-RI

Start [Min]	Time [Min]	End Time[Min]
25.07	25.92	27.64

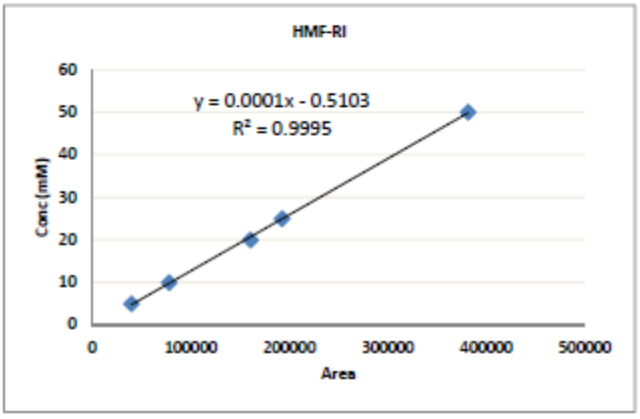

Levulinic acid-UV

Start [Min]	Time [Min]	End [Min]
15.63	16.1	16.96

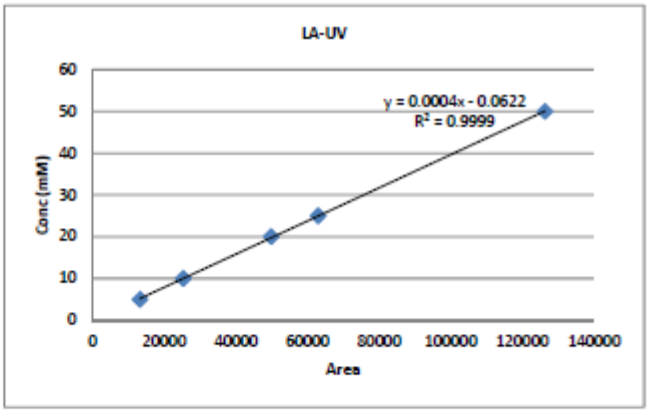

Levulinic acid-RI

Start [Min]	Time[Min]	End [Min]
15.47	16.15	17.37

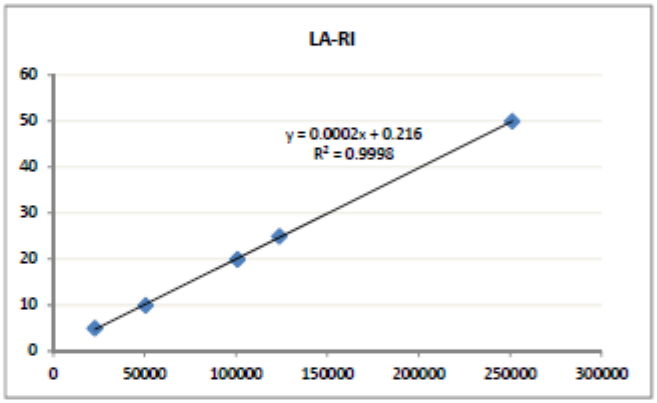

Glucose-RI

Start [Min]	Time [Min]	End [Min]
10.3	10.8	11.87

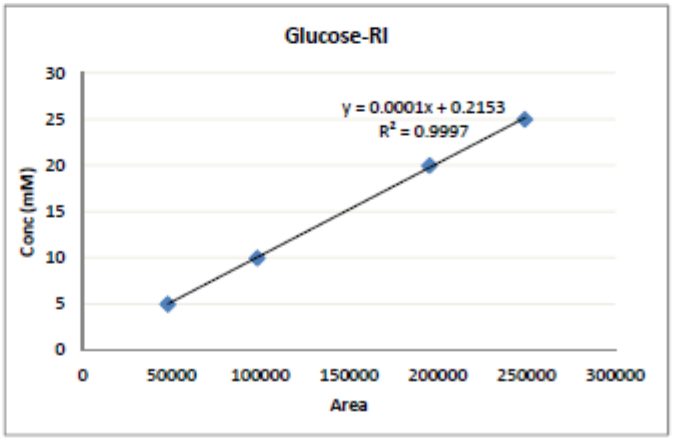

Formic acid:

Start [Min]	Time [Min]	End [Min]
14.24	14.8	15.57

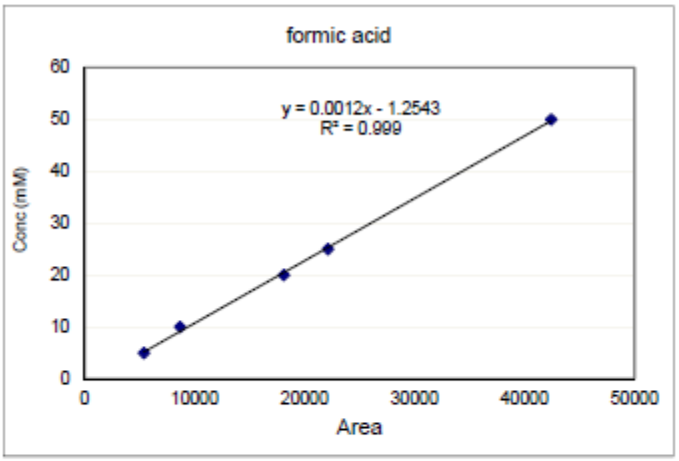

Xylose_RI

Start [Min]	Time [Min]	End [Min]
10.9	11.38	12.29

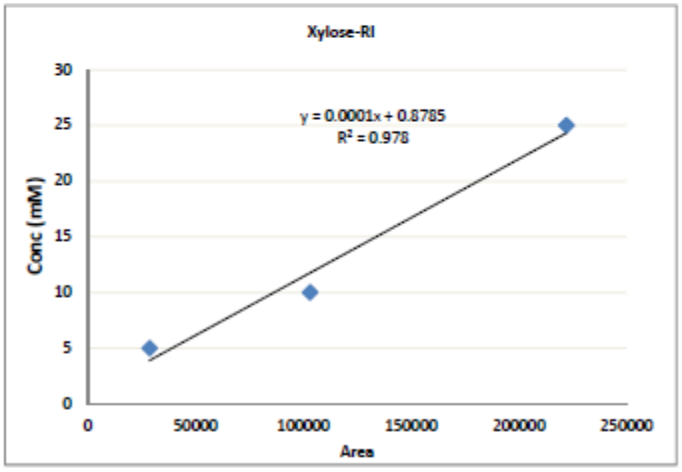

Attachments IV: Calibration line HPX

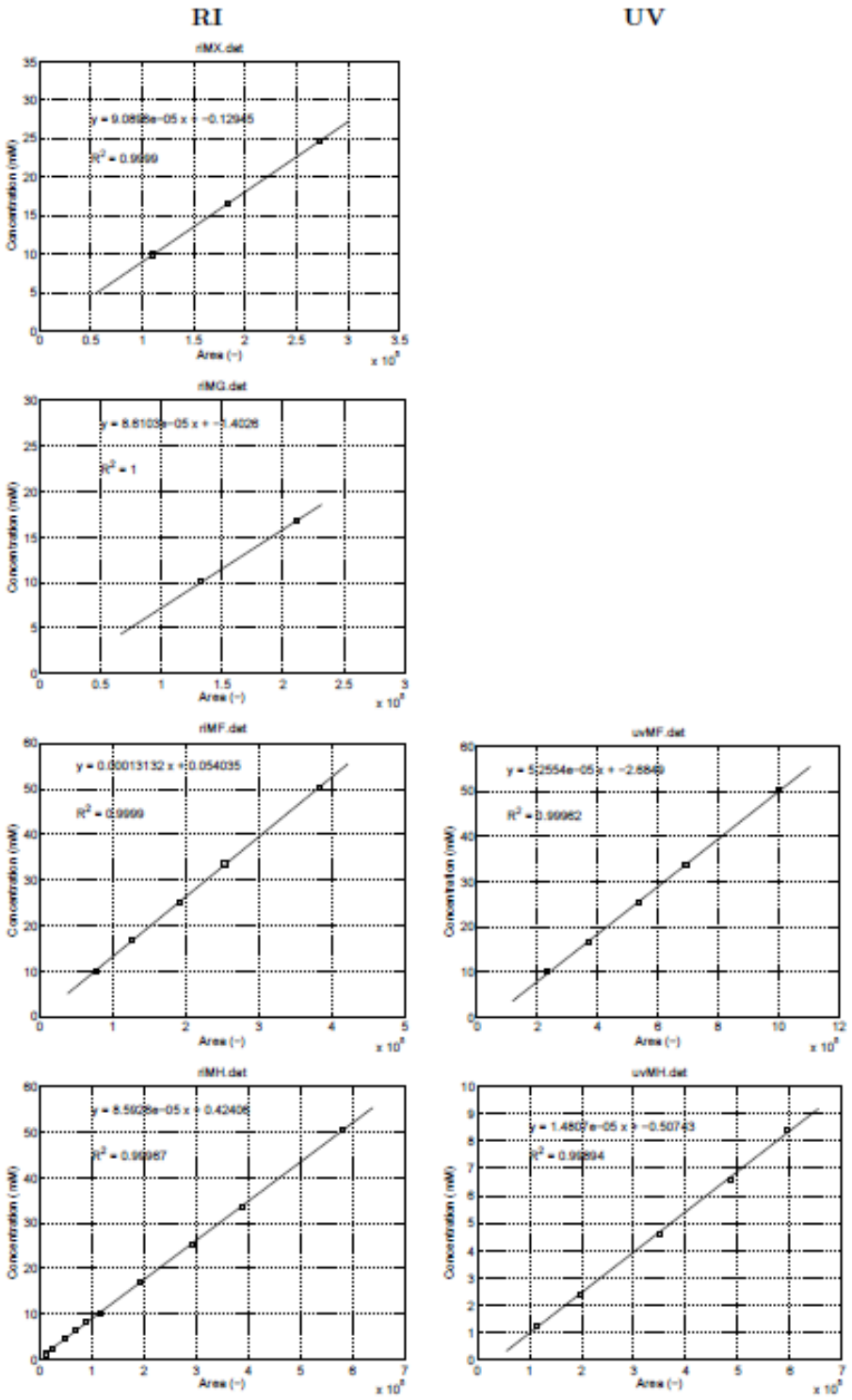

Figure 1: Calibration curve of HPX-87H column @60℃, 0.005N H_2SO_4 eluent, 0.6 mL/min. X = xylose, G = glucose, F = furfural and H = hydroxymethyl-furfural.

1

Attachments V: Calculation stirrer

All formulas and parameters not known from the reactor design are taken from Zlokarnik [1].

Because nothing is known of the behaviour of the reaction mixture some assumptions were made to simplify the calculations:

- The mixture is homogeneous
- The mixture behaves as a Newtonian fluid

The fluid probably does not behave as a Newtonian fluid, but this assumption simplifies the calculations to a great extent.

The stirrer power can then be calculated using:

$$P_{stir} = Ne * n^3 * d^5 * \rho \qquad \text{Equation 0-1}$$

Where *Ne* is the Newton number, *n* is stirring frequency, *d* is the diameter of the blade and *ρ* is the density of the fluid.
The Newton number is dependent on the Reynolds number. The Reynolds number was calculated using the viscosity of water at the reaction temperature. With the Reynolds number known the Newton number can be obtained from a graph in the book of Zlokarnik.

Table 0-1: Used parameters

n_stirrer	3,44	min-1
n_stirrer	0,057	s-1
v_water (kin.visc.)	1,38E-04	m2/s
d_blade	2	m
eff_stir	0,95	%
Reynolds number	1,00E+05	-
Newton numb.	0,2	from Zlokarnik pp80

With the parameters from Table 0-1 the stirrer power was calculated:

$$P_{stir} = 0{,}97\ kW$$

This is negligible in comparison to the heat needed as input for the process.

1. M. Zlokarnik, Stirring: theory and practice, Wiley-VCH, 2001, pp70-80